ARCH D5.2

Handbook on Heritage Asset Vulnerability

Deliverable No.	D5.2
Work Package	WP5
Dissemination Level	PU
Author(s)	Andrea Dall'Asta, Michele Morici, Graziella Roselli, Enrica Petrucci (UNICAM), Sonia Giovinazzi, Ludovica Giordano, Maurizio Sciortino (ENEA)
Co-Author(s)	Lucia Barchetta, Claudia Canuti (UNICAM)
Contributor(s)	-
Due date	2021-11-27
Actual submission date	2021-12-14
Status	Final
Revision	1.0
Reviewed by	Quintilio Piattoni (CAMERINO), Nicolas Buxens, Olatz (TECNALIA)

This document has been prepared in the framework of the European project ARCH – Advancing Resilience of historic areas against Climate-related and other Hazards. This project has received funding from the European Union's Horizon 2020 research and innovation programme under grant agreement no. 820999.

Contact

arch@iais.fraunhofer.de

www.savingculturalheritage.eu

This project has received funding from the European Union's Horizon 2020 research and innovation programme under Grant Agreement no. 820999

Executive Summary

This deliverable has been prepared for the European Commission-funded research project ARCH: Advancing Resilience of historic areas against Climate-related and other Hazards. It is the key output of task 5.2 “Handbook on Heritage Asset Vulnerability” within work package 5 “Impact & Risk Assessment”.

The aim of task 5.2 is to develop and adapt models and methods to assess the vulnerability of historic areas and to estimate potential consequences, based on the hazard models from T5.1 and the data about the current condition of heritage assets from T4.4. This has been performed by defining state indices for heritage assets (e.g. material degradation, structural capacity, soil-foundation capacity, population density, education levels, age and gender distribution, etc.) and quality parameters for measuring service degradation. Damage functions are developed and adapted to quantify different consequences deriving from a variation of the asset state and hazard characteristics (e.g. intensity).

Subsequently, the relationships (damage functions) between hazards (stresses or shocks) and state indices variations are defined by combining information from literature and data collected during the co-creation activities (WP3). The main objective of this action consists in calibrating damage functions coherently with the information detail available. The proposed damage functions will be validated based on historical data recorded during previous disasters.

The definitions of state indices, quality parameters and damage functions provide a contribution for the design of the monitoring actions and the work are carried out in connection with relevant monitoring activities of WP4.

Table of contents

Table of Abbreviations

Abbreviation	Explanation
BTM	Building Typology Matrix
CLRTAP	Convention on Long-range Transboundary Air Pollution
CULT-STRAT	Assessment of Air Pollution Effects on Cultural Heritage
CV	Contingent Valuation
Da.D.O.	Observed Damage Database
DInSAR	Differential Interferometric techniques
DPM	Damage Probability Matrices
EAPMBSP	Effects of Airborne Particulate Matter on Building Surfaces Project
HR	High Rise
ICP	International Co-operative Programme
InSAR	Interferometric Synthetic Aperture Radar
LR	Low Rise
LTSM	Limiting Tensile Strain Method
MINNI	Italian National Integrated Model to support the International Negotiation on air pollution issues
MQI	Masonry Quality Index
MR	Middle Rise
MULTI-ASSESS	Model for Multi-pollutant Impact and Assessment of Threshold Levels for Cultural Heritage

PGA	Peak Ground Acceleration
PGV	Peak Ground Velocity
PMF	Probability Mass Function
PPASDC	Particulate Pollution And Stone Damage Contract
PS	Permanent Scatterers ®
RC	Reinforced Concrete
REACH	Rationalised Economic Appraisal of Cultural Heritage
SAR	Synthetic Aperture Radar
Sa(T)	Pseudo Spectral Acceleration
SRI	Subsidence Related Intensity
UNECE	United Nations Economic Commission for Europe
WTP	Willingness To Pay

1. Introduction

(A. Dall'Asta, S. Giovinazzi)

This deliverable has been prepared for the European Commission-funded research project ARCH: Advancing Resilience of historic areas against Climate-related and other Hazards. ARCH will develop decision support tools and methodologies to improve the resilience of historic areas to climate change-related and other hazards. These tools and methodologies are developed with the pilot cities of Bratislava (Slovakia), Camerino (Italy), Hamburg (Germany), and Valencia (Spain), in a co-creative approach, including local policy makers, practitioners, and community members.

Deliverable can be used by technicians and researchers and, more generally, persons in charge of implementing tools for risk assessment, (WP5 content) and persons in charge of developing maps and communication tools for stakeholders and communities; the document is not intended to be used directly by stakeholders or end users.

1.1. Purpose of this report and relation to other deliverables

This handbook will describe the developed state indices, quality parameters, and damage functions and how they can be employed in vulnerability assessments of historic areas. It includes descriptions of interrelations between heritage assets and the social and economic fabric, as well as impacts related to intangible and artistic values.

This report (D5.2) is the accompanying document to the demonstrator for activity 5.2 "Vulnerability and consequence analysis" within Work Package 5 (WP5) " Impact & Risk Assessment". The objectives of WP5 are:

- To provide methods and tools to assess, calculate, and visualise the risk in historic areas;
- To define service quality parameters for measuring service degradation due to predicted impacts.
- To define state indices for heritage assets (e.g. material degradation, structural capacity, soil-foundation capacity, content vulnerability);
- To transform environmental data into hazard models, according to the format of the selected response functions;
- To estimate potential consequences to heritage assets by defining and adapting damage functions selected from the technical literature;
- To extend the CIPCast decision support system for impact and risk estimation for historic assets.

Accordingly, to the purposes mentioned above, this document illustrates models and methods to assess the vulnerability of historic areas and estimate potential consequences, based on the hazard results obtained inT5.1 and the data about the current conditions of heritage assets collected in T4.4. This document defines state indices for heritage assets (e.g. material degradation, structural capacity, soil-foundation capacity, population density, education levels, age and gender distribution, etc.) and quality parameters for measuring service degradation. Damage functions are developed and adapted to quantify different consequences deriving from a variation of the asset state and hazard characteristics (e.g. intensity).

Vulnerability assessment has been focused on the following points.

- Physical-chemical degradation indexes for architectural components, as mortar, bricks or stones, and artefacts, as frescos, statues, depicts, books;
- Parameters controlling the mechanical vulnerability of construction with cultural values, as churches and historical buildings
- Risk perception indexes representing the perception of the population with regard to severity of expected risks and threats
- Geotechnical, hydrological, and hydrogeological parameters, and in particular those related to that portion of terrains (rocks and soils) strictly interacting with the heritage asset and influenced by hazards considered in WP4
- Road blockage index, which is related to the risk of blockage of the road network due to debris produced following a disaster event
- Socio-economic impacts at regional scale

Therefore, the D5.2 is directly related to the following deliverables:

D3.4 Report on co-creating the information system

D3.5 Report on co-creating the Impact and Risk Assessment

D4.1 Sensing and Repositories

D4.2 Historic Area Information Management System (HArIS)

D4.3 Threats and Hazard Information Management System (THIS)

D4.4 Knowledge information management system for decision support

D5.1 Hazard models for impact assessment

D5.3 CIP Cast DSS modification and integration

D6.1 Inventory of resilience options

D6.2 Assessment of long-term implementation options

D7.5 Requirements description

D7.6 Interface specification and system architecture

D7.7 System design and realization

1.2. Gender statement

This document has been developed taking into consideration the guidance on gender in research provided in the Project Handbook (D1.2) as well as State-of-the-Art report number 5 of deliverable D7.1 on "*Gender aspects in conservation and regulation of historic areas, disaster risk management, emergency protocols, post-disaster response techniques, and techniques for building back better*".

In particular, special attention has been paid to those risk evaluations where gender differences may play a role in the procedure, as in the evaluation of socio-economic impacts, illustrated in Chapter 8, and in the selection of sample of persons called to respond to the questionnaire about the social value attributed to historical assets, included in Chapter 6.

1.3. Structure of this report

The report is divided in eight sections:

- Following this introduction, **Section 2** illustrates the general framework for risk assessment and the specific role of the models to be used for vulnerability analysis.
- **Section 3** focuses on damage in materials due to environmental conditions, presenting response models relating environmental chemical-physical parameters to degradation of the material surface. Here and in the following chapters, the topics are analysed discussing the following points: a) description of the problem, b) scientific background, c) suggestion for implementation, d) applicative examples.
- **Section 4** focuses on seismic vulnerability of historical constructions and towns. Metrics for seismic hazard and construction damage are presented, as well as consequence functions relating them.
- **Section 5** concerns hydrological and hydrogeological vulnerability of historical construction presenting results related to subsidence at town level..
- **Section 6** provides suggestions for the assessment of intangible values, presenting a strategy to handle non measurable quantities related to social values perceived by human communities and artistic values attributed by experts. Two examples regarding social and artistic value, developed at district level, are reported
- **Section 7** focuses on the road network functionality in historic areas, analysing the efficiency in the aftermath of seismic events and potential consequences on post-event emergency activities. A response model relating seismic intensity to road blockage due to the debris produced by building collapses is presented.
- Finally, in **Section 8** the assessment of socio-economic consequences at regional scale are considered. In this field analytical models are not yet available, and a different approach is illustrated. Criteria to select indicators influencing the impacts, and to define numerical indexes are presented, as well as two examples of application.

Bibliographic references are collected in the **References** section.

2. General concepts and preliminary definitions

(A. Dall'Asta)

The aim of this handbook consists in providing tools for a quantitative assessment of vulnerability of cultural heritage, going beyond a qualitative assessment and providing a solid base for risk and impact assessment and evaluation of the effectiveness of risk mitigation actions.

2.1. Consequence functions and vulnerability framework

The handbook provides *consequence functions* (or impact functions), intended as analytical expressions relating hazardous event, with specific properties and intensity, to potential damage on cultural heritage-related systems. Systems must be intended in a general sense, as objects, more or less complex, that may suffer a damage as a consequence of a specific hazard. So, systems may span from single monument or building to historical town or communities living in a district. It is evident that different systems are prone to different type of damage, e.g. a material degradation can be of interest for a monument, the loss of escape ways can be of interest for historical centres or the loss of employments can be of interest at regional scale. As well as it is evident that the consequence functions are not exclusively related to the objects, but they depend on the specific cause-consequence pair of interest, e.g. damage produced by flooding is not the same as damage caused by earthquake, even if they act on the same system.

So, the overall properties of a consequence function give a formal and operative description of the general concept of vulnerability, defined according to the ARCH-glossary D7.1.

However, despite the study on this topic strongly increased in the last decades ([1], [2]), nowadays it is not possible to analyse a so large number of different problems by models with the same level of accuracy, so that strong simplifications are required in many cases. A general conceptual framework is reported below (Figure 1), and this should help to give evidence to the simplification assumptions introduced time after time.

Hazard occurrence generally triggers a variation in the vulnerable system. This type of phenomena can be efficiently contextualized in the very general formal framework of *dynamical systems*, whose behaviour can be described by introducing the concept of *state*, intended as the minimum set of information necessary to characterize the object condition at a particular instant, and the *transition law* describing the variation of the state due to the external cause, the hazard.

This general concept can be formally defined in different ways according to the intrinsic property of the problem studied and to our level of knowledge of the dynamic mechanisms involved.

In many cases the object is clearly bounded, hazard and state descriptions are based on measurable quantities and transition is described by analytical relationship providing the description of the state variation following from a particular hazard.

The problem is usually formulated by considering a family of similar objects (e.g. residential buildings or district with similar governance structure) and transition laws maintain the same structure but they have some internal parameters that are different case by case. These differences describe the intrinsic different vulnerability of considered systems. The specific properties of a single transition law can be related to general characteristics, such as susceptibility, exposure, or resilience.

It is worthy to note that information about the state is complete, in the sense that identifies in a unique way the current system and it is sufficient to evaluate its future evolution due to a hazard. However, state variation is a *direct consequence*, but in many cases other consequences may be of interest for the assessment of potential impacts. This other information should be derived from the state by one or more *derived consequence functions*, at least if it is correctly defined (e.g. the state of historical building is described by deformation measures but the impact of interest may consist in the repairing costs that follow from the former information). In this case, the consequence function consists of the combination of the transition law and the derived consequence functions. Derived consequences may be often organised in a series of *consequence chain*.

The most refined consequence functions generally include uncertainties affecting the prediction ([3], [4]), in this case the output is not a numerical value measuring the consequence, but the output is a probability density function associated to the random variable measuring the consequence.

The compatibility between consequence functions and hazard description should be carefully considered because the same hazard can be described in different ways (e.g. flooding may be described by the evolution in time of water level or simply by the maximum value attained by the water level or earthquake description may or may not include information about frequency content and time duration of the ground motion). The consequence functions are organized to receive a specific format only for hazard. So that it is necessary to check that the input form of interest be available for the system studied.

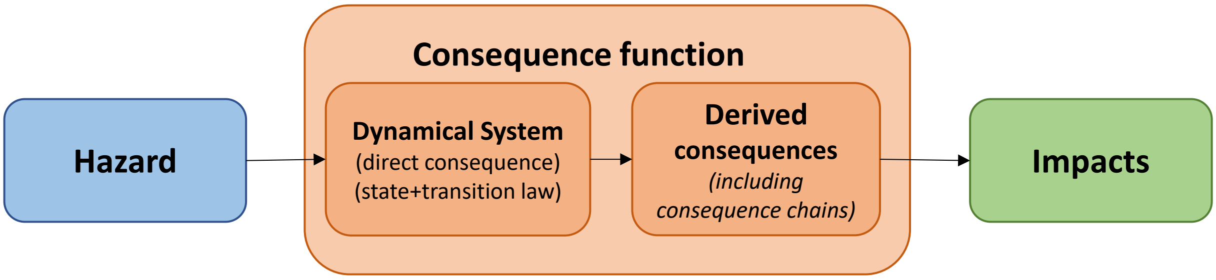

Figure 1: Conceptual framework

However, this type of analytical approach is not always possible, at least based on the current level of knowledge. Sometimes, the problem is too complex, in the sense that involves a lot of inter-dependent phenomena, and the consequence is a multi-dimensional entity whose components can be defined only in a qualitative way. The assessment of socio-economic vulnerability at a regional case is a typical example (see relevant chapter).

In this case, it is not possible to define in a precise and operative way state and transition law with a satisfactory reliability level and the vulnerability problem is approached by selecting a list of parameters, *vulnerability indicators,* that play a role in the system vulnerability.

On one hand, these vulnerability indicators, measured by numerical *vulnerability indexes*, only provide a qualitative information about the vulnerability of the system while cannot give a quantitative information about consequences related to a specific hazardous event. However, a comparison between indexes concerning different vulnerability causes makes it possible to select the most efficient actions. At the same time, the comparison among synthetic indexes related to different systems makes it possible to prioritize actions, addressing resources toward the most vulnerable contexts. So that, this approach is surely effective from the point of view of the decision-making process.

On the other hand, this approach is very flexible and inclusive, and very complex system can be handled.

In this case, the risk, including both hazard and vulnerability, is usually obtained by a simple multiplication of hazard and vulnerability indexes and results is a consequence index. So that, the general concept of vulnerability is formally described by the set of vulnerability parameters and compatibility with hazard requires that the latter be described by a single index too.

In the following, the two approaches will be used, according to the particular properties of the considered vulnerability problem.

2.2. Vulnerability analysis of different scale

Results from vulnerability analysis are often reported in maps connecting vulnerability of unitary elements with their location. This is useful to show a global overview of the problem and maps make it possible to give evidence to the most critical situations.

Characteristic properties of a map are the *granularity*, dictated by the geometrical dimension of the *unitary elements*, and the *extension*, related to the global dimension of the area reported in the map (Figure 2). Maps can be more or less extended (large/small scale maps) and they may include a large/small number of unitary elements (high/low resolution maps).

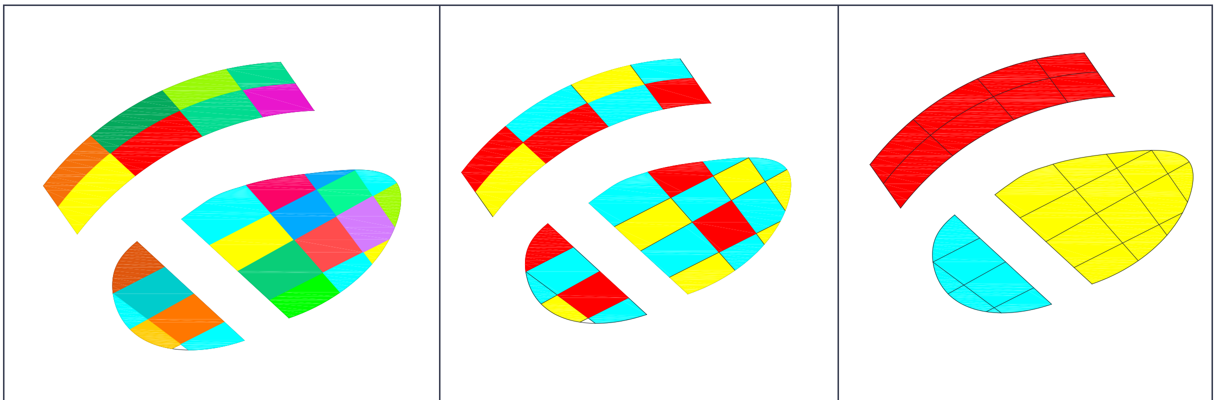

Refined models	Model reduction	Granularity reduction

Figure 2: Different approaches to scale transition problem

The decision-making process and the selection of the actions that are mostly effective in risk mitigation often requires the same problem (relationship between hazard and damage) is analysed at different scales and a connection among results at different scales must be clearly defined. In general, analysis at district level (large-scale) can be easily related to socio-economic dynamics of the territory and may guide the distribution of the resource available for prevention in a more effective way. This type of analysis also gives evidence to the most critical areas where heavier consequences are expected but the resolution of their prediction is not accurate, so that the problem is re-analysed at a smaller scale to improve prediction and refine preventive actions.

To establish a connection among analysis at different scales it is necessary to identify a measure (or metric) for hazard and damage that holds at all the scales considered. The use of the same metric makes it possible to compare not only the vulnerability but also the risk, combining damage models with hazard. This is an essential requisite to analyse the same problem at different scales.

However, different damage functions (or response models) can be equally used in the analysis at different scales, given that they are compatible in the sense that they use the same metrics.

Starting from the analysis at small scale, it can be observed that it generally involves few elements for which a lot of information are available, and this leads to the use of refined models providing accurate and reliable relationship between hazard and damage (damage functions). Generally, a refined model requires a strong computational effort, and the model definition may be very demanding. For example, in vulnerability analysis of historical construction subjected to mechanical actions, such as earthquakes or subsidence, the analysis involves Finite Element Model [5] of each building (*element*) and the geometrical characteristics of all the components (walls, roofs, girders, vaults,…) are required, as well as the mechanical properties of components (Figure 3). In this case, the extension of the analysis is limited to a small number of elements and analysis is frequently limited to a single element.

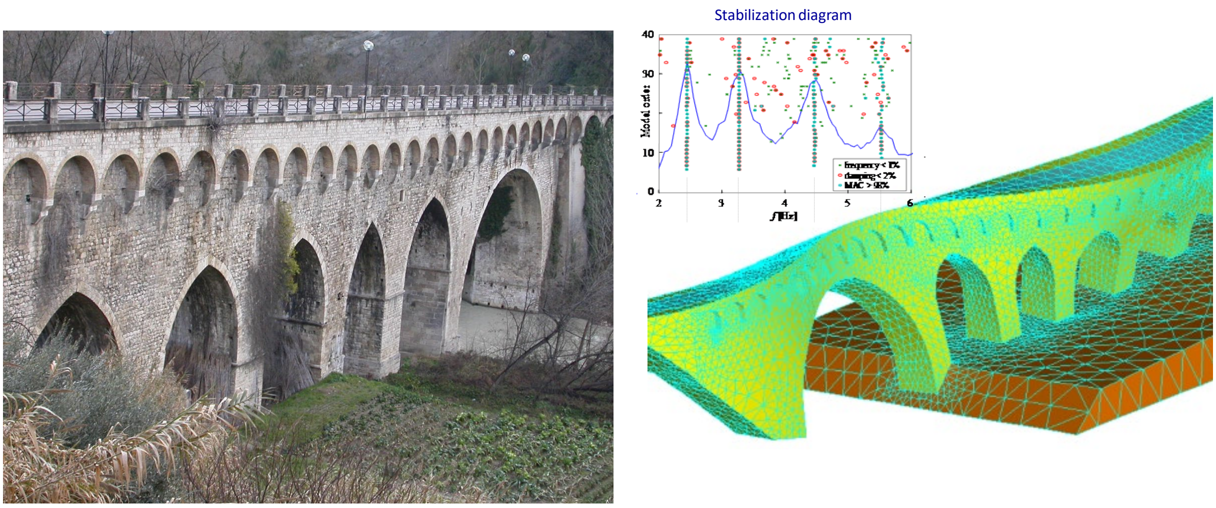

Figure 3: Finite Element Model of historical construction

Moving towards and analysing the problem at higher scale, granularity and models can be preserved and theoretically no problem is involved in the scale variation. However, this is only a hypothetical conclusion because, at least, two problems arise. On one hand, a larger number of elements are involved in the analysis and the computation effort con be unsustainable. On the other hand, information required to build up a refined model for each of the elements included in the map is not available. So that, a strategy is generally required to move from a small-scale analysis to a large-scale analysis, preserving the possibility to compare results. Technical literature does not provide a support to this problem because existing studies focused on specific scales of the problem, and metrics used at one scale are generally not compatible with metrics used in other scales.

Two strategies can be defined to approach the problem. The former one is based on the *model reduction*. In this case, the granularity of the problem is preserved but the response model varies and models requiring a reduced number of data are considered, to recover the opportunity of defining a model for all the elements included in the map. Obviously, also the computational effort is notably reduced. The damage function must be formally equal, in the sense that it relates the same hazard metric and damage metric used previously, and the reduced model must be “compatible” with this statement. It is expected that the level of accuracy of outcomes is reduced. This approach can be interpreted as a sort of classification, in the sense that elements that showed different responses in the small-scale analysis, now are described by a unique model and provides the same output. So, the whole set of elements is partitioned into a reduced number of subsets with different damage functions.

Taking up the previous example of historical buildings, reduced models are available, and they are based on a very small set of information, such as material typologies, number of storeys, construction typologies and relevant damage functions are expressed by analytical expressions depending on few parameters ([6], [7], [8], [9], [10])

The alternative approach is based on a *granularity reduction*. In this case, elements are grouped into subsets here too, but the joining is based on the location, while the response model remains the same. The map is subdivided into cells and the parameters necessary to define the response models are obtained averaging parameters of cell components (or choosing the parameters of the most representative elements). Results suffer of this averaging and generally cells are defined by grouping elements with similar properties. Given that the model is not varied, the related damage function provides results compatible with the starting scale.

Considering again the example of historical construction, a common strategy for analysis at large-scale consists in defining cells for which census data are available, so that risk/vulnerability information can be linked to information regarding people living in that area (distribution of age, gender, occupation, and so on) ([11], [12]).

3. Physical-Chemical damage at material level

(G. Roselli, M. Materazzi, M. Sciortino, L. Giordano)

3.1. Environment, Pollution and Effects

The damage to architectural heritage from air pollutions mainly derive from the gases that increase the corrosivity of the atmosphere and black particles that dirty light-coloured surfaces.

The main mechanism occurs when acid chemicals released from industrial factory and other sources form are incorporated into rain, snow, fog, or mist. In the ‘‘acid rain’’, the ‘‘acid’’ arises from oxides of sulphur and nitrogen, largely products of domestic and industrial fossil fuel burning. The burning produce two strong acids: sulphur dioxide (SO_2) and nitrogen oxides (NOx), which falling with the rain that damage both heritage materials. In dry areas, the acid chemicals may become incorporated into dust or smoke, which can deposit on buildings and cause corrosion when later wetted ([13], [14]).

One further gas, ozone (O_3), has also been shown to be important. Indeed, it is the major component of photochemical smog and is a product of reactions among the chemicals produced by burning coal, gasoline and other fuels as well as those found in solvents, paints, hairsprays, etc. [15].

Particulate matter is much more complicated because it is a mixture rather than a single substance that includes dust, soot and other tiny bits of solid materials produced by many sources, including burning of fossil fuels. Particulate pollution can cause increased corrosion by involvement in several chemical reactions and, often more importantly, it is the source of the black matter that makes buildings dirty.

Weather factors mostly act on monuments in a synergistic way. The simultaneous action of temperature and water in repeated freezing/thawing cycles is a typical example of a situation, which is very dangerous for wet porous, brittle and quasi-brittle materials. The interaction of temperature and moisture causes repeated and uneven volumetric changes and results in material deterioration and propagation of defects such as cracks. In combination with abrasive particles, the wind can cause remarkable surface erosion (e.g., on monuments in sandy deserts). However, there are numerous other examples: moisture and deposition mechanisms, wind plus water plus pollutants forming weak acids and penetrating materials [16]. In recent years it has become clear that there may be one more climatic parameter that must be considered, that is the long-term fluctuations in climate including the long-term trends which are generally grouped together as the ‘‘greenhouse effect’’. A method of examining responses of buildings and materials to future climates is to review information on the sensitivity of materials to the present climate. However, this shows that there is a substantial lack of understanding and information. Some of the problems stem from the ever-present problem of linking accelerated laboratory testing to performance under atmospheric conditions.

Knowledge of basic damaging mechanisms of historic materials is indispensable for their appropriate and effective protection and safeguarding (Figure 4) [17].

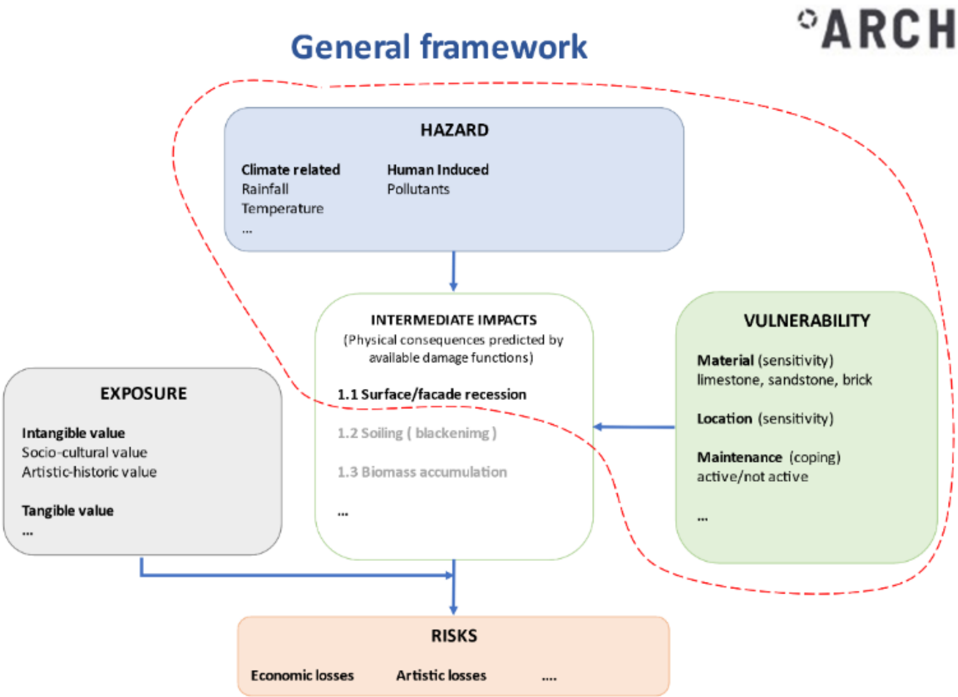

Figure 4: General framework of stone degradation and climatic-environmental data correlation

3.2. Physical-chemical mechanisms producing material degradation

We have many different types of monuments, made of many different materials, ranging in age over centuries and located in radically different environments. Air pollution is only one of the risks that threaten this heritage and may frequently not be the most pressing.

Physical damage regard mechanical deterioration of the material mainly due to the action of physical external action (from loads, movements, impacts, human actions, etc.) ([18], [19]) or internal forces, (e.g., generated by forced deformations at uneven temperature and moisture changes). The time factor may be important for some materials, e.g., long-term overloading of timber. Further, erosion problems decreasing cross-sectional characteristics belong to this group. Physical damage typically results in a mechanical breakdown.

In the case of chemical and biological damage, material is chemically attacked by reactive compounds present in the surrounding environment or produced by biological agents. In the latter case materials is a nutritional source for biological organisms that can, for example, decompose cellulose in organic materials. Chemical damage can be initiated or accelerated by physical factors, e.g., temperature or light (or another form of radiation), usually termed thermal damage (which is well known for timber and marble) and photochemical damage.

A great deal of the research was undertaken within a series of projects sponsored by the UNECE and the European Commission and others. The International Co-operative Programme (ICP) on effects on materials including historic and cultural monuments is one of several effect oriented ICPs within the United Nations Economic Commission for Europe (UNECE) and the Convention on Long-range Transboundary Air Pollution (CLRTAP). The main research projects on the topic are:

“CULT-STRAT” Project: Assessment of Air Pollution Effects on Cultural Heritage – Management Strategies 2004–2007. Contract number: SSPI-CT- 2004-501609.

“MULTI-ASSESS” Project: Model for Multi-pollutant Impact and Assessment of Threshold Levels for Cultural Heritage. Contract EVK4-CT-2001-00044 MULTI-ASSESS.

“REACH” Project: Rationalised Economic Appraisal of Cultural Heritage. EU: Environment and Climate Programme under Topic 2.2.4. PROJECT No: ENV4-CT98-0708 (REACH).

“PPASDC” Project: Particulate Pollution And Stone Damage Contract. EU Contract: EV5V CT94 0519 1/07/94 to 31/10/96.

“EAPMBSP” Project: Effects of Airborne Particulate Matter on Building Surfaces Project. CE Contract STEP-CT90-0097.

3.2.1. *Corrosion Processes*

Atmospheric corrosion is a complex field. Degradation processes can be physical, chemical, biological or a combination of there (Figure 5). The effect of pollution is, however, mainly associated with a chemical attack, which is the focus of the present treatment. Cultural heritage uses many materials, but this discussion is limited to limestone as indicator materials particularly sensitive to pollution. Corrosion attack is mostly a non-desirable effect that causes a loss of aesthetic value and mechanical strength. One of the reasons for the complexity of the degradation process is the many phases involved [20]. In almost all cases, water is a necessary requirement for corrosion to occur. The water is absorbed in the porous stone material or corrosion products.

Many parameters affect the degradation process. Usually, they act together in different combinations ([21], [22], [23]):

- The effect of SO_2 in combination with NO_2/O_3 and temperature/relative humidity
- The effect of HNO_3 in combination with temperature/relative humidity
- The effect of precipitation and acid rain
- The effect of particulate matter including NaCl in combination with temperature/relative humidity.

The water film provides the link to the atmosphere in which corrosive species can dissolve and attack directly or indirectly by modifying the properties of the water layer [24].

3.2.2. *Synergistic Effects*

The gas SO_2 is dissolved into the water layer as sulphite and with the help of an oxidiser (e.g., NO_2/O_3) it is then converted to sulphate. SO_2 is an acidifying pollutant and the acidification of the water layer in turn accelerates the corrosion process. In ambient atmospheres, however, the levels of SO_2 are usually small in comparison to the levels of the oxidation agents, which therefore determine the corrosion rate [25]. The dry deposition of SO_2 is influenced by both temperature and relative humidity since they are the main factors that determine the thickness of the moisture layer and therefore its ability to dissolve gases.

The effect of temperature is more complicated and for several materials a maximum is observed at about 10°C. At annual temperatures below 10°C corrosion increases with temperature, and this can be related to the increased time of wetness.

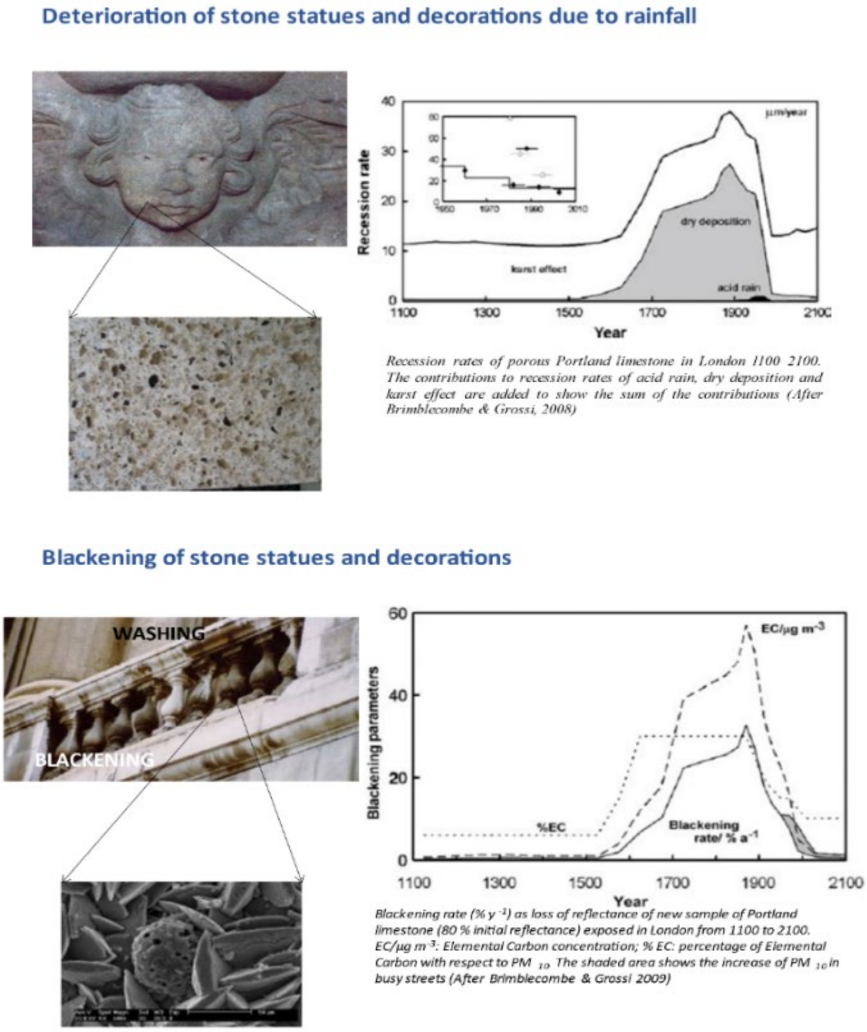

Figure 5: Deterioration due to rainfall and blackening

The role of nitric acid (HNO_3) on atmospheric corrosion has so far received little or no attention. However, the last decades of decreasing sulphur dioxide (SO_2) levels and unchanged HNO_3 levels in many industrialised countries have resulted in an increased interest in possible HNO_3 -induced atmospheric corrosion effects. Recent results indicate that the corrosion effect of HNO_3 by far exceeds that of SO_2, with a factor between 2 and 20 depending on the material. The pollution level of HNO_3 is typically around 1–2 mg m^3 (annual average) and is generally below the SO_2 concentration. However, due to the aggressiveness of this pollutant compared to SO_2 the effects of SO_2 and HNO_3 can be comparable in the present multi-pollutant situation. In the field, empirical data has proved HNO_3 to have an effect limestone. The Effect of Precipitation and Acid Rain ([14], [15]).

When rain starts to fall the amount of water on the surface becomes so large that water may dissolve aggressive substances such as chlorides and transport them away from the surface, i.e., rain has a washing effect that may decrease the attack. In addition, it also has a corrosive effect, by wetting the surface and dissolving protective layers depending on the pH of the precipitation (acid rain effect). These two effects act in opposite directions and the net result can be either positive or negative, depending on the type of environment and material.

The Effect of Particulate Matter in Combination with Temperature/Relative Humidity Particulate matter in general is hygroscopic and starts to attract substantial amounts of water at a relative humidity below 100% ([21], [26]).

Water plays a predominant role as a damage factor despite the fact that temperature is often attributed as the main variable of climate change, if we consider cultural heritage, the role not only of extreme events such as intense rainfall, floods and storms seems to prevail, but also of the less evident and more widespread ones that cause structural damage in the roofs and in the ornamental elements of the buildings, penetrating into the materials up to their complete decohesion. Water is involved in the changes in humidity responsible for the growth of microorganisms, in particular on stone materials and wood, and the formation of salts that degrade surfaces and accelerate corrosion. Finally, more intense precipitation can both increase the risk of floods and favour the penetration of water into materials and structures. On the other hand, increasingly dry summers could lead to a greater drying of the soils that play a protective role against archaeological finds not yet excavated. Furthermore, an increase in the phenomena of crystallization of salts can occur in the masonry structures, producing decohesion of the materials and superficial aesthetic damage [27].

3.2.3. *Dose-Response Functions*

Emissions of pollutants or other chemical, physical, and biological effects lead first to impacts. It is only if people consider these impacts as undesirable and put a value on them that they can be referred to as damages [28]. A dose of a pollutant depends on both the concentration and the time of exposure and in a strict sense the dose is defined as the quantity of a pollutant that is actually delivered to the receptor.

However, the term ''dose-response function'' is often used in a broader sense where the dose is replaced by the concentration, implicitly assuming that there is a direct relation between the concentration and deposition of the pollutant. For these types of functions, also the term exposure-response function is frequently used.

In the case of SO_2 dominating situation, the dose-response relations from ICP Materials were all expressed in the general form

$$K = f_{dry}\left(T, Rh, [SO_2], [O_3], ...\right) + f_{wet}\left(Rain, [H^+]\right) \tag{1}$$

were K is the corrosion attack, f_{dry} is the dry deposition term and f_{wet} is the wet deposition term. A list of all dose-response functions for exposure of unsheltered materials is shown in Table 1 [29].

In the case of multi-pollutant situation, the dose-response function consider the measurements of HNO_3 and particulate [EU 5FP MULTI-ASSESS project]; a list of all dose-response functions for exposure of unsheltered materials is shown in Table 2 ([15], [29], [30], [31]).

Table 1. Dose-response functions for unsheltered materials for the SO2-dominating situation [29]

Material	r^2	n
Structural metals		
Weathering steel (C<0.12%, Mn 0.3–0.8%, Si 0.25–0.7%, P 0.07–0.15%, S<0.04%, Cr 0.5–1.2%, Ni 0.3–0.6%, Cu 0.3–0.55%, Al<0.01%)		
$ML = 34[SO_2]^{0.13}\exp\{0.020Rh + f(T)\}t^{0.33}$	0.68	148
$f(T) = 0.059(T\text{-}10)$ when $T \leq 10°C$, otherwise $-0.036(T\text{-}10)$		
Zinc		
$ML = 1.4[SO_2]^{0.22}\exp\{0.018Rh + f(T)\}t^{0.85} + 0.029Rain[H^+]t$	0.84	98
$f(T) = 0.062(T\text{-}10)$ when $T \leq 10°C$, otherwise $-0.021(T\text{-}10)$		
Aluminium		
$ML = 0.0021[SO_2]^{0.23}Rh \cdot \exp\{f(T)\}t^{1.2} + 0.000023Rain[Cl^-]t$	0.74	106
$f(T) = 0.031(T\text{-}10)$ when $T \leq 10°C$, otherwise $-0.061(T\text{-}10)$		
Copper		
$ML = 0.0027[SO_2]^{0.32}[O_3]^{0.79}Rh \cdot \exp\{f(T)\}t^{0.78} + 0.050Rain[H^+]t^{0.89}$	0.73	95
$f(T) = 0.083(T\text{-}10)$ when $T \leq 10°C$, otherwise $-0.032(T\text{-}10)$		
Bronze (Cu $Sn_6Pb_7Zn_5$, ISO/R 1338)		
$ML = 0.026[SO_2]^{0.44}Rh \cdot \exp\{f(T)\}t^{0.86} + 0.029Rain[H^+]t^{0.76} + 0.00043Rain[Cl^-]t^{0.76}$	0.81	144
$f(T) = 0.060(T\text{-}11)$ when $T \leq 11°C$, otherwise $-0.067(T\text{-}11)$		
Stone materials		
Limestone (Portland)		
$R = 2.7[SO_2]^{0.48}\exp\{-0.018T\}t^{0.96} + 0.019Rain[H^+]t^{0.96}$	0.88	100
Sandstone (White Mansfield dolomitic sandstone)		
$R = 2.0[SO_2]^{0.52}\exp\{f(T)\}t^{0.91} + 0.028Rain[H^+]t^{0.91}$	0.86	101
$f(T) = 0$ when $T \leq 10°C$, otherwise $-0.013(T\text{-}10)$		
Paint coatings		
Coil coated galvanized steel with alkyd melamine		
$L = [5/(0.084[SO_2] + 0.015Rh + f(T) + 0.00082Rain)]^{1/0.43}$	0.73	138
$f(T) = 0.040(T\text{-}10)$ when $T \leq 10°C$, otherwise $-0.064(T\text{-}10)$		
Steel panels with alkyd		
$L = [5/(0.033[SO_2] + 0.013Rh + f(T) + 0.0013Rain)]^{1/0.41}$	0.68	139
$f(T) = 0.015(T\text{-}11)$ when $T \leq 11°C$, otherwise $-0.15(T\text{-}11)$		

where

ML = mass loss, g m^{-2}
R = surface recession, µm
t = exposure time, years
L = maintenance interval (life time), years
Rh = relative humidity, % – annual average
T = temperature, °C – annual average
$[SO_2]$ = concentration, µg m^{-3} – annual average
$[O_3]$ = concentration, µg m^{-3} – annual average
$Rain$ = amount of precipitation, m $year^{-1}$ – annual average
$[H^+]$ = concentration, mg l^{-1} – annual average
$[Cl^-]$ = concentration, mg l^{-1} – annual average

Table 2. Dose-response functions for unsheltered materials for the multi-pollutant situation ([15], [29], [30], [31])

Material
Carbon steel
$R = 6.5 + 0.178[SO_2]^{0.6}Rh_{60}e^{f(T)} + 0.166Rain[H^+] + 0.076PM_{10}$
$f(T) = 0.15(T\text{-}10)$ when $T<10°C$, $-0.054(T\text{-}10)$ otherwise
Zinc
$R = 0.49 + 0.066[SO_2]^{0.22}e^{0.018Rh+f(T)} + 0.0057Rain[H^+] + 0.192[HNO_3]$
$f(T) = 0.062(T\text{-}10)$ when $T<10°C$, $-0.021(T\text{-}10)$ otherwise
Cast Bronze
$R = 0.15 + 0.000985[SO_2]Rh_{60}e^{f(T)} + 0.00465Rain[H^+] + 0.00432PM_{10}$
$f(T) = 0.060(T\text{-}11)$ when $T<11°C$, $-0.067(T\text{-}11)$ otherwise
Portland limestone
$R = 4.0 + 0.0059[SO_2]RH_{60} + 0.054Rain[H^+] + 0.078[HNO_3]Rh_{60} + 0.0258PM_{10}$

where

Rh_{60} = Rh – 60 when Rh > 60, 0 otherwise

$[HNO_3]$ = concentration, μg m^{-3} – annual average

$PM10$ = concentration, μg m^{-3} – annual average

3.3. Essential data and suggestion for implementation

A dose of a pollutant depends on both the concentration and the time of exposure and in a strict sense the dose is defined as the quantity of a pollutant that is delivered to the receptor.

A dose-response function links the dose of pollution, measured in ambient concentration and/or deposition, to the rate of material corrosion (Figure 6, and Figure 7).

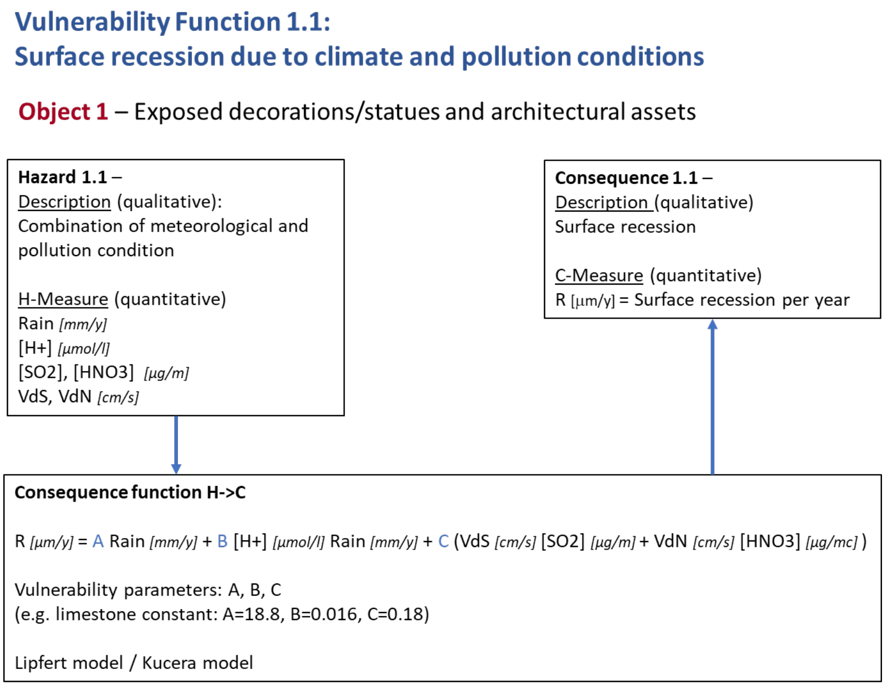

Figure 6: Vulnerability function: Surface recession due to climate and pollution conditions ([32], [33])

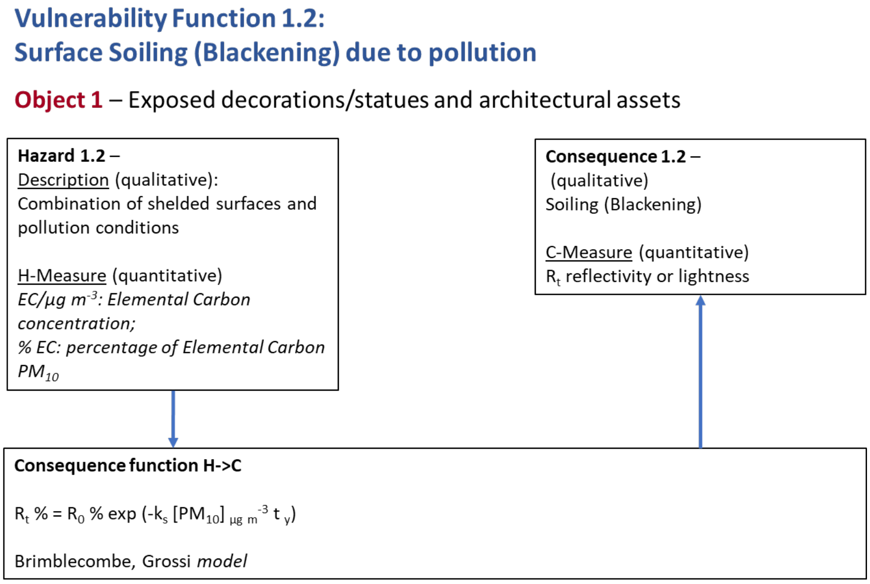

Figure 7: Vulnerability function: Surface soiling (Blackening) due to pollution

Dose-response functions are useful for mapping areas of increased risk of corrosion and maps are a powerful tool to illustrate the effects of pollutants on cultural heritage objects. The dose-response functions can also be used for calculation of corrosion costs and for assessing tolerable levels of pollution.

3.4. Example

Camerino, about 670 meters above sea level, is located in a hilly median depression enclosed by lateral mountainous areas, known as the "syncline of Camerino". The orography obstructs the hot-humid westerly winds, while in winter the easterly winds blow, which help to lower the temperature. The weather station of Camerino is one of the oldest in Italy, with records of daily maximum and minimum temperatures dating back to 1865. The oldest data come from the archive of the Experimental Geophysical Observatory of Macerata, while from 1957 onwards they are managed by the Civil Protection Agency of the Marche Region. Camerino has a mean annual temperature of 12.8°C calculated over the last 30-year standard reference period (1991-2020) and this value showed a significant increase compared to the previous 1961-1990 (11.9 °C) and 1931-1960 (12 °C) thirty years periods. Historically, the lowest minimum temperature ever recorded by the Camerino weather station is -13.4°C on 02/04/2020; the highest maximum temperature, on the other hand, was reached on 28/07/1983 with 38.6°C. The annual temperature range is quite high and approaches and values typical of the continental climate. The diurnal temperature variations are often higher than 10 °C in summer and less than 5 °C in winter, this is because the cloud cover and the humidity of the air reduce the thermal differences. The relative humidity for the period 1991-2020 is around 68%, while the average wind was 1.7 m/s.

Concerning rainfalls, the mean annual precipitation in the last standard reference period was 968 mm, higher than the 933 mm of the 1961-1990 period, but much lower than 1931-1960 when the average was 1066 mm.

Camerino, similarly to many other areas in the world, is undergoing climate extremes that are increasing both the number of continuous wet days and the number of continuous dry days. Moreover, some climate indices such as R95p, R99p, RX1day, RX5day and SDII are increasing with a significance greater than 95% [34].

In particular, R95p and R99p are indices expressing the total amount of precipitation over the year which exceeds the 95th and 99th percentiles, with respect to the standard reference period (1961-1990), RX1Day is the maximum monthly precipitation recorded in 1 day, the RX5day is the maximum monthly precipitation value in 5 days and SDII is the total annual precipitation compared to the number of rainy days in the year, (Figure 8).

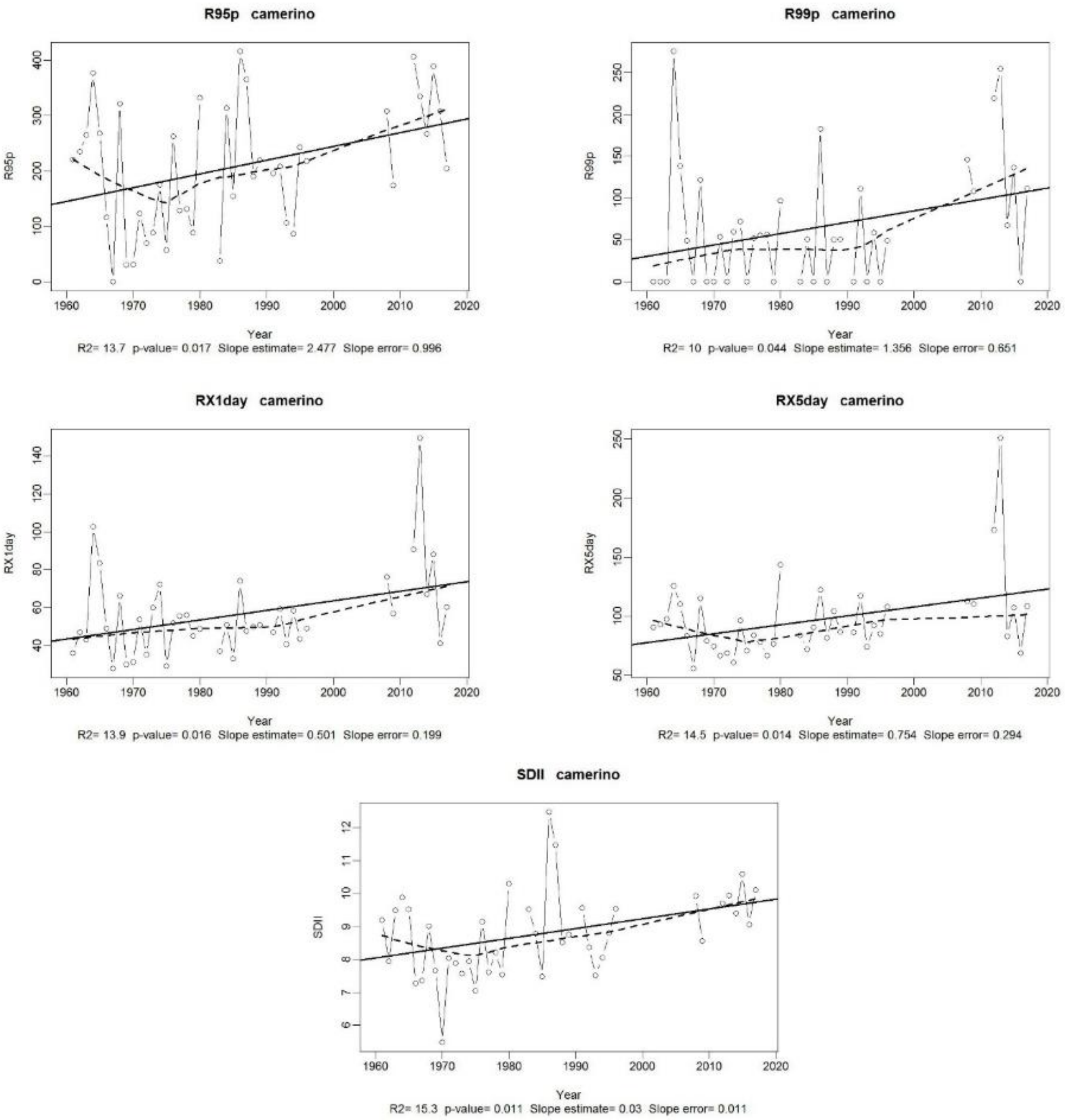

Figure 8: Climatic indices from the weather station of Camerino

Using historical data it is also possible to perform probabilistic calculations and provide rainfall height values for assigned duration of the event (in hours) and return times (in years) [34]; chosen a standard return time of 100 years (PR100) values of 53 mm (1 hour), 82.9 mm

(3 hours), 87.4 mm (6 hours), 114.7 mm (12 hours) and 173 mm (24 hours) are obtained (Figure 9).

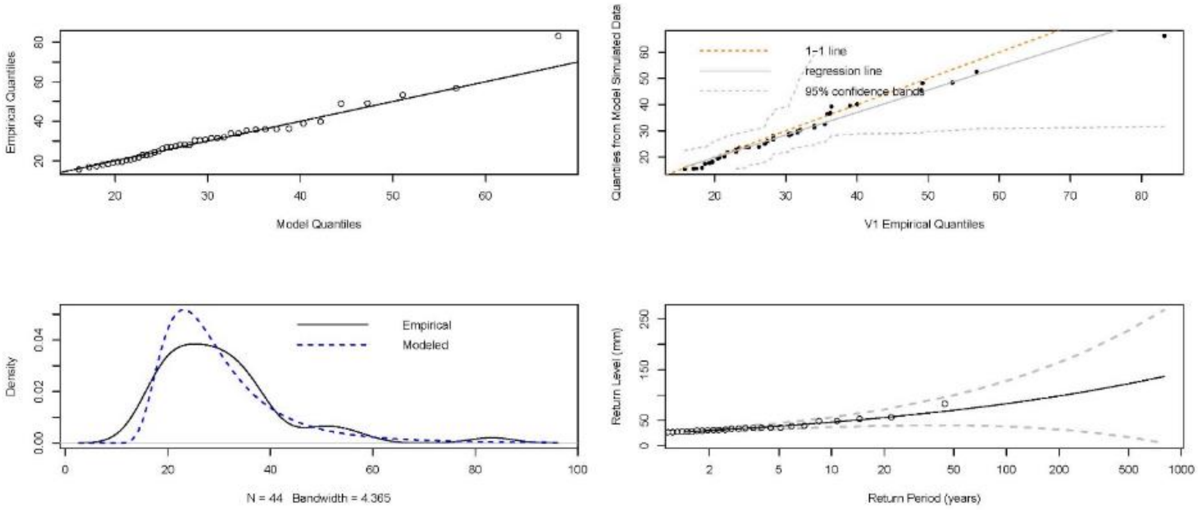

Figure 9: Camerino weather station: statistical analysis and rainfall height evaluation for a return time of 100 yrs and a duration of 3 hours

Concerning pollutant concentration, the data is evaluated adopting MINNI Modelling System (Italian National Integrated Model to support the International Negotiation on air pollution issues) developed by ENEA group. The MINNI Modelling System was developed by ENEA to simulate the behaviour of pollutants in the atmosphere and produce hourly maps of gas and particulate concentration, in particular of fine dust. The territorial resolution is 4 km^2 in Italy (the size of a small municipality) and 20 km^2 in Europe. Figure 10 shows the territorial resolution and the pollutant prevision; historic Centre of Camerino falls in the cells 181-129 and 182-129. Table 3 reported the data of pollutant concentration for 3 years (2003, 2005, 2007).

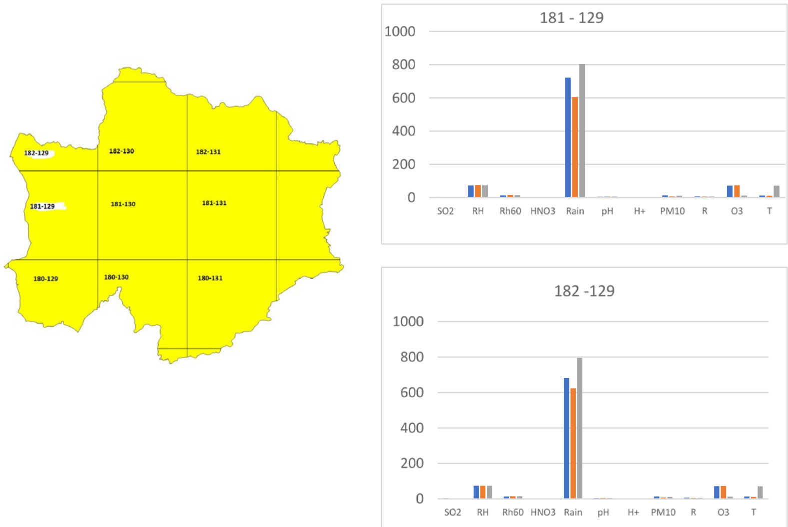

Figure 10: Map of environmental and air quality data collection areas 182-129, 181-129 of Camerino area (Provided by ENEA)

Table 3. Environmental and air quality data collection areas from 2003 to 2007. 182-129, 181-129 Camerino area (Provided by ENEA)

ET_Index	SO2	RH	Rh60	HNO3	Rain	pH	H+	PM10	R	O3	T	year
181--129	3,35843	73,4422	13,4422	1,30454	722,33	4,612403	0,024607	13,6722	6,89671	72,2692	12,643	2003
181--129	1,7552	75,3541	15,3541	0,823574	604,3778	5,396	0,00405	7,68658	5,425824	73,6969	11,052	2005
181--129	1,87498	74,5637	14,5637	0,957078	803,8237	5,396	0,00405	10,8113	5,65305	12,328	71,2457	2007

3.4.1. *Building level*

Sandstone, a useful and beautiful building stone, combining ease of processing with aesthetic value, has been widely used in the historic structures of Camerino. Research on stone degradation due to atmospheric agents has focused on granite and limestone, while sandstone remains a relatively neglected element as a building stone and object of study despite being an important architectural stone in many parts of the world.

However, this model is not always reliable for estimating the extent of the degradation suffered over time and this is due to the very nature of the arenaceous material. In fact, we applied the dose-response function to calculate the regression undergone by the columns of the portico of the Ducal Palace and the results obtained differed by several orders of magnitude from the real measured value.

A major problem in understanding sandstone weathering in the landscape lies in the inheritance of stress by exposed stone, which is extremely difficult to estimate, measure, or recreate artificially. Thus, the operation of weathering processes must be set within an historical context of changing conditions associated with environmental change or alterations to material properties. In other words, an increase in stress derived from external variables may induce a weathering route, such as surface exfoliation, that has not originated in the effects of previous weathering or decay, such as etching of grain surfaces. Nevertheless, existing material properties exert a profound influence on development of weathering and decay forms, and changes to these structural and compositional properties on a microscale are likely to play a significant role in stone response to processes of deterioration across a range of spatial scales.

Most of the monuments and artifacts built in Camerino were made with sandstone as it is easily found both for the very extensive and accessible deposits and for the short distance from the town.

Upon a superficial examination, the sandstone blocks of both the load-bearing structures and the decorative elements of the Ducal Palace have at times undergone, even in contiguous blocks, processes of decay and markedly differentiated alteration. Alongside the intact ashlars there are elements in which the detachment of the altered superficial outer layer occurred. Other blocks then have almost totally lost their crust and have a porous surface, with marked detachments and with evident superimposed "flakes' ' separated by totally decohesive layers. Sometimes the degradation process has acted profoundly by removing thicknesses greater than 5 cm easily observable on both the external and internal walls of the Palazzo Vecchio of the "Loggia Magna " which is part of the Palazzo Nuovo. In many cases there has been the partial or total disappearance of the friezes and decorations that adorned the colonnade and the portico of Piazza Cavour.

3.4.2. *Town level*

The surface recession represents the direct measure of the loss of material caused by the synergistic action of atmospheric pollutants and climatic factors characteristic of a given territory. For the estimation of the superficial recession, in the literature, different algorithms are available, obtained mainly in an experimental way. To estimate the loss of material of the cultural heritage present in the pilot site, the damage function defined by the European project MULTI-ASSESS (Model for multi-pollutant impact and assessment of threshold levels for cultural heritage) was used as part of the international program ICP Materials, (International Co-operative Program on Effects on Materials, including Historic and Cultural Monuments - Mapping of Effects on Cultural Heritage).

For the assessment of the level of vulnerability at urban scale, it is necessary to evaluate the distribution of the materials that constitute the facades of the buildings to locate the most vulnerable architectural buildings. For this, through a reconnaissance of the historic centre, can be possible to verify the distribution of materials constituted the facades.

Most of the artifacts were made with stone which is readily available in situ. The problem of the alteration and degradation of these lithotypes, which falls only partially within the cases of degradation of sandstone, has been recently addressed with a series of research that examine more specifically the native material [35].

A reconnaissance of the historic centre of Camerino, the distribution of the façade materials is reported in Figure 11. The main material that constitutes the facades is the sandstone, in variable percentages (Figure 12). The degree of deterioration is linked to these percentages and must be related to the exposure of the facade to the agents that accentuate the process of recession.

Starting from the data of pollutants and environmental conditions, it is possible to evaluate the recession of the most widespread material (sandstone) that constitute the historic centre of Camerino.

Recession function adopted to evaluate the surface recession of sandstone is

$$R=4+0.0059\cdot\left[SO_2\right]\cdot RH60 + 0.054\cdot Rain\left[H^+\right]+0.078\cdot\left[HNO_3\right]\cdot RH60+0.0258\cdot M10 \qquad (2)$$

where R is the surface recession in the unit of time (μm/year), $[SO_2]$ the concentration of SO_2 (μg/m3), RH60 the relative humidity measurement (when RH> 60, otherwise = 0). Rain is the rainfall (mm/year), [H+] is the pH, concentration of H+ in precipitation (mg/l), $[HNO_3]$ is the HNO_3 concentrations (μg/m^3) and PM10 is the concentration of atmospheric particulate matter (μg/m^3).

Table 4 report the sandstone recession in the interval 2003-2016 year adopting the Equation (3).

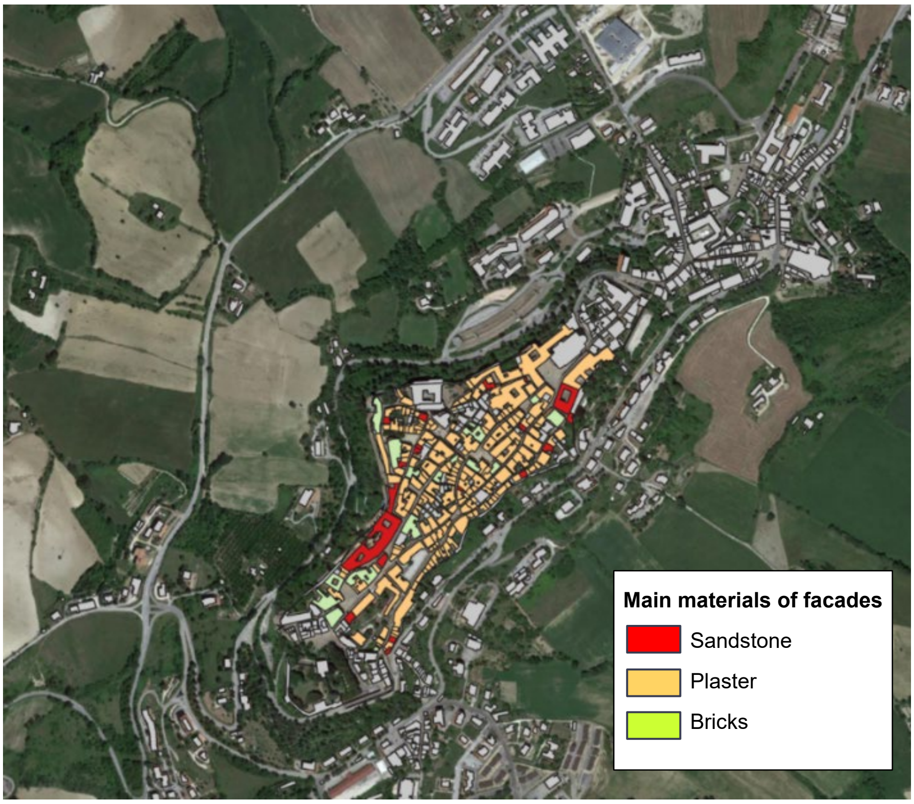

Figure 11: Main materials of facades

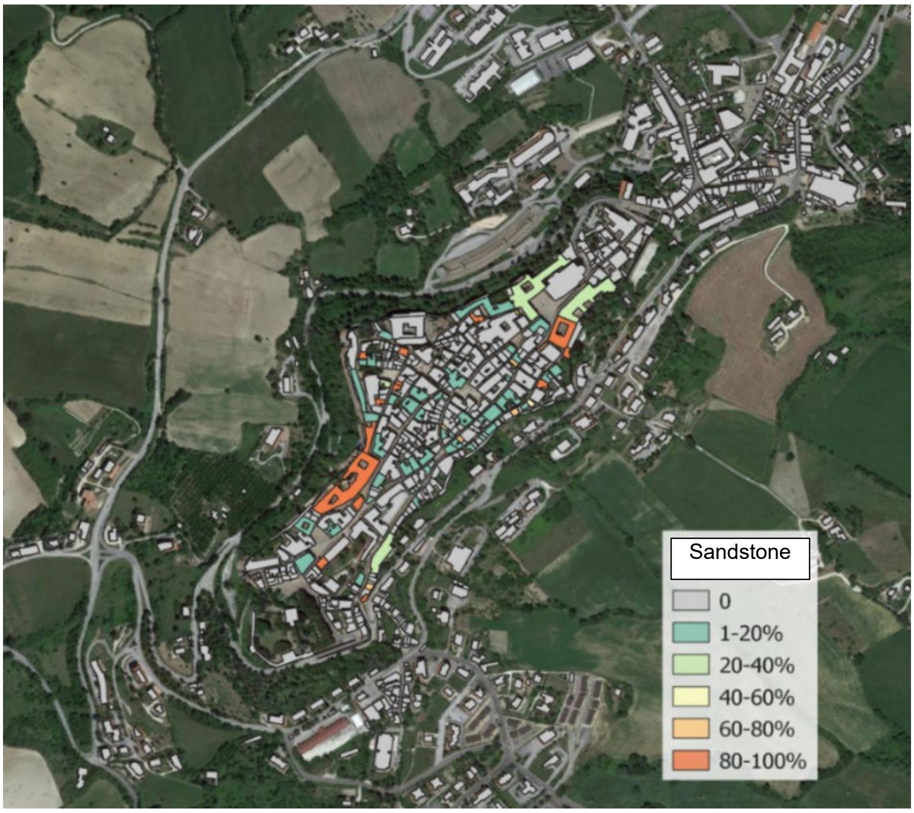

Figure 12: Percentage of sandstone in the facades

Table 4. Sandstone recession year 2003-2016

date	year	Temp °C	RH_{60} %	SO_2 μ/m³	HNO_3 μ/m³	PM_{10} μ/m³	H+(pro) μ/m³	Rain m/y	R µm/y
2003	1	16.87	5.994121	0.017671	1.1831	13.352	0.021	0.63082	4.89897
2004	2	16.27	10.75316	0.01721	0.946737	11.03758156	0.006261	0.926078	5.080247
2005	3	15.58	10.23023	0.016342	0.808473	9.683733568	0.003084	1.041866	4.896128
2006	4	16.40	10.59775	0.016853	0.710374	8.723163128	0.001866	0.701676	4.813394
2007	5	16.81	7.492692	0.015504	0.634282	7.97808681	0.001264	0.656271	4.577258
2008	6	16.54	9.804371	0.01532	0.57211	7.369315132	0.00092	0.832926	4.628572
2009	7	16.58	10.5466	0.015237	0.519545	6.854606012	0.000703	0.950873	4.605229
2010	8	15.72	13.06517	0.0147	0.47401	6.408744692	0.000556	1.04186	4.649566
2011	9	16.65	8.650132	0.016002	0.433846	6.015467136	0.000453	0.7112	4.448754
2012	10	16.92	6.653322	0.014765	0.397918	5.663668374	0.000377	0.882561	4.353224
2013	11	16.36	13.03361	0.014393	0.365418	5.345427684	0.000319	1.048468	4.510529
2014	12	16.85	15.36522	0.014071	0.335747	5.054896696	0.000274	1.016106	4.534095
2015	13	17.05	9.920781	0.014019	0.308452	4.787634095	0.000238	0.87996	4.36304
2016	14	16.84	11.95241	0.013881	0.283181	4.540187576	0.000209	0.957308	4.382133
2017	15	17.08	7.6839	0.012984	0.259655	4.309820379	0.000186	0.787472	4.267413
2018	16	17.11	15.28317	0.013126	0.237647	4.094326256	0.000166	0.927208	4.390122

4. Seismic vulnerability of historical constructions and towns

(M. Morici, A. Dall'Asta, E. Petrucci, C. Canuti, L. Barchetta)

4.1. Construction damage due to seismic actions

From the history of architecture emerges that earthquakes have always represented one of the main causes of damage and losses of cultural heritage, and post event damage observation can be a remarkable source of information on the recurrent damage patterns. The damages observed in various countries due to recent earthquakes (e.g. Umbria-Marche, Italy (1997-98); Açores, Portugal (1998); Molise, Italy (2002); Andravida, Greece (2008), Abruzzo, Italy (2009); Central Italy, (2016) etc..), as well as the results of both experimental and analytical research carried out in the last decades, shows that the recursive damages are related to the intrinsic vulnerability and relative mechanisms to resist to earthquakes. Indeed, damage to masonry buildings can be essentially interpreted on the basis of two fundamental collapse mechanisms: the "First Damage Mode" is produced by seismic actions perpendicular to the wall (out-of-plane) that cause the overturning of the whole wall panel or of a significant portion of it; the "Second Mode of Damage" is produced by seismic actions parallel to the wall (in-plane) and is usually marked by inclined cracks associated with shear forces that often result in an "X" pattern [36]. Figure 13 shows a typical mechanism of First and Second Mode of seismic damage.

Figure 13: Example of damage mechanisms: (a) First mode damage and (b) Second mode damage

Generally, masonry structures exhibit enhanced vulnerability to out-of-plane bending (low bending moment capacity). This pronounced vulnerability is negatively affected by all the conditions that limit the box action of buildings, as the poor quality of construction type of masonry and the building materials adopted.

Needless to say, previous non-repaired damages, lack of maintenance, decay of materials, etc… further aggravate the effects of a seismic event. The observations of masonry buildings when subjected to earthquakes have shown that the behaviour is strongly dependent on how the walls are interconnected and anchored and to floors and roofs. In old structure the unfavourable effect of insufficient anchorage between walls and between walls and floors was often observed. Irregular structural layout in plan, large openings, and lack of bearing walls in both directions often caused severe damage or even collapse. A good quality of the connections between floors and walls, between roof and walls and between perpendicular walls is also crucial to reach a good global seismic behaviour of the building. Good quality connections will drive the collapse of the construction to a configuration that requires a stronger seismic action, [40].

In historic centres, building has evolved in the time adding adjacent constructions or portions, without strong connections between the parts with the effects of high fragility of the structures towards the seismic actions. This aspect involved that the most recurrent failure mechanism is the overturning of the façade. However, if the building structural capacity has been improved by means the introduction of ties or ring beams, this simple overturning mechanism is prevented.

Other contributing factors that influence the earthquake resistant capacity are: the original configuration and craftsmanship of the masonry; the modifications made over time, such as buttresses and ties (which improve the general performance) and additional storeys (which tend to compromise the performance); the characteristics, quality, and condition of the masonry; the appropriate thickness of the bearing and non-bearing walls and discontinuities; the method and configuration of the connection of the floors and roof to the walls; and the materials and design of the floors and roofs themselves. The most important factors tend to differ with the building typology.

The presence of in-plane flexible diaphragms, typically timber floors and roofs as well as thin masonry vaults, is very common in the existing masonry buildings. Even though proper connections between walls and floors allow to prevent local first mode mechanisms, in masonry buildings with flexible floors the global seismic response is quite complex. In the case of the flexible diaphragms, the coupling effect by the horizontal structures is limited or null, and vertical structures (walls) tend to behave independently; in addition, the sealing effect against the out of plane mechanism is limited. However, an acceptable approach in practice could be to analyse separately the in-plane seismic response of each masonry wall as extracted from the global structure with its pertaining loads and inertial masses.

4.1.1. *Walls Damage mechanisms*

As detected by the post-earthquake damage surveys carried out after strong earthquakes events that stuck areas where cultural heritage buildings are common, the main vulnerability is associated to local failure modes, relate to “First Damage Mode”, mainly due to out of plane response of walls ([36], [37], [38], [39], [41], [42], [43], [44]).

Generally, the seismic response is governed by such mechanisms when connections between orthogonal walls and between walls and floors are particularly poor. This is often the case in existing stone masonry buildings without tie rods, with lack of interlocking at the connection of intersecting walls, presence of simply supported wooden floors and thrusting roofs. Only if connections are improved by proper devices (e.g. tie-rods), local mechanisms can be prevented and a global behaviour governed by the wall in-plane response can develop.

The structural behaviour of a very complex building can be analysed in meaningful structural portion called macro-element and related to the damage and collapse mechanism.

Simple overturning

The simple overturning of external walls could be considered as one the most frequent and brittle collapse mechanism. The mechanism involves a rigid rotation of a wall or of a portion of a wall around a horizontal hinge, (Figure 14). The out of plane actions due to the earthquake start the mechanism.

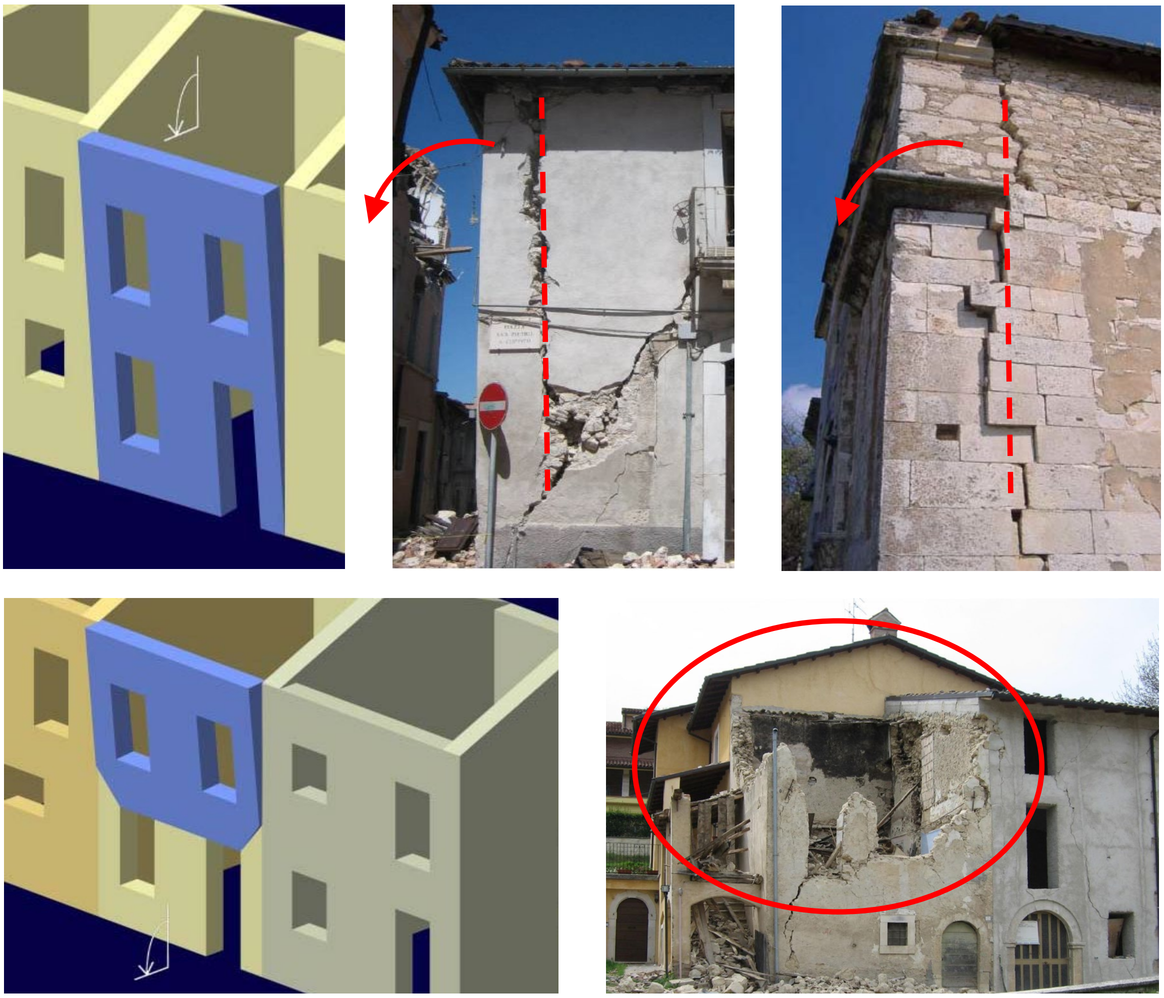

Figure 14: Example of Simple out of plane walls mechanism [45]

Vertical out-of-plane bending

A common situation in masonry buildings concerns a wall restrained at the extremity and free in the central area. This could happen in case of irregular layout of restraints or tie beams, (Figure 15).

The ties prevent the wall global overturning but other actions or the floor hammering, or the masonry quality could start the vertical instability and the wall bulging. The upper and the lower bonds in general are effective to prevent the global overturning of the wall.

In a damaged building, a relevant out of plumb or the wall bulging reveals the mechanism that could involve one or more floors.

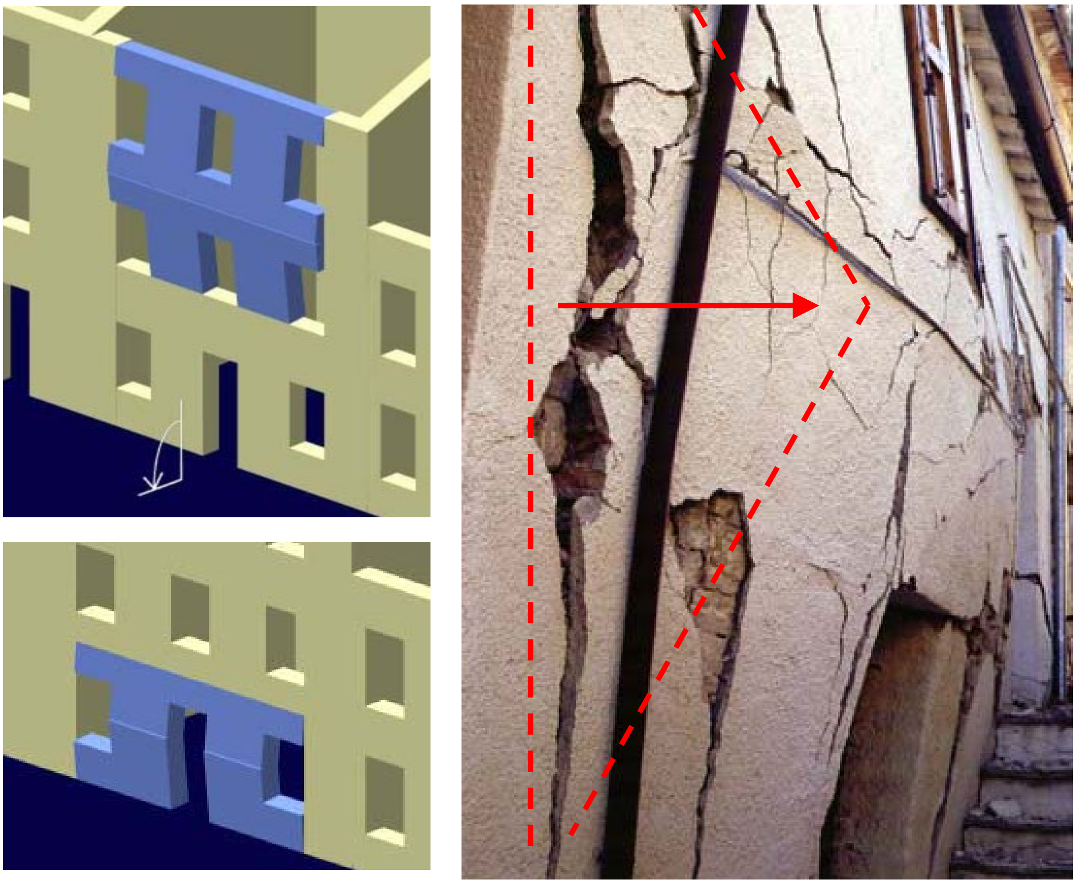

Figure 15: Separation of wall due to out-of-plane bending [45]

Horizontal out-of-plane bending - Arch mechanism

Restrained panels to orthogonal walls but not in the upper side could be damaged by bending in the horizontal plane. Floor or roof beams could thrust the wall but are restrained to the side walls connection. The general behaviour involves an arch mechanism within the wall section caused by the out of plane actions, (Figure 16). The condition of limit equilibrium is characterised by the developing of three hinges, one in the middle and the others close to the connection of the lateral walls.

The mechanism is typical of walls restrained by ties. The beam hammering or the roof thrust, and the low quality of the masonry could produce the whole mechanism or local damages.

Furthermore, the opening geometry and position could affect the behaviour and the extension of the damaged area.

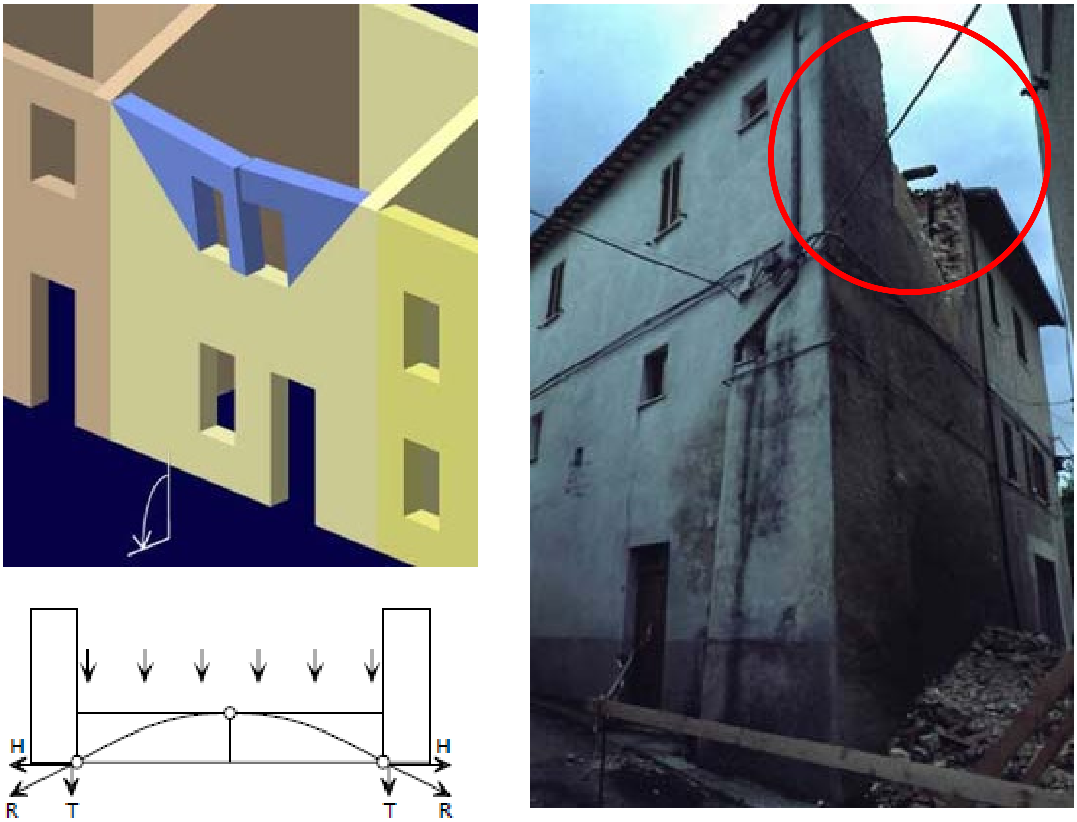

Figure 16: Arch mechanism [45]

Complex overturning mechanism

In most cases, the mechanisms are triggered by complex damages (Figure 17). In this case, the overturning of a wall involves also the orthogonal walls and on the corners, which could be damaged by in plane action. The mechanism is generated by the lack of constraints at the top of the masonry panel but the effective side connections with the orthogonal walls is present.

Many factors affect the damage mechanism, such as the masonry quality, the openings geometry e positions in the shear walls, the discontinuity localisation (e.g. chimney flues, plants, etc.) and connections between floor and orthogonal walls.

In the case of shear walls without openings the inclination of the diagonal crack increases with the masonry quality corners. The presence of openings close to the wall intersection affects the geometry and the shape of the damaged area. Furthermore, the damage mechanism is the frequent cause of the corner damages, particularly if coupled with roof thrust.

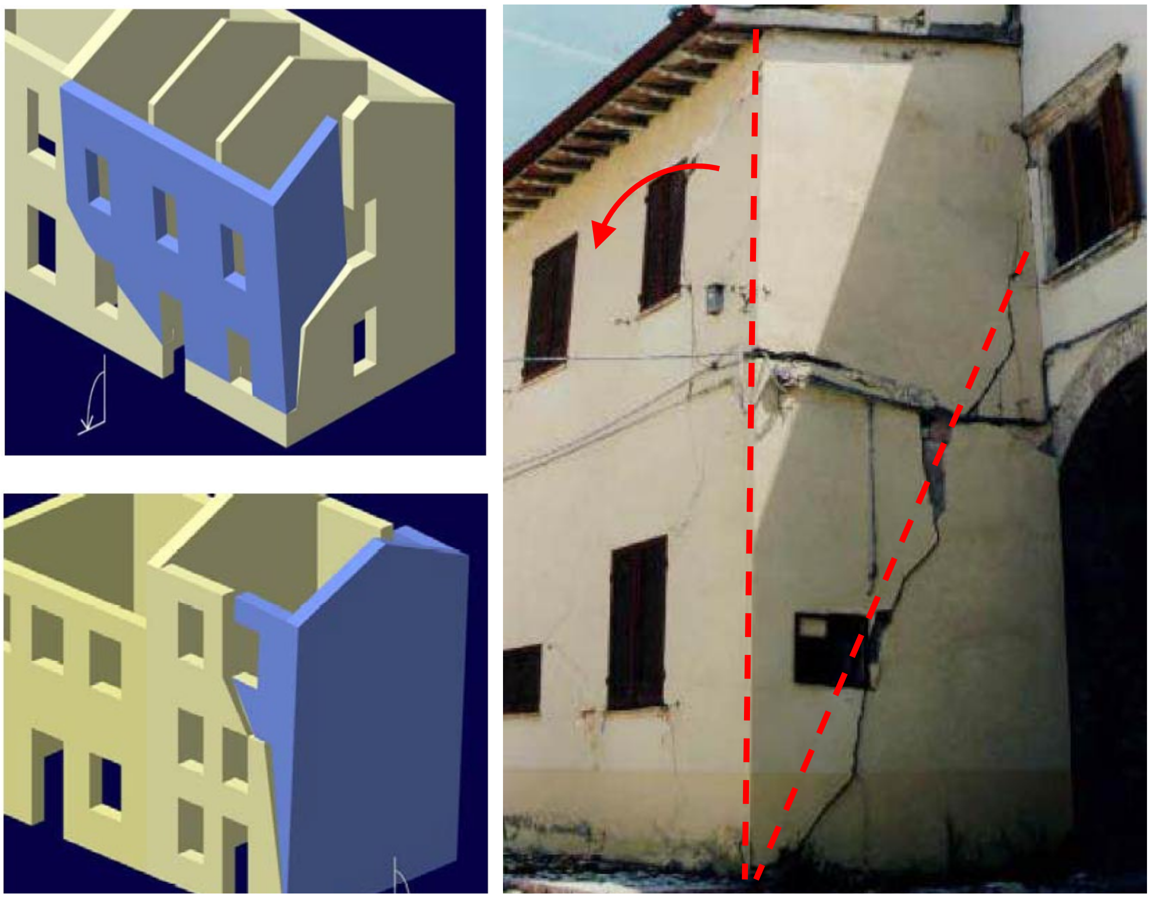

Figure 17: Overturning of the façade with damage of the orthogonal wall [45]

Roof damage

Roof damage could be revealed by a movement of the joints or of the ridge. Local damages caused by the movement of the tile coverings are frequently causes of the beams decay (Figure 18). In addition, thrusting elements could contribute to the local or global overturning of unrestrained walls (Figure 18).

Aggregate buildings

The generalized characteristic of the historical centres' layout is the structural continuity of the buildings [46]. In fact, excluding exceptional cases, frequently masonry buildings are structurally connected with the adjacent ones to form a block. The latter can be defined as a buildings system - also of remarkable dimensions - delimited by public and/or private un-built spaces. The buildings can evolve in curtains along a street, in rows. The reconstruction of the row evolution is a key point in the vulnerability evaluation because it can clarify the effectiveness of the restrains between the walls and locate discontinuity between masonry portions.

Damage often affects whole rows of contiguous buildings, with the damage concentrated at the base of the structures on the up-slope side of the buildings. This indicates that the rows of buildings lagged the ground motion as a unit, rather than pounding each other, which would have caused the most damage at the upper story points of collision. Instead, as the earthquake waves cause the buildings to sway, shear cracks opened on the ground floor walls.

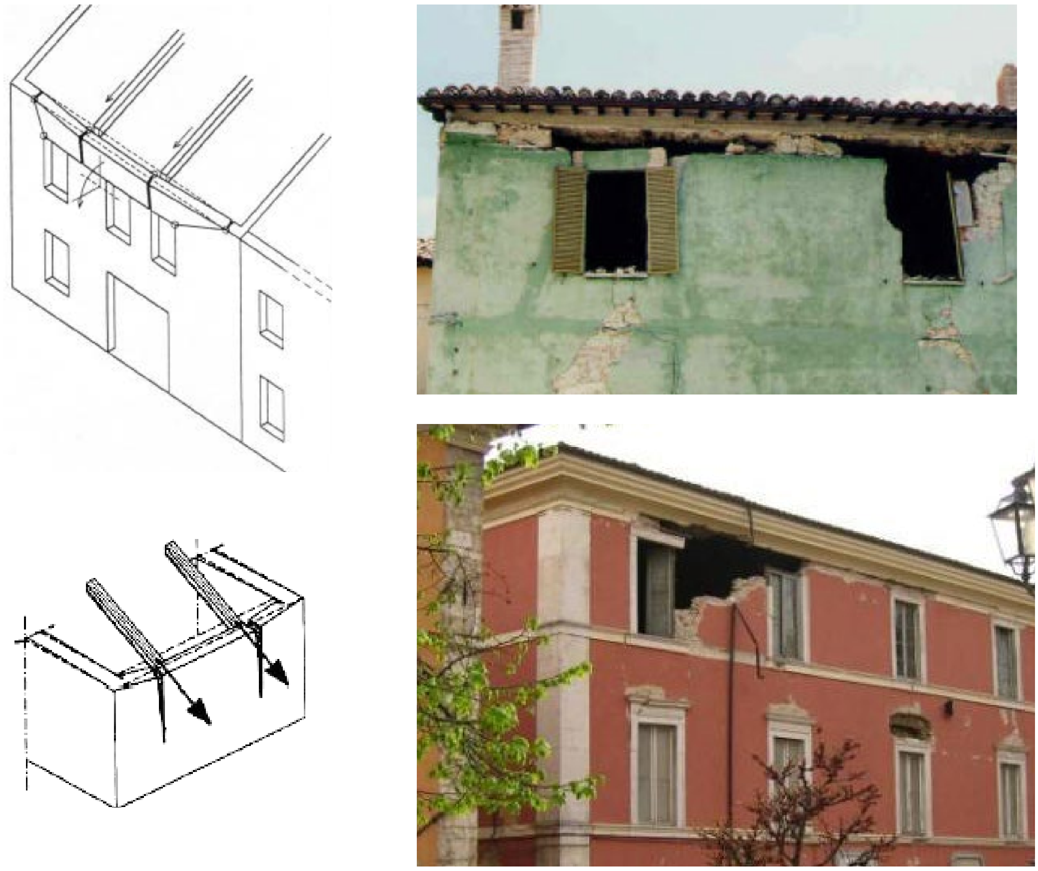

Figure 18: Hammering of the roof structures to the load bearing walls, [45]

4.2. Scientific background and damage functions

Earthquakes are known to be natural hazards that have affected tremendously historical constructions characterised by a low level of resistant capacity and hight seismic vulnerability. The heterogeneity of the Italian civil building stock and cultural heritage, typical for each region, in terms of both materials and structural configurations, represents an element of complexity for the assessment and mitigation of seismic risk ([48],[49],[50]). Furthermore, the classification of regional and local, i.e., more specific, building types is a complex process that can be successfully addressed only by a systematically elaborated and well-organized methodology [47].

The vulnerability assessment of the buildings is a process that can be implemented at different levels, from the single building up to the territorial scale. The selection of a proper method to evaluate the vulnerability is a crucial issue that depends on the accuracy of the expected results, the scale of the assessments (single building or urban area) and the computational effort related to the scale to which the assessment is addressed.

Regarding the territorial scale, in the evaluation of seismic vulnerability of the buildings, one of the main application problems is the limited information on the characteristic buildings, with respect to the required level of investigation. The information concerning building types generally used in the risk studies can be obtained by census databases (e.g., ISTAT in Italy) [48], that provide only very basic data to carry out vulnerability assessments at urban levels; indeed, ISTAT database in Italy report number of the floors, age of construction and type and structural materials. Therefore, the uncertainty of the input data does not allow to obtain consistent prediction models, which are necessary for the calculation of prevention and risk reduction strategies.

Regarding of the single building, more sophisticated analyses could be carried out and the obtained results could be extended to the whole urban area; in this case is necessary thorough knowledge of geometry, architecture, material, and structure of the building with the aim to define a refined response model for the structure. Instead, when limited information are available or the vulnerability assessment is performed to a territorial scale, simplified procedures are commonly considered to predict damage scenarios. In both cases, the level of vulnerability of a structure can be evaluated using seismic vulnerability functions and/or fragility functions.

The methodologies for assessing the seismic vulnerability of buildings use different approaches (empirical, analytical, hybrid); they are based on the purposes of the analysis and the various levels of detail of the information available on the morphological-structural features of the buildings. Empirical methods refer to the observed damage and express the seismic vulnerability of building types through: (i) Damage Probability Matrices (DPM) ([49], [50], [51]); (ii) analytical methods, which perform numerical analyses applied to a mechanical model of a building (capacity spectrum and collapse mechanism-based methods) ([52], [53]); (iii) hybrid procedures, which combine aspects of both previous methods based on the expert judgment and on simulated analytical damage statistics for the definition of vulnerability and fragility functions [54].

Seismic vulnerability functions represent the relationship between seismic shaking intensity and damage level, cost of repair for a particular asset (building) or asset class (category of buildings). On the other hand, seismic fragility functions represent the relation between shaking intensity and the probability of reaching or exceeding different limit states (such as physical damage or injury levels) given a level of ground shaking ([55], [56]). In Figure 19a a classical shape of the vulnerability function is reported while typical fragility functions are reported in Figure 19b.

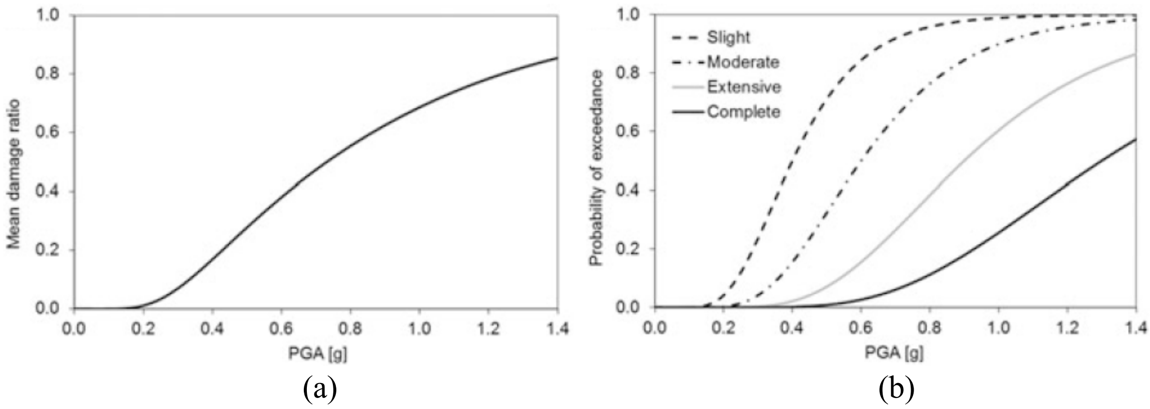

Figure 19: Examples of (a) vulnerability function and (b) fragility function ([55], [56])

Generally, vulnerability function can be derived from fragility functions using consequence functions that describe the probability of loss conditioned to damage state. Fragility curves are one of the key elements of seismic risk assessment that relate the seismic intensity to the probability of exceeding a level of damage for the elements at risk.

The evaluation of the seismic risk is strictly connected with the assessment of direct losses such as the repairing damage cost of a structure, injuries and casualties and indirect losses associated with the loss of income due to business disruption. Generally, these forms of losses (damage, death and downtime) are known as the '3D's' [57] and the analysis of the seismic loss is important for the decision-making process.

Analytical loss estimation can be determined by following a direct method, where the annual rate of exceedance of a loss value is determined by considering all the uncertainties in a unitary way and by assuming probabilistic models for all of them. As an alternative approach, the problem can be separated in blocks, as proposed in the PEER frameworks ([58], [59]), by exploiting some advantages coming from the conditional evaluation of rare events. The latter approach the annual rate of exceedance of losses can be evaluated by the equation:

$$\lambda_C(c) = \iint G_C(c \mid d) f_D(d \mid i) dd \left|\lambda_I^{'}(i)\right| di \tag{3}$$

were, "loss" is referring to the random variable C providing the cost required to repair/replace the facilities after an earthquake, the random variable D describes the building damage (fragility or vulnerability functions) and I is a random variable measuring the ground motion intensity. Notation $G_X(x)$ indicates the complementary distribution function of the argument x, and $f_X(x) = -G_X^{'}(x)$ denotes the related probability density function and apex denotes derivative.

Regarding the damages, fragility curves describe the probability of exceedance of a given damage level as a function of the intensity measure of the seismic ground motion. Generally, the damage state is described by a discrete variable $d_k \quad k = 0,1,..,N_D$

$N_D + 1$ of ordered possible damage states. By denoting by D the random variable that describes the church damage, the fragility curve $G_D(d_k \mid i)$ ($k = 1,..,N_D$) describes the probability that, for a seismic intensity i, the damage state is equal or higher than d_k. Usually, the fragility curves are efficiently approximated by the two-parameter function [57]:

$$G_D\left(d_k \mid i\right) = \Phi\left(\frac{\ln\left(i\right) - \theta_k}{\beta_k}\right) \tag{4}$$

where Φ is the cumulative normal distribution function, i is the intensity measure generally expressed in Peak Ground Acceleration (PGA) and θ_k and β_k are the two-parameters associated to the response of the structure. The most common way to define earthquake consequences is a classification based on qualitative approach (0 = no damage; 1 = slight/negligible; 2 = moderate; 3 = heavy; 4 = very heavy, 5 = destruction) according to EMS98 scale [60], which requires a description of each damage state.

Starting from the definition of discrete fragility functions is possible to derive the vulnerability curve in terms of damage index or mean damage $\mu_D\left(i\right)$ normalised in the interval $\left[0,1\right]$ by mean

$$\mu_D\left(i\right) = \frac{\sum_1^k G_D\left(d_k \mid i\right) d_k}{\sum_1^k k} \tag{5}$$

The capacity of the fragility or vulnerability curves to predict the damage probability distribution depends on the level of details of the collected data that could best simulate the building behaviours in numerical model generation. This shows the importance of defining damage levels for seismic hazard by considering the variability in building types through probabilistic distributions of the damage levels.

In this work, the macro seismic method developed by [61] that propose a semi-empirical expressions for the evaluation of the building's mean damage grade as a function of its vulnerability and the macro-seismic intensity IMS_{98}, with $0 \le \mathrm{IMS}_{98} \le 12$ [60], is considered. The representative range of the mean damage grade is $\overline{\mu}_D\left(i\right) \in \left[0,5\right]$ following the EMS-98 approach.

The correlation between the seismic input and the expected damage, as a function of the assessed vulnerability, is expressed in terms of vulnerability curves described by a closed analytical function [61]:

$$\overline{\mu}_D\left(i\right) = 2.5 \cdot \left[1 + \tanh\left(\frac{i_{MCS} + 6.25V - 13.1}{Q}\right)\right] \tag{6}$$

This is a two parameters function, namely vulnerability V and ductility index Q, that represents the rate of increase in damage with intensity and controls the slope of the curve. Parameters V and Q are defined based on the typological categories of buildings (e.g. churches, towers, palaces or others) and they were introduced in [61]. For unreinforced masonry buildings Q assume value of 2.3. Starting from Equation (6) is possible to define the damage index $\mu_D(i) \in [0,1]$, divide the damage $\overline{\mu}_D / 5$.

In the framework of Work Package [62], a classification system, finalized to vulnerability models, and an occupational classification system were proposed for ordinary buildings. On the one hand, a typological classification system was introduced (referred to as the Building Typology Matrix (BTM)) to group together structures that would be expected to behave similarly during a seismic event. In fact, for each building type is associated a series of vulnerability indices obtained by proper survey (Table 5): V is the most probable value for the vulnerability index, V^+ and V^- bounds of the plausible range of the vulnerability index V (usually obtained as 0.5-cut of the membership function) and V^{++} and V^{--} upper and lower bounds of the possible values of the vulnerability index V.

If additional information is available, it is possible to improve the vulnerability characterization for the generic building adopting

$$\overline{V} = V + \Delta V \tag{7}$$

with $\overline{V}$ final vulnerability index, ΔV behaviour modifier score, accounting for the effect of relevant vulnerability factors (Table 6).

Table 5. Vulnerability index values for building typologies, where the mean and the value of probable and less probable vulnerability index are reported [61]

Typologies		Building type	V^{--}	V^{-}	V	V^{+}	V^{++}
Masonry	M1	Rubble stone	0.62	0.81	0.873	0.98	1.02
	M2	Adobe (earth bricks)	0.62	0.687	0.84	0.98	1.02
	M3	Simple stone	0.46	0.65	0.74	0.83	1.02
	M4	Massive stone	0.3	0.49	0.616	0.793	0.86
	M5	U Masonry (old bricks)	0.46	0.65	0.74	0.83	1.02
	M6	U Masonry—r.c. floors	0.3	0.49	0.616	0.79	0.86
	M7	Reinforced /confined masonry	0.14	0.33	0.451	0.633	0.7
Reinforced Concrete	RC1	Frame in r.c. (without E.R.D)	0.3	0.49	0.644	0.8	1.02
		Frame in r.c. (moderate E.R.D.)	0.14	0.33	0.484	0.64	0.86
		Frame in r.c. (high E.R.D.)	−0.02	0.17	0.324	0.48	0.7
	RC2	Shear walls (without E.R.D)	0.3	0.367	0.544	0.67	0.86
		Shear walls (moderate E.R.D.)	0.14	0.21	0.384	0.51	0.7
		Shear walls (high E.R.D.)	−0.02	0.047	0.224	0.35	0.54

Table 6. Vulnerability modifiers [62]

Vulnerability modifiers	Masonry M	ΔV	Reinforced Concrete RC	ΔV
State of preservation	Good state	-0.04	Good state	+0.0
	Bad state	+0.04	Bad state	+0.04
Ns	LO (1, 2)	-0.08	LO (1, 2, 3)	-0.02
	ME (3, 4, 5)	+0.0	ME (4, 5, 6, 7)	+0.0
	HI (≥6)	+0.08	HI (≥8)	+0.0
Plan irregularity	yes	+0.04	yes	+0.04
Elevation irregularity	yes	+0.04	yes	+0.04
Retrofit intervention	yes	-0.08		
	no	+0.08		
Horizontal structure	steel slabs	-0.06		
	wood slabs	-0.02		
	vaults	+0.08		

The probabilistic assessment, in terms of both damage distributions and fragility curves for the mean damage value $\overline{\mu}_D$ evaluated according to Equation (7), can be obtained assuming a binomial distribution. Therefore, the probability of having each damage grade, d_k for a certain mean damage $\overline{\mu}_D$, is evaluated according to the Probability Mass Function (PMF) of the binomial distribution [49]

$$G_D\left(d_k \mid i\right) = \frac{5!}{k!(5-k)!}\left(\frac{\overline{\mu}_D}{5}\right)^k\left(1-\frac{\overline{\mu}_D}{5}\right)^{1-k} \tag{8}$$

Being more versatile than the binomial model, the beta distribution better approximates empirical damage distributions, as also demonstrated by other literature studies (e.g. [61], [63]). Despite its limited flexibility, the advantage of the binomial model is, however, the fact that damage repartition in the different damage states can be described through a unique parameter, representing the mean damage of the discrete distribution. However it is also possible to consider a damage variable d continuous in the interval [0,1], as in the approach proposed by [65] for the churches.

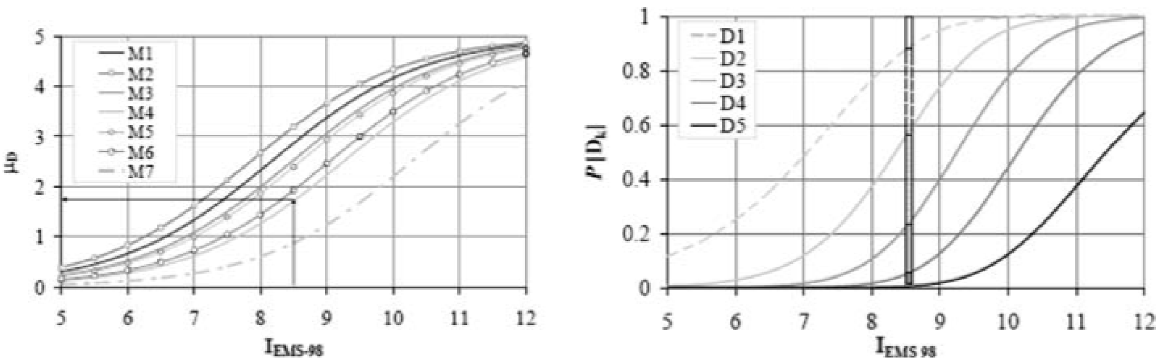

Figure 20: Example of the use of the macroseismic method: (a) vulnerability curves for different masonry building typologies; (b) fragility curves for a building typology as a function of Lagomarsino and Giovinazzi [61]

If a proper correlation law between macro seismic intensity MCS and PGA is assumed, the fragility functions may be converted in terms of PGA. To this aim, many correlations may be found in literature, which have been calibrated in different areas and are usually in the form

$$i_{MCS} = a_1 + a_2 \log\left(i_{PGA}\right) \tag{9}$$

were a_1 and a_2 are the parameters defined in ([68], [69]).

4.3. Essential data and suggestion for implementation

Regarding the analysis at small scale or single building, it is necessary to know more information regarding the construction to define an accurate vulnerability curves or fragility functions. Generally, at level of single building, is preferable to implement mechanical model of the building that provide accurate and reliable relationship between hazard and damage (damage functions). Thus, at building scale, numerical models need to be developed and a compromise must be made between the accuracy of the representation of the nonlinear behaviour and the robustness and cost-efficiency of the model. Generally, for the case of buildings, two used methods to model the nonlinear structural behaviour are plastic hinge modelling (i.e. concentrated inelasticity) and fibre element modelling (i.e. distributed plasticity).

Furthermore, “direct” assessment methods can be used that produce fragility curves as a function of the types of intensity measurement (eg. PGA, PGV, Sa(T), etc.) and “indirect” methods which estimate the damage probability with respect to structural response parameters (e.g. spectral displacement at the inelastic period).

Moving towards a higher scale (urban scale/territorial scale), a larger number of buildings are involved in the analysis and so the vulnerability assessment at territorial scale requires to group the buildings that have a similar seismic behaviour to evaluate the damage and losses of the built environment due to a given hazard assessment. Thus, the vulnerability assessment at territorial scale requires, first, to group the buildings of the exposure, that have a similar seismic behaviour, to evaluate the damage and losses of the built environment due to a given hazard assessment. To this aim, a proper taxonomy can be used to classify the buildings and then select the classes which the computation of fragility or vulnerability functions must be addressed to.

For urban-scale seismic vulnerability analysis, one of the main application problems is the limited information on residential buildings, with respect to the required level of investigation. The basic information concerning building types generally can be find in the census databases (e.g., ISTAT in Italy), that provide only very basic data to carry out vulnerability assessments for urban areas, such as number of buildings and floors, age of construction and type and structural materials. Alternatively

The procedure involves the construction of regional inventories, more specific with respect to census databases, carried out by the CARTIS approach [70] in the framework of the Reluis 2015–2018 project. The first level CARTIS form (issued on 2014), based on an interview protocol, recognizes the common residential types within sub-municipal areas (districts). For each building type, relevant parameters are collected, such as number of floors, construction period, use, shape and surface, type of aggregation, vertical and horizontal structural configuration, type of foundations, and conservation state. The form presents distinct sections addressed to the survey of vulnerability aspects of both masonry and reinforced concrete buildings. The second level CARTIS form (issued on 2016), within the same framework, permits to gather information relevant to the seismic response of specific buildings for more in-depth investigations (vulnerability studies) ([71], [72]).

Following important seismic events in Italy, the evaluation of the usability of a damaged buildings is carried out through a compilation of AeDES forms by specialized technicians. Data collected in the AeDES form have been used also to develop fragility functions for ordinary masonry buildings [64] and for Reinforced Concrete buildings [65] with similar structural behaviour, classifying the fragility curves for classes of buildings (Par. 4.2 - Table 5 and Table 6). These results have been used to carry out the National Italian risk platform, to evaluate seismic risk at territorial level for specific consequences such as collapses, or number of evacuated people [66]. Many works have been used this form to provide empirical vulnerability functions. In particular, the role of several vulnerability factors has been highlighted, to get the empirical damage and vulnerability distribution [73]. To this aim, a Web-Gis platform named Da.D.O. (Observed Damage Database) has been developed, to store and share information from past-earthquakes surveys in a comprehensive way, inserting data from AEDES form [67].

Regarding the quality of the masonry the classification procedure adopted consists in the assignment of a Masonry Quality Index value (MQI), calculated in accordance with the “score method” recently developed by the Italian researchers [74]. The MQI value has been correlated to the normal strain arising from in situ double flat-jack tests. MQI method is based on the identification of masonry buildings typical features evaluated with respect to the “rules of art”, as reported in ancient and modern handbooks; from the visual inspection of masonry texture in façade and in cross section, a numerical evaluation is given to different parameters and the quality index can be obtained.

The following list of the essential data is divided into 5 sections: building geometry, building typology, site morphology, seismic damage, and masonry characterization.

Building geometry

- Georeferencing
- Nr Storeys (above ground)
- Average storey height
- Construction/renovation
- Position in aggregate

Building typology

- Structure typology
- Vertical structures (prevailing typology)
- Horizontal structures (prevailing typology)
- Roof

Site Morphology

- Site morphology
- Foundations

Masonry characterization

- Masonry typology
- Horizontality of bed joints
- Stagger properties of vertical joints
- Stone/brick regularity
- Stone/brick dimension regularity
- Bed joint regularity (Mortar)
- Quality of the mortar
- Masonry Quality Index (MQI)

4.4. Example

4.4.1. *Town level (by building aggregation)*

The seismic activity that has always shaken the Italian territory and especially the latest events (earthquake in Central Italy 2016) - highlighted again the structural fragility of the historic centres, which are mostly made up of masonry buildings, often of poor quality, and characterized by typical and specific vulnerabilities that do not allow sufficient resistance to the seismic phenomenon. In particular, the small historical centres in the Marche region are mainly characterized by a “spontaneous” architecture, generally made up of poor materials.

The historic centre of Camerino has been identified as a case study as it represents one of the most affected historical centres after the 2016 seismic events and which still has a very large “red area” (not accessible area due to the damages). Camerino has a high historical-cultural value, and it is possible to find a vast amount of available data on local seismic history. The macro seismic approach is implemented to evaluate the vulnerability and damage scenario after a simulation of earthquake event. The procedure foresees four steps: (1) Definition of a GIS data storage that collect information deriving from AeDES sheet; (2) Definition of a Vulnerability Index, and assignment to each building of a vulnerability function; (3) Simulation of a seismic event; (4) Evaluation of a damage scenario. The management and processing of the essential data collected was managed through a GIS platform.

GIS data storage

Concerning geographic data, the cadastral register of the centre of Camerino is necessary as in whose attributes table there are the data concerning the parcels. The building footprints and street network are useful as well. For each building the geometric and structural properties, among the type of material, will be collected and organized in the GIS database.

The GIS database permits an effective management of all information and the implementation of damage and loss estimation models (probability functions). To automate and optimize the procedure, all computations were performed inside the GIS environment through query, field calculator, array, buffer, join, etc. The analysis was carried out by mapping all outputs through the open-source software Quantum GIS (QGIS), released by the Open-Source Geospatial Foundation. All information contained in the AeDES form is implemented in GIS system to facilitate the selection for each building the correct vulnerability index value.

Figure 21 reports the distribution of building according with their construction material: blue colour represents the Reinforced Concrete buildings (RC), while the orange ones are the masonry buildings. Figure 22 reports the distribution of the buildings considering the number of floors: Low Rise (LR) characterized by 1-3 floors (green), Middle Rise MR by 4-7 floors (orange) and High Rise (HR) constituted by 8 and more floors (red). Finally, Figure 23 shows if the buildings have withstood thanks to retrofitting intervention or not.

The quality of the masonry is defined adopting the MQI, based on the photographic survey campaign of the walls. Figure 24 shows the survey campaign on the walls of the historic centre of Camerino, carried out through a filing of the different types of walls and the quality of the masonry.

Figure 21: Building classification according with their construction material

Figure 22: Building classification according with the number of storeys

Figure 23: Building classification according with the presence of retrofitting technique.

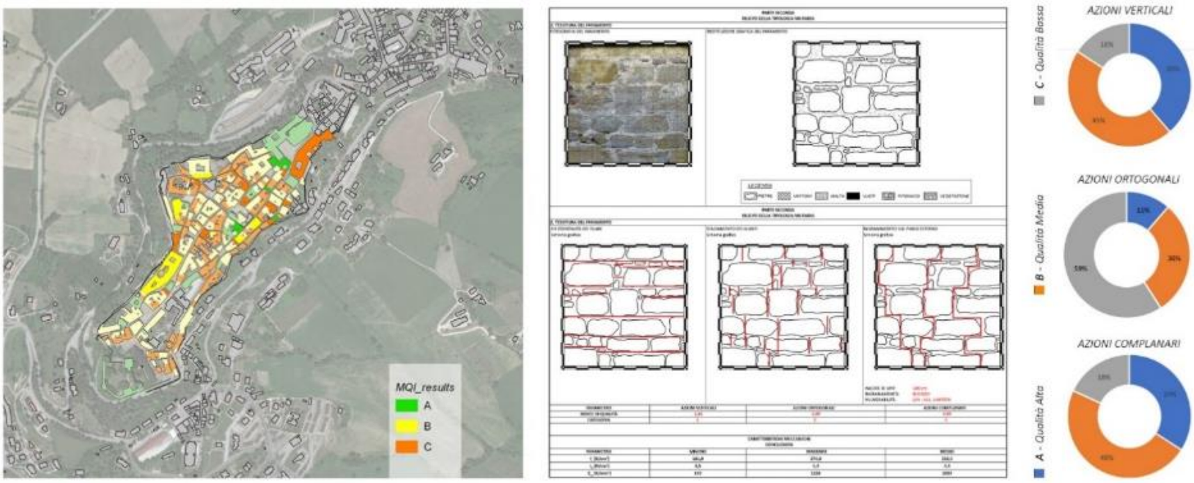

Figure 24: Survey campaign on the walls of the historic center of Camerino

Definition of Vulnerability Index

Starting from data collected in the database is possible to attribute, for each building, the initial vulnerability index V

Table 6. The MQI can been considered in the state of preservation vulnerability modifier ΔV . In particular, the maximum value of MQI is associated with the “Good state” of masonry (ΔV = -0.04, while the minimum value of MQI is associated with the “Bad state” (ΔV

= +0.04); medium value of MQI is associated with “Normal” state (ΔV = 0.00). Figure 25 shows the result of the Vulnerability Index applied to the Historic centre of Camerino.

Figure 25: Distribution of the vulnerability Index for the historical centre of Camerino

Simulation of seismic event

In the application the seismic sequence occurred in 2016 in Central Italy began on August 24th with a Mw = 6 is simulated. It causes 299 fatalities and important huge economic losses due to building damage. The epicentre was at 1 km W from Accumoli, and the Peak Ground Accelerations (PGAs) recorded nearby the epicentre was about 0.45g. A second strong event characterised by Mw = 5.9 occurred on October 26th 3 km away from Visso, extending the activated seismogenic area toward NW. Four days later, on October 30th, a third earthquake with Mw = 6.5 occurred 4 km NE from Norcia. During this last mainshock, the maximum PGA recorded nearby the epicentre was about 0.48g. Moreover, the area was interested by about 6500 aftershocks with Mw ranging from 2.3 to 5.5, occurred between August 2016 and January 2017. Figure 26 shows the locations of the mainshock epicentres, the shake maps of the three main events, reporting the distribution of PGA, and their envelope. These shake maps have been obtained by handling the shake data provided by the Italian National Institute of Geophysics and Volcanology (INGV. Shake maps data) through the QGIS Opensource GIS software (QGIS. Development Team 2015). The value of PGA processed by INGV is referred to stiff soil characterised by shear wave velocity higher than 800 m/s and it is estimated by means of empirical attenuation laws starting from shakings recorded in the accelerometric stations distributed over the territory. It should be noted that the PGA estimated by INGV does not include possible local shaking amplification due to the geological conditions. In the sequel only the event of October 30th is considered and Figure 26 report the shake map of the event in terms of PGA.

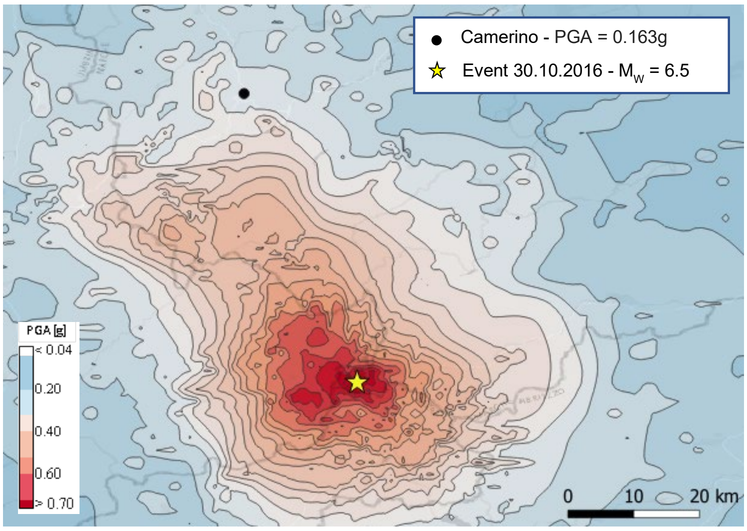

Figure 26: Shake maps of the October 30th event of the 2016 seismic sequence.

Expected damage scenario

The correlation between the expected damage and the seismic input is expressed in terms of vulnerability curves depending on the assessed vulnerability, described by a closed analytical function as seen in Par. 4.2. In Equation 6, the intensity i_{MCS} is computed from the PGA according to correlation reported in Equation 9 proposed by Faccioli and Cauzzi [68], assuming coefficients a_1 and a_2 equal to 6.54 and 1.96 respectively. Figure 27 shows the distribution of the expected damage, grouped in 5 intervals, for the Camerino historic centre considering the event of the 30th October 2016.

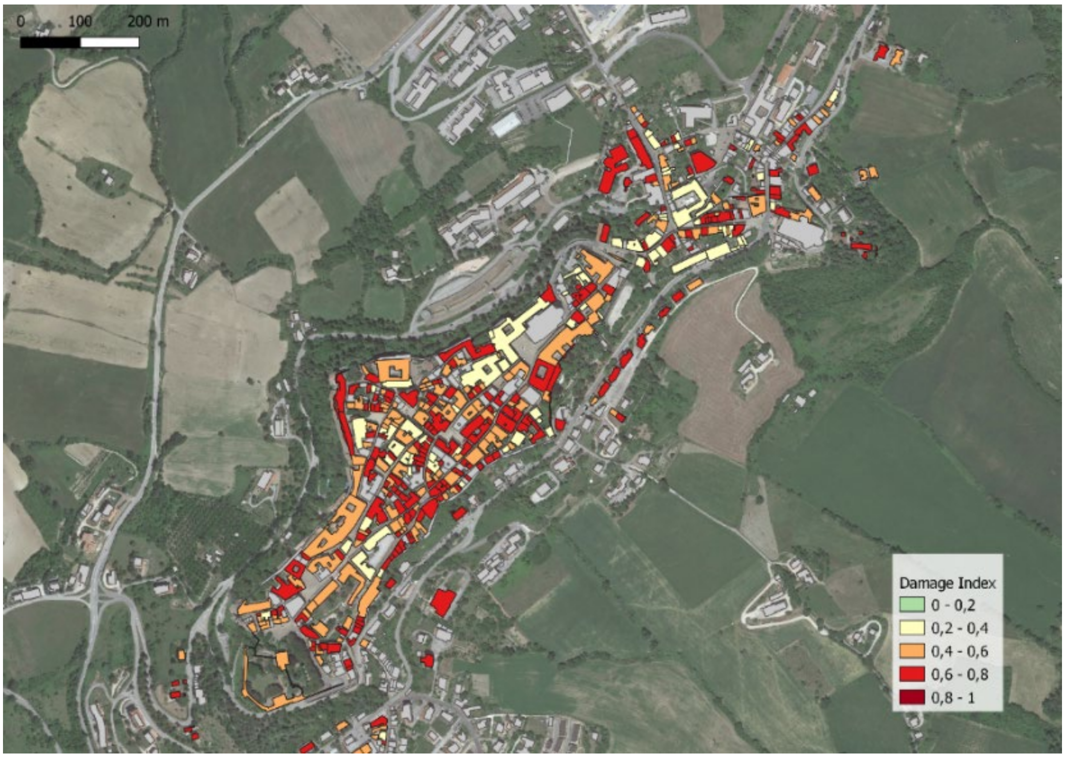

Figure 27: Predicted damage after the event of the 30th October 2016

5. Hydrological and hydrogeological vulnerability of historical constructions and towns

(M. Morici, S. Giovinazzi)

5.1. Historical construction damage due to subsidence

Subsidence is the sinking of the ground beneath buildings, that can be caused by natural processes or by human activities. Regarding the natural events subsidence can also be caused by earthquakes, soil compaction, glacial isostatic adjustment, erosion, sinkhole formation, and adding water to fine soils deposited by wind (a natural process known as loess deposits). Regarding the human activity, the extraction of minerals by underground, pumping water from underground, mining often causes ground subsidence phenomena.

These ground movements due to natural and manmade hazards (subsidence, landslides, consolidation...) induce a differential settlement on the buildings, producing a different level of damage, from simple cracking to partial or total collapse. In urban regions, these phenomena may induce in historical areas an important damage due to the building limited capacity to adapt the settlements.

To evaluate this damage, several empirical and analytical methods have been developed. Empirical relationships between the foundations settlements and the damage induced to superstructures have been developed by several researchers. Early on, Skempton and MacDonald [75] reported observations of settlements and the onsets of cracking to 98 buildings with isolated/continuous footings resting on fine/coarse grained soils, while Bjerrum [76] retrieved useful relationships between the maximum settlement and the maximum differential settlement, recommending the limiting values of angular distortions for buildings. Burland and Wroth [79] addressed the conditions leading to settlement-induced damage and, like Polshin and Tokar [90], concluded that visible cracking is related to the exceedance of certain values of tensile strain. Indeed, based on the above-mentioned damage criteria, placing a limitation on the values of some Subsidence Related Intensity (SRI) parameters (e.g., angular distortion/relative rotation) is currently used in several design codes [86].

Peduto et al. 2019 [9] defined the correlations between the damage category and the building movements, through Subsidence Related Intensity (SRI) parameters evaluated starting from Spaceborne Synthetic Aperture Radar (SAR) images, processed via advanced Differential Interferometric techniques (DInSAR). This technique uses radar images acquired by satellites. Millions of measurements can be acquired simultaneously by satellite in a single pass. InSAR is the only aerial monitoring technique that can map ground deformation along line-of-sight and cover the whole territory field with very high point density. Spirit levelling and GPS data may be used for calibration and cross validation. To be able to measure both horizontal and vertical deformation by InSAR it is planned to use both ascending and descending geometries.

These correlations may then be used to assess the damage due to a predicted future ground movement combining the DInSAR to evaluate the potential damage on buildings affected by land subsidence. The main advantage of this method is that it represents a realistic image of the real vulnerability of buildings since it is based on actual recorded damage and measured ground displacements.

Additionally, InSAR datasets allow the calculation of the vertical displacements that affect every building. Consequently, since InSAR data cover the territory and provide information about the vertical displacement of all buildings, we can calculate the probability of damage certainty level of damage.

In the following the functions defined in [9] were used to predict the damage starting from the estimation of SRI parameters evaluated by means the DInSAR-derived ground displacements.

5.2. Scientific background and damage functions (subsidence)

The state of the art on building damage for masonry buildings is mainly based on the work of Boscardin and Cording [78] and Burland [81]; it is more commonly known as the Limiting Tensile Strain Method (LTSM). This method is generally adopted in the cases of tunnelling or other ground-related works. The LTSM involves classifying the damage severity according to the system proposed by Burland [80] for brickwork or blockwork and stone masonry, which mainly reflects the attainment of damage affecting the building aesthetics (D0 = negligible, D1 = very slight and D2 = slight), causing a loss of functionality (D3 = moderate and D4 = severe) or even compromising the stability (D5 = very severe). According to LTSM, a given damage severity level is attained if the combination of bending, shear and horizontal strain (combined into one tensile strain) reaches a certain limiting value. Factors influencing the limiting values of the tensile strain are, for example, the geometrical and mechanical characteristics of the building [93].

Considering the inherent uncertainties involved in the problem, an interesting perspective is offered by probabilistic tools relating different (measured) SRI parameter values with (surveyed) damage severity levels in the form of empirical fragility curves [9].

Fragility curves describe the probability of exceedance of a given damage level as a function of the intensity measure of the SRI_i parameter values (SRI_i = Differential settlement δ_ρ, deflection ratio Δ/L, rotation (Θ). Generally, the damage state is described by a discrete variable d_k ($k = 0,1,..,N_D$) which denotes the damage within a finite number $N_D + 1$ of ordered possible damage states. By denoting by D the random variable that describes the church damage, the fragility curve $G_{Di}\left(d_k \mid SRI_i\right)$ ($k = 1,..,N_D$) describes the probability that, for a SRI_i parameter values intensity, the damage state is equal or higher than d_k. Usually, the fragility curves are efficiently approximated by the two-parameter function:

$$G_{Di}\left(d_k \mid SRI_i\right) \approx \Phi\left[\frac{\ln\left(SRI_i\right) - \left(\overline{SRI}_i\right)_k}{\beta_k}\right] \tag{10}$$

where Φ is the cumulative normal distribution function, SRI_i is the intensity measured of Subsidence Related Intensity, and $\left(\overline{SRI}_i\right)_k$ and β_k are the two-parameters associated to the response of the structure.

Starting from Equation (1) according to Saeidi et al. [91], is possible to evaluate the mean damage index $\mu_{Di}\left(SRI_i\right) \in \left[0,1\right]$ that relate the mean damage with the ground displacements

$$\mu_{Di}\left(SRI_i\right) = \frac{\sum_{j=1}^{N_D+1} G_{Di}\left(d_k \mid SRI_i\right) d_k}{\sum_{j=1}^{N_D+1} d_k} \tag{11}$$

The mean damage is a continuous variable defined in the interval 0-1.

Regarding the SRI parameters differential settlement (δ_ρ), deflection ratio (Δ/L) and rotation (Θ) can be selected [9] and defined as (Figure 28):

- Differential settlement δ_ρ is computed along the profile as the difference between the maximum and the minimum values of the recorded settlements;
- The deflection ratio is obtained as Δ/L according to the definitions provided by Burland and Wroth [79], where D is the displacement of a point relative to the line connecting two reference points and L is the distance between these two points;
- The rotation Θ, or slope, is assumed as $\Theta = \delta_\rho / L_\rho$, where L_ρ indicates the distance at the foundation level between the two points where δ_ρ was computed.

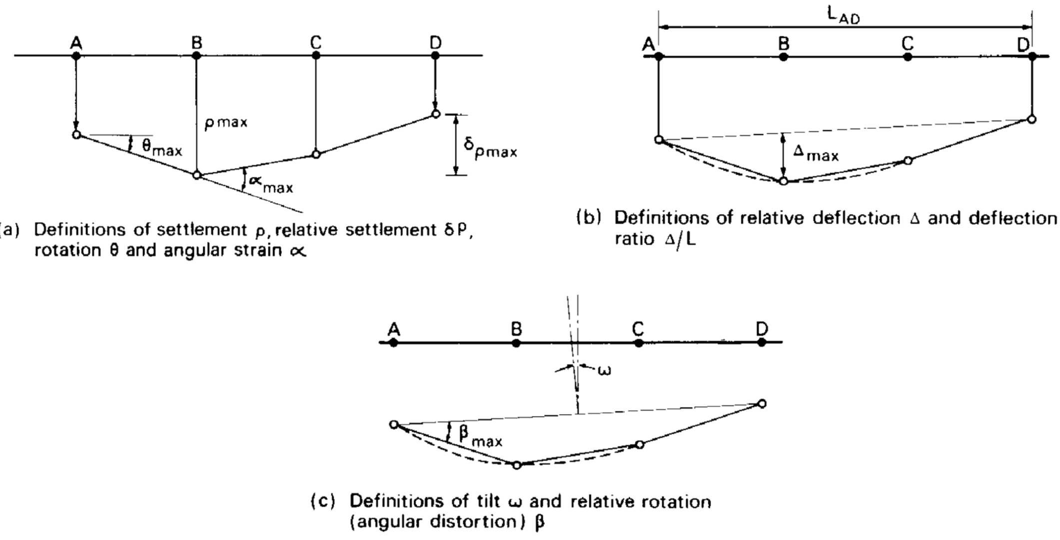

Figure 28: Definition of settlement damage mechanism

In addition, for the SRI parameter [9] defined 3 levels of damages $N_D = 3$ and in Table 7, are reported the parameters to evaluate the fragility function.

Table 7: Median $\left(\overline{SRI}_i\right)_k$ and standard deviation β_k of the lognormal distribution function for each considered SRI parameter distinguished by the foundation type and damage level.

SRI parameter	Damage level	Foundation type			
		Shallow		Piled	
		$\overline{SRI}_i$	β	$\overline{SRI}_i$	β
δρ [mm]	D1	9.04	0.99	12.57	0.57
	D2	25.06	0.99	23.26	0.57
	D3	41.53	0.99	36.81	0.57
	D4/D5	–	–	48.60	0.57
θ [rad]	D1	2.16×10^{-4}	6.04	3.10×10^{-4}	4.14
	D2	4.67×10^{-2}	6.04	8.69×10^{-3}	4.14
	D3	6.38×10^{-1}	6.04	9.08×10^{-2}	4.14
	D4/D5	–	–	1.69×10^{-1}	4.14
Δ_1/L_1 [mm/mm]	D1	3.16×10^{-4}	2.56	5.00×10^{-4}	1.76
	D2	3.26×10^{-3}	2.56	2.21×10^{-3}	1.76
	D3	1.01×10^{-2}	2.56	6.45×10^{-3}	1.76
	D4/D5	–	–	1.26×10^{-2}	1.76

The evaluation of building vulnerability to groundwork-induced displacements is based on a combination of different approaches available in literature [10] regarding mining ([77], [94], [84]), tunnelling [87] and seismic risk ([88], [60]). In the procedure proposed by [10], the Vulnerability Index (I_v) was defined following the procedure of [82] and [83], but using a reduced number of parameters for the index evaluation grouped into three different categories: geometrical characteristics, structural characteristics, and condition of the building (Table 8). Each category is assessed by vulnerability parameters: building length and shape for the geometrical characteristics; type of structure and foundation for the structural characteristics; and visible damages for the current condition of the building. For each i-parameters ($i = 1-6$) are defined four classes of scores A, B, C, and D were the class score C_{vi} assumes value of 0, 5, 20, and 50 respectively.

Table 8: Vulnerability classes for a building, based on a common evaluation of five attributes. Rating method adapted from Dzegniuk et al. [84]. The score for each class is shown in square brackets.

Characteristic	Parameter	Class vi				Weight Pi	Max value	Relative weight
		A [0]	B [5]	C [20]	D [50]			
Geometrical	Building length (m)	≤10	11–15	16–30	>30	0.75	37.5	30%
	Building shape[1]	>0.75	0.75–0.5	0.5–0.35	<0.35	0.75	37.5	
Structural	Structure type	Steel	Reinforced concrete	Wooden, Mixed	Masonry, special structure	1	50	50%
	Foundation type	To bedrock, Piles	Raft	Strip	Wooden piles, isolated	1.5	75	
Condition	Visual damage	Excellent	Good	Medium	Bad	1	50	20%

The overall vulnerability is calculated as a weighted sum of the six parameters, associating a weight p_i for each parameter, ranging from 0.75 (for the less important parameters) up to 1.5 (for the most important). The normalised I_v can be evaluated by the expression

$$I_v = \frac{1}{4}\sum_{i=1}^{6} C_{vi} \cdot p_i \qquad [\%] \tag{12}$$

In the case of one or more vulnerability parameters is missing, then the highest class C_{vi} can be considered in the calculation, and the weights can be changed as a function of the database at hand [10].

The I_v can be grouped in classes: Negligible (V_1), $I_v = \left[0 \div 25\right)$; Low ($V_2$), $I_v = \left[25 \div 50\right)$; Medium ($V_3$), $I_v = \left[50 \div 75\right)$; Hight ($V_4$), $I_v = \left[75 \div 100\right]$.

Regarding the category related to geometrical characteristics, the assessment of vulnerability parameters building length and building shape, are calculated as follows

- Building length: maximum length in plant of the building along the direction of the maximum slope of the plane that interpolate the measured settlements;
- Building shape: number representing the geometric squareness or complexity of a building polygon, evaluated considering the "isosquarimetric" version of the Polsby-Popper score $s_n = 16\,\mathrm{A}/\mathrm{P}^2$ [89] where A is the area P is the perimeter at level of the foundation of the building.

5.3. Essential data and suggestion for implementation (subsidence)

The procedure followed for the analyses consists of three phases preceded by a preliminary data preparation phase. In the following only two SRI parameters were considered, i.e. the differential settlement δ_ρ and the rotation Θ, while the deflection ratio Δ/L is neglected.

In Phase I, the cumulative settlement pertaining to each Permanent Scatter (PS) over the observation period is derived by multiplying the available PS velocity by the monitoring period (mean of both ascending and descending orbits). In this way, settlements are implicitly assumed as occurring at a constant rate in the study area during the observation period. This assumption is acceptable if such widespread settlements in the analysed areas are mainly related to the long-term creep processes [85].

PS-derived settlement δ_e are interpolated over each building by a plane defined by

$$\delta_e\left(x_m, y_m\right) = \delta_g\left(x_g, y_g\right) + \Theta_y x_m - \Theta_x y_m \tag{13}$$

where $\left(x_m, y_m\right)$ are the coordinate of the point inside the plant of the building, $\left(x_g, y_g\right)$ are the coordinate of the centre of the plant shape of the building and δ_g, Θ_y, Θ_x are the parameters of the interpolation plane. Parameters δ_g, Θ_y, Θ_x are evaluated minimizing the ordinary least squares between measured data and approximated data

In Phase II, starting from the interpolated plane are estimated the maximum displacement and rotation and are evaluated the mean SRI parameters

$$\mu_{D\delta}\left(\delta\right)_b = \frac{\sum_{j=1}^{N_D+1} G_{D\delta}\left(d_k \mid \delta_v\right) d_k}{\sum_{j=1}^{N_D+1} d_k} \;;\; \mu_{D\Theta}\left(\Theta\right)_b = \frac{\sum_{j=1}^{N_D+1} G_{D\Theta}\left(d_k \mid \Theta\right) d_k}{\sum_{j=1}^{N_D+1} d_k} \tag{14 a,b}$$

Adopted fragility curves for differential displacement and rotation evaluated adopting the parameters reported in Table 7, the correspond to fragility curves reported in Figure 29.

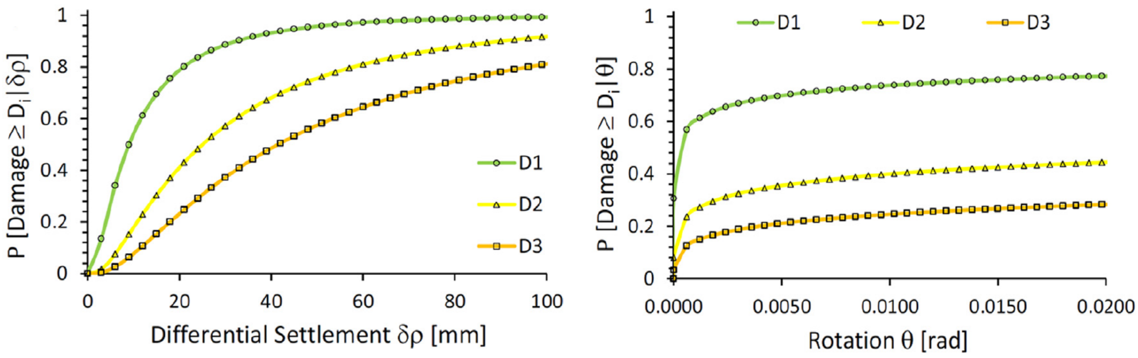

Figure 29: Adopted fragility curves for differential displacement and rotation

5.4. Historical construction damage due to pluvial flooding

Pluvial flooding occurs because of high rainfall rates when surface runoff (flowing along preferential path- ways, typically roads, footpaths, natural ground depressions, small water courses, etc.) cannot be efficiently conveyed into the underground storm water drainage system (surface drainage deficiency) [95]. In other cases, the underground storm water drainage system itself overflows (drainage system failure) ([96], [97]).

The hydraulic performance of urban drainage systems can be dramatically affected by the operational condition of its components as in the case of inlets, through which surface storm-water runoff enters the underground storm water drainage ([98], [99], [100]). In fact, partial and full blockage of inlets due to the accumulation of debris is a common occurrence that can be influenced by a number of factors, including maintenance regimes, relative location of the inlet, year season (e.g. leaf fall-rate in autumn) and antecedent weather conditions (e.g. higher accumulation of tree leaves, branches and debris may occur after previous storms). Because of these deficiencies, pluvial flooding events usually occur quite frequently because of rain events of lower intensity than the design one and may involve only limited portions of the urban area, even in case of proper dimensioning of the drainage system.

Many individual historic buildings suffer flooding due to defective or poorly managed ground drainage. On a local scale, this is commonly due to rising ground levels and defective street drainage, which may allow local surface water to 'run off' and drain into, rather than out of, ground floor or basement structures. On a larger scale, mismanagement of the river catchment drainage system by the local authority can result in surface and ground drainage water being 'held back' to create unplanned 'flood plains'. This can occur due to poor maintenance and blocking of drains or culverts, but sometimes it is the result of a deliberate policy to prevent flooding in other more sensitive areas. In this way, historic buildings built on relatively high ground can be put at risk by measures taken to prevent further flooding of a larger number of new buildings built on flood plains or water meadows downstream.

Impacts of pluvial flooding in historic buildings can be further exacerbated due to failures of the roof drainage systems or other building services such as water mains. In these cases, water will often flood through buildings, causing damage to structures, furnishings, and fittings, and accumulate in porous materials such as masonry, pugging or other insulation. These can then act as 'moisture reservoirs', providing the conditions for long-term damp and decay. This can be a particular problem in poorly maintained and infrequently occupied structures such as storerooms or the unoccupied parts of buildings in multiple occupation.

5.5. Scientific background and pluvial flooding damage functions

The scientific community has been intensively working to define models and approaches for the estimation and assessment of potential damage of flood events, including pluvial-induced flood events, as an important component in flood risk management.

Depth-damage curves, which denote the flood damage that would occur at specific water depths per asset or per land-use class, have been widely used for the estimation of direct flood damage on the built environment. Huizinga et al. [101] worked on a systematic revision and organization of such curves developing a globally consistent database of depth-damage curves. This dataset contains damage curves depicting fractional damage as a function of water depth as well as the relevant maximum damage values for a variety of assets and land use classes. Based on an extensive literature survey normalized damage curves have been developed for each continent, while differentiation in flood damage between countries is established by determining maximum damage values at the country scale. These maximum damage values are based on construction cost surveys from multinational construction companies, which provide a coherent set of detailed building cost data across dozens of countries. A consistent set of maximum flood damage values for all countries was computed using statistical regressions with socio- economic World Development Indicators. Further, based on insights from the literature survey, guidance is also given on how the damage curves and maximum damage values can be adjusted for specific local circumstances, such as urban vs. rural locations or use of specific building material (Figure 30).

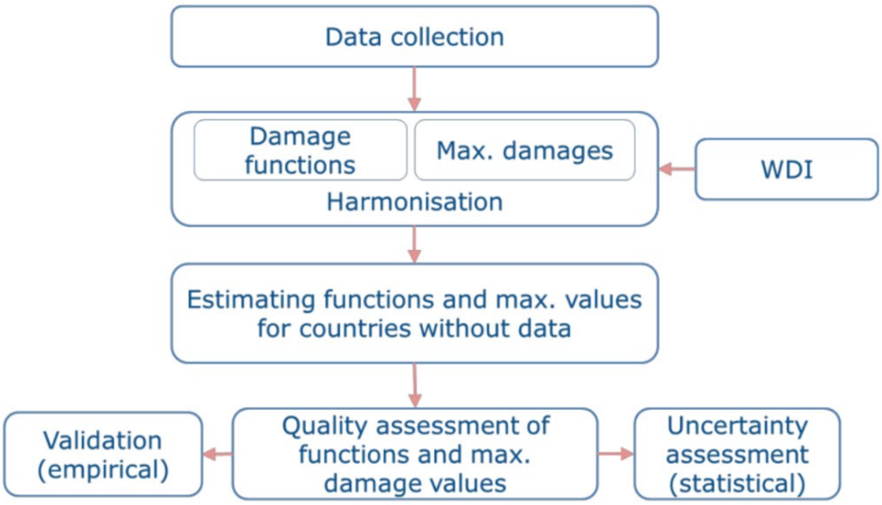

Figure 30: How the damage curves and maximum damage values can be adjusted for specific local circumstances

Flood-damage functions for EU member states for European countries (from [101]) are reported in figures Figure 31 to Figure 34 in term of damage per square meter as a function of flooding depth for: residential buildings including inventory; commerce including inventory; road infrastructures; and agriculture.

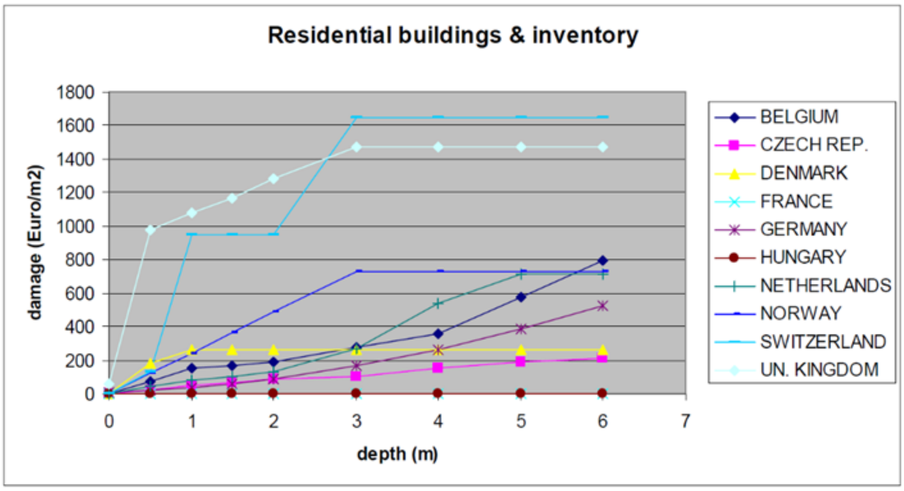

Figure 31: Damage per square meter for residential buildings including inventory.

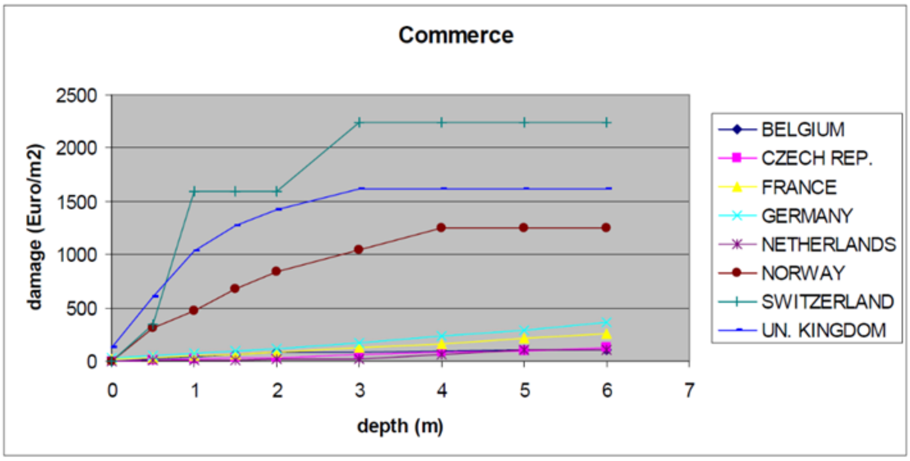

Figure 32: Damage per square meter for commerce

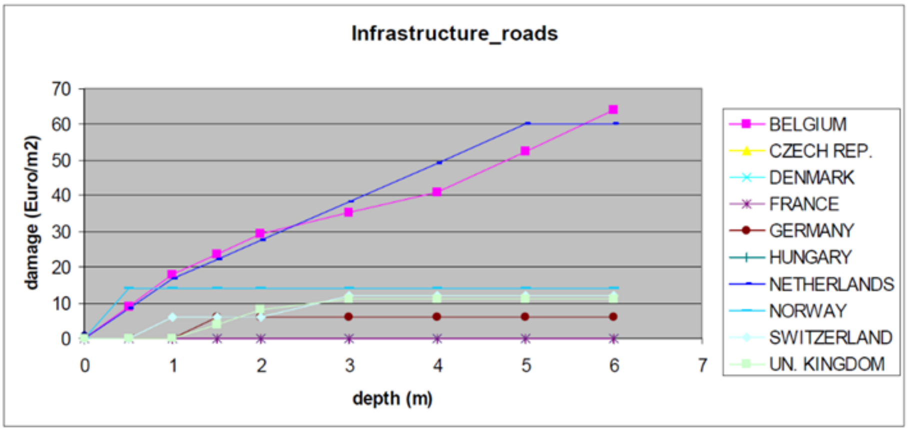

Figure 33: Damage per square meter for infrastructure (roads)

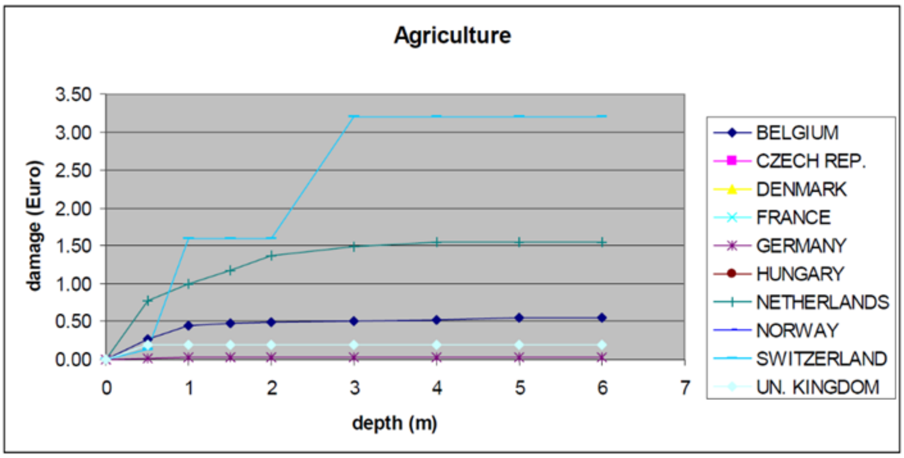

Figure 34: Damage per square meter for agriculture.

Switzerland & the UK have by far the largest damage values, the rest of the explored countries have more or less equal maximum damage values. The average maximum damage value for the category residential buildings including inventory at 6m depth is 2 750 €/m.

Switzerland has by far the largest damage value; Norway and UK are in the intermediate region and have quite similar functions, while on the other hand Germany, France, the Czech Republic and The Netherlands have quite low values. The average maximum 2 damage value for the category commerce at 6 m. depth is 621 €/m.

Maximum damage for roads differs largely between the considered countries. Belgium and Switzerland have by far the largest damage values, the rest of the explore countries have quite low values. The average maximum damage value for the category roads at 6 2 m. water depth is 24 €/m.

For agriculture large differences exist between the functions. Switzerland has by far the largest damage values; the Netherlands has an intermediate value and the rest lower values. The average maximum damage value for the category agriculture at 6m depth is 0.77 2 €/m.

The aforementioned flooding Depth-damage curves proposed for EU countries by Huizinga et al. [101] refer to the building use as the only discriminatory element. A more sophisticated approach is available from FEMA Federal Emergency Management Agency’s, i.e. HAZUS-MH [102] a multi-hazard impact assessment approach (Figure 35) develop for United States (USs) underpinning earthquake, flood and hurricane models. The flood events considered by HAZUS are either riverine or coastal. Pluvial flood is not explicitly considered by HAZUS-MH.

The vulnerability model proposed by HAZUS Flood model is assumed as the reference model for implementation within the ARCH project as it provides a more detailed classification of the built exposed asset with respect to the one proposed by Huizinga et al. [101]. The riverine (non-velocity zone) depth-damage functions provided by HAZUS Flood model are deemed to be appropriate for assessing pluvial flood induced damage (Figure 36).

Direct building damage is expressed by HAZUS Flood model in terms of cost to repair ($), damage ratio, i.e. repair cost relative to replacement cost or as a damage state. In ARCH similar to what done in different projects and platforms, five damage states are adopted as a function of the damage ratio, to align the damage state scale to the one from EMS-98 already adopted for the assessment of damage induced by earthquakes and subsidence among the other in Table 9.

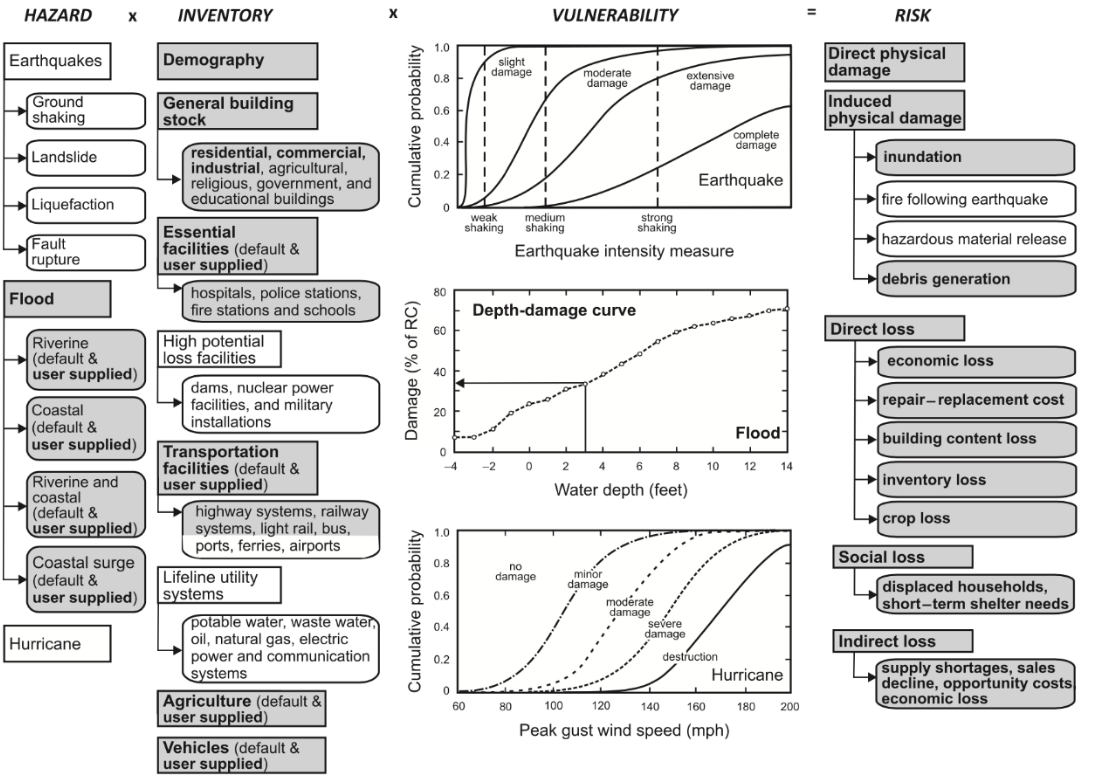

Figure 35: Schematic representation of the hazards, inventory, damage functions, and risks in Hazus. In grey are characteristics of the Hazus Flood model (picture courtesy of Nastev M.,Todorov N. [101])

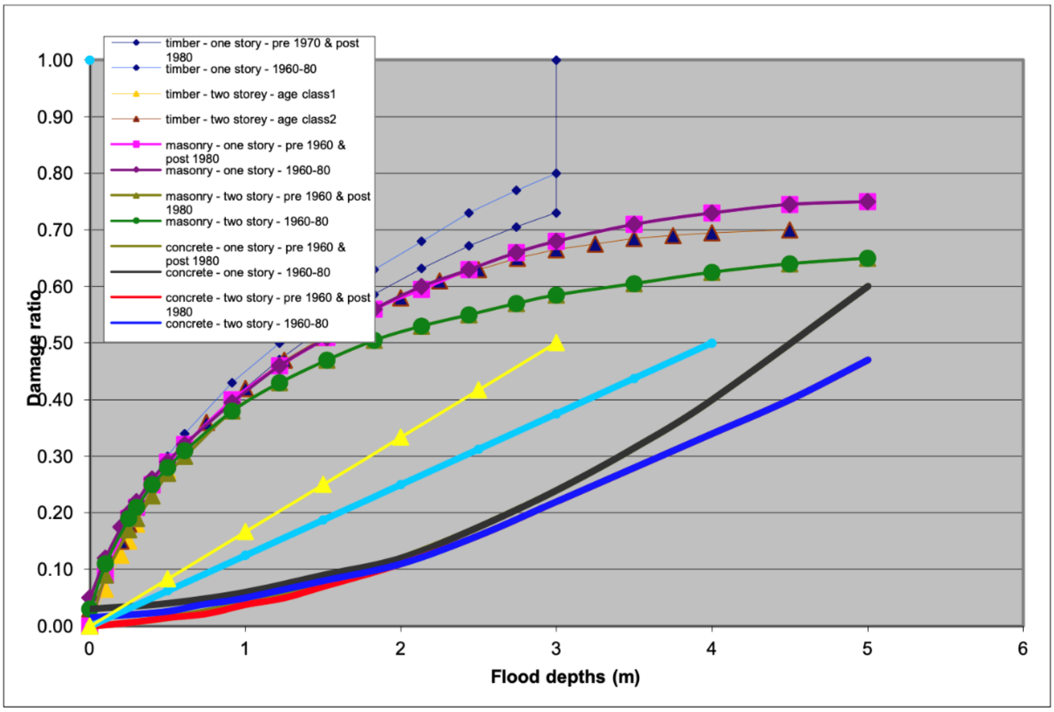

Figure 36: Flood fragility curves (adapted from HAZUS-MH) for various building types, with inundation depth above the floor level (m) along the horizontal axis and average damage ratio along the vertical axis (picture courtesy of NIWA Technical Report [103])

Table 9: damage induced by earthquakes and subsidence adopted also in the flooding damage

Damage state	Description	Damage ratio
DS0	Insignificant	0–0.02
DS1	Light—Non-structural damage, or minor non-structural damage	0.02–0.1
DS2	Moderate—Reparable structural damage	0.1–0.5
DS3	Severe—Irreparable structural damage	0.5–0.95
DS4	Collapse—Structural integrity fails	> 0.95

5.6. Essential data and suggestion for implementation of pluvial flooding vulnerability approaches

Hazus Flood uses five basic construction classifications (wood, concrete, steel, masonry, and manufactured housing) and seven general occupancy categories (residential, commercial, industrial, agricultural, religious/ non-profit, governmental and educational buildings). In addition, the flood model considers essential facilities (hospitals, schools, police and fire stations), selected transportation facilities (highway, light rail and railroad bridges), selected utility facilities (water treatment plants, pumping stations), agriculture products and vehicles (Figure 37 above).

In the vulnerability assessment, the foundation type and its associated typical height are also considered and come together with information for the elevation of the first floor from grade (Figure 37). Both have significant impact on the loss estimation. The foundation type can be selected from among the following types with default values of the first-floor height in parentheses: pile (7–8 ft), pier (5–6 ft), solid wall (7–8 ft), basement (4 ft), crawlspace (3–4 ft), fill (2 ft) and slab-on-grade (1 ft). In Hazus, “first-floor” refers always to the lowest floor. The number of stories is also taken into consideration (Table 10).

The algorithm for estimating direct physical damage to the general building stock is quite simple, with default damage functions as a function of the characteristics of the building and of estimated water depths.

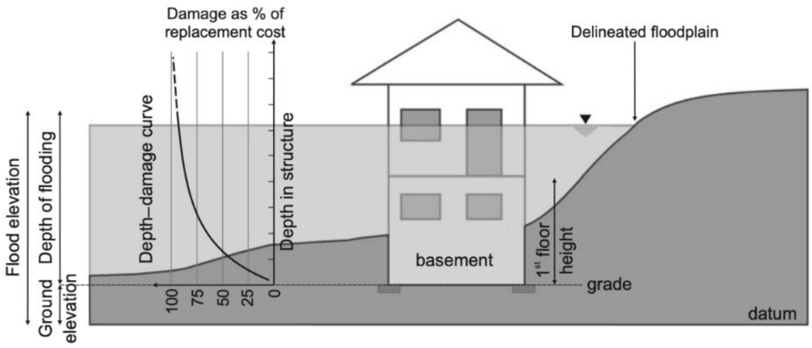

Figure 37: Schematic representation of the hazard parameters for a typical Canadian house with a basement [1st floor in Hazus]. Depth-damage functions are applied to relevant depth of flooding (depth in structure). (Picture courtesy of Nastev M., & Nikolay Todorov N. [101])

Table 10: Hazus Flood model: building classification by main constructive material and height.

No.	Label	Description	Height			
			Range		Typical	
			Name	Stories	Stories	Feet
1	Wood	Wood (light frame and commercial and industrial)		All	1 to 2	14 to 24
2	Steel	Steel frame structures including those with infill walls or concrete shear walls	Low-rise Mid-rise High-rise	1-3 4-7 8+	2 5 13	24 60 156
3	Concrete	Concrete frame or shear wall structures including tilt-up, precast, and infill walls	Low-rise Mid-rise High-rise	1-3 4-7 8+	2 5 12	20 50 120
4	Masonry	All structures with masonry bearing walls	Low-rise Mid-rise High-rise	1-3 4-7 8+	2 5 12	20 50 120
5	MH	Mobile Homes		All	1	10

5.7. Example

5.7.1. *Subsidence – town/district*

Within the domain of ground deformation measurements, a multi-temporal Interferometric SAR (InSAR) technique, namely the Permanent Scatterers ® (PS) technique [104] is adopted. The procedure allows to generate mean ground velocity and the related time series of deformation, starting from the collection of a large stack of SAR images. In particular, the PS technique implemented in SARScape ® software has been used to elaborate data collected by the ESA SAR mission Sentinel-1, over the city of Hamburg [D 4.1 ARCH].

The analysis aims to provide the basic information for the planned subsidence risk analysis in WP5. Therefore, a subset area has been selected to focus the analysis in the zone of the city most prone to subsidence. Afterwards, the InSAR analysis has been performed, over a small region of about 10km x 10 km, centred on the main interesting district of Speicherstadt (Figure 38). For the data processing, we selected and downloaded 93 images from ascending path and 107 from the descending one from the Alaska Satellite Facility repository. The temporal window of the S1 observations range from 30/04/2015 to 10/01/2020, and from 1/06/2016 to 24/01/2020, for the ascending and descending set, respectively.

The maps show a general stable behaviour with some small parts that report slow subsidence between -5 and -10 mm per year, along the SAR Line of Sight (yellow-orange points in the maps of Figure 39).

Only two points in the ascending dataset, inside the HafenCity district which contains the world heritage site, have mean ground velocity of about -18 mm/yr. However, new buildings are in this zone, therefore probably this higher value could be related to construction works. Figure 40 reports the mean velocity registered in the district of the Speicherstadt evaluated in the temporal window of the observations range and implemented in the HArIS system.

Assuming the observation time window of 6 years, the cumulative displacements were evaluated for to each PS points multiply the mean velocity for the time; in this operation, the "zero" point of evaluation of the problem was considered 2015.

The PS-derived settlement δ_e are interpolated over each building by a plane defined by Equation (14), starting from the interpolated plane are evaluated the maximum displacement and rotation (SRI parameters) necessary to evaluate the damage level.

For each building the mean damage level is assessed using the fragility curves defined starting from the structural characteristics of the building considered i.e. typology of foundation, superstructure (masonry, concrete, steel building etc); in this application, given the limited number of information available, only the type of foundation is taken into consideration in the definition of fragility curves.

The mean damage represented by vulnerability curve is evaluated applying Equation (15) as reported in D4.1. In the definition of gravity of damage, the level of damage is between 0 (no damage) to 3 (intermediate damage). Vulnerability curves adopted in the analysis is reported in Figure 41.

Figure 42 and Figure 43 reports the mean damage relate to rotation and maximum displacements of the Speicherstadt area; the damage intervals were defined considering the median values contained in the Table 7.

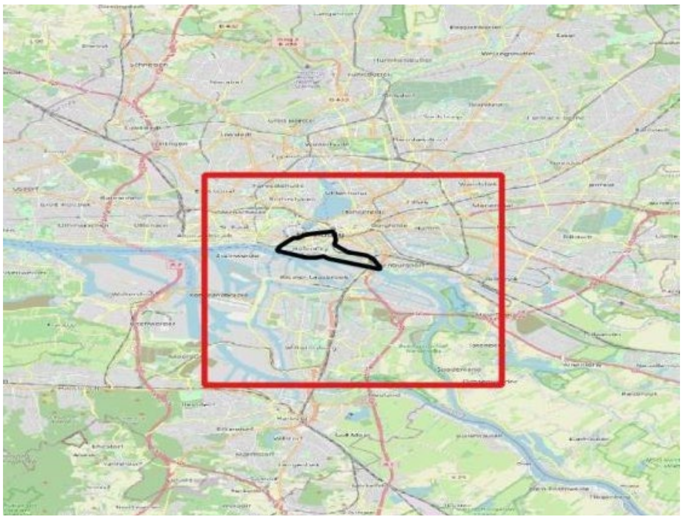

Figure 38: Location map: red rectangle refers to the area used to process SAR data; black polygon refers to Speicherstadt district

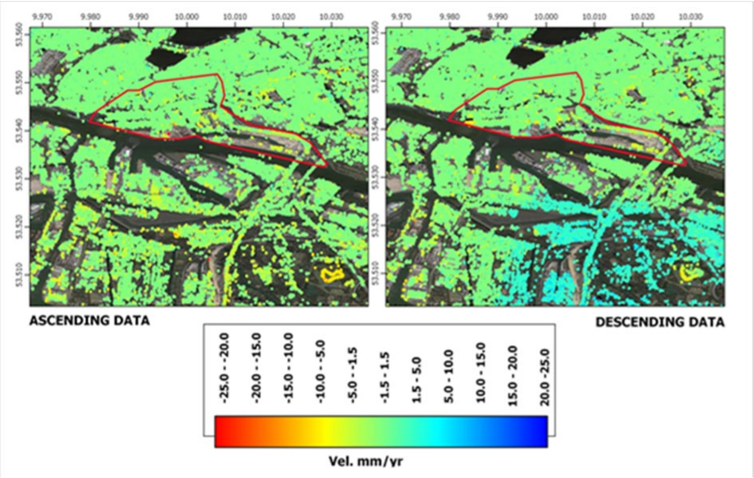

Figure 39: Left: PS ground velocity map from ascending data; Right: PS ground velocity map from descending data

Figure 40: Velocity of vertical displacements

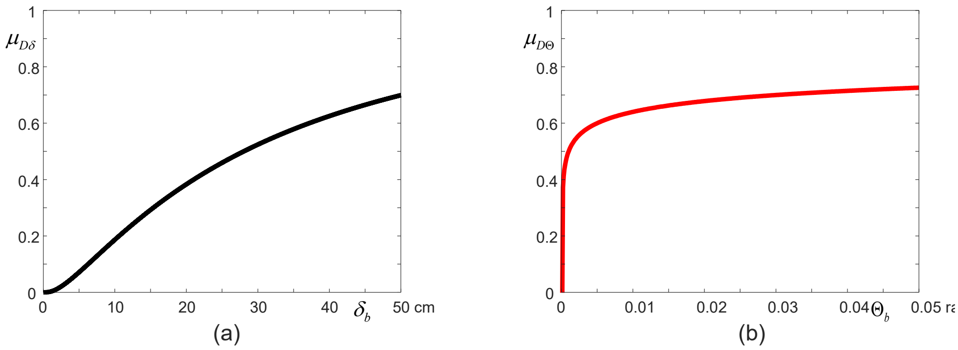

Figure 41: Vulnerability curves: (a) vertical displacement and (b) rotation

Figure 42: Mean damage referred to maximum vertical displacement

Figure 43: Mean damage referred to maximum rotation

6. Vulnerability of intangible values

(E. Petrucci, A. Dall'Asta, G. Roselli))

6.1. Intangible values and risk perception

Loss analysis presents specific aspects which need to be correctly addressed as they are normally focused on the evaluation of the costs related to construction strengthening and maintenance. This may be satisfactory for new constructions, but it is inadequate for heritage structures as unique and non-reproducible artefacts.

Associating a value to a historical building and its contents is a complex operation that cannot be limited to costs but should involve the evaluation of its symbolic and social value (Intangible Values) considering the cultural identity of communities, the quality of life of citizens and the economical processes related to tourism and cultural activities.

Cultural heritage is the legacy of tangible and intangible heritage assets of a group or society that is inherited from past generations. In 2005, the Faro Convention introduced a much broader and innovative concept of "cultural heritage", considered a "set of resources inherited from the past, which populations identify, regardless of who owns them, as a reflection and expression of their values, beliefs, knowledge and traditions, in continuous evolution" (art. 2). Therefore, cultural heritage can create a sense of community by connecting the individual to the city as it is considered a resource to be protected and witness of traditions, history of the community, symbols, and spiritual values.

Planning actions oriented to preserve intrinsic properties of cultural assets generally requires a preliminary assessment of their value to establish a ranking. This is a necessary step towards the use of limited resources to provide the basis for a decision-making process regarding resilience improvement and disaster risk reduction.

6.2. Background and strategy for the assessment

Assessing an objective value for cultural heritage requires the acknowledgement of its historically conditioned and largely composite nature to conserve, restore, and spread it.

In the first stage, detailed knowledge of every single element or structure must be acquired. In the second stage, the available knowledge about the various monuments must be combined and the monumental complex must be re-examined concerning its original status and its historical modifications. As soon as a great amount of information and profound knowledge has been acquired it is possible to propose valid hypotheses on each architectural artefact as well as to propose an interactive data system for risk analyses and risk assessment concerning the preservation of the complex. The development of a new system will make it possible to cross-reference the data acquired within the various fields of investigation.

The horizon of the reflection should be expanded to enrich the estimative paradigm of the cultural good with knowledge and results from different disciplinary areas. Two elements descend from the bipolarity of physical object and ideal value and the new immaterial idea of "good". On the one hand, it is possible to justify some apparent notional contradictions due to the incontrovertible historical dimension of the item, for example, its increase or loss of value over time or the lack of correspondence between something's cultural and commercial value. On the other hand, the opportunity exists to define the cultural good as a public tout court. Its inherent cultural value makes it a "good for use" destined to satisfy public interest, that is, for citizens to enjoy the culture inherent in the goods themselves, independent from its ownership, which could be either public or private [105].

In the last years, researchers developed their studies based on the concept of Contingent Valuation (CV), previously used to assign a value to the environmental heritage or libraries and adopt tools as the Willingness To Pay (WTP) for enjoying the good or the willing to accept (WTA) a possible loss [106].

These methods are specifically useful to evaluate goods that are partially external to market rules and provide values and benefits not simply related to their use (existence value, indirect value, option value). Cultural goods, defined by economists as "public goods", are particular goods: by their value, they cannot be efficient products and offers on the market due to the difficulty (or impossibility) of putting a price on them [107]. They cannot be consumed or renewed, but rather are used and enjoyed individually or collectively. As it happens with other types of goods, they require the financial flow necessary to realize and manage policies and produce various benefits which cannot be identified exclusively with a monetary advantage but primarily derive from their complex cultural value. Public goods, in addition, are characterized by the non-competitiveness of their consumption and by their non-exclusiveness. Their non-rivalry refers to the fact that a subject's consumption of the good does not prevent consumption by another subject. Non-excludability refers to the fact that no one can be excluded from enjoying the good. The production of public goods gives rise to advantages (external) in favour of other individuals whose producers cannot be repaid by applying the mechanism of prices. When there is no private economic convenience to their production, this should occur in the public sector through an organization that has the capacity, the force of compulsion, to have consumers pay with a mechanism different from a price [108]. Economic assessment is thus proposed to estimate the cultural value and help the decision-maker choose solutions commensurate with the pre-defined objectives [109].

In recent decades, especially in the work of economists, mathematicians, statisticians, and psychologists, different systems of "integrated", "dynamic" assessment have been developed. These systems aim to consider the different values of the cultural heritage, quantify them in numerical terms, and classify them according to priority, using specific software to simplify complex decision-making processes. For this to be possible, it is first necessary to convert the data, i.e., the value, into objective scales and codes of reference, keeping two precise warnings in mind. Firstly, the quantitative descriptions that the qualitative definitions are transformed into are intended as temporary tools, given the historical determination of the value in question. Secondly, it is unthinkable to eliminate the variable components associated with the person who, in this context, evaluates and decides; however, the risk of subjectivity and the ability to control evaluation criteria can be contained by compiling tables of values based on mathematical matrices and by making pair comparisons [110]. But what are the values that can be considered? The French philosopher and sociologist Jean Baudrillard identifies different types of value assigned to objects: the value of use, the value of exchange, and symbolic value. From the point of view of cultural goods, the first is connected to the monument's potential for versatility and adaptation to reuse. The second implies historical and aesthetic educational values and is divided into local symbolic value of a place − internal, spontaneous, and quantifiable through interest indicators such as the citizen's desire to live in the middle of the historical centre or on the outskirts − and the symbolic value of importation − connected to tourism and therefore to the economic development determined by accommodation and transport services.

The most noted American multi-criteria, multi-objective methods are echoed in Italian research that investigates a complex approach based on the definition of built cultural heritage, together with archaeological, architectural, environmental, and artistic goods. The literature shows a market failure concerning public goods. Consumers are prevented from expressing their real preferences since each individual has them freely or at least at a lower price than a private producer; it is consequently difficult to optimally allocate the resources.

Local institutions that intend involvement as a keyword for change should be increasingly committed to a culture of participation. This can be possible only by involving citizens in protection, preservation, care but also by the management of the urban heritage, increasing the sense of responsibility towards an asset common that contributes to the formation of personal identity and of the community itself. From this perspective, shared revitalization becomes a significant means of action that can contribute to the construction of the city's identity, capable of increasing its attractiveness. If well managed, it can also trigger the development of economic activities for creativity, culture, community interaction and social integration.

6.3. Essential data and suggestion for implementation

Cultural heritage value cannot be measured by completely objective metrics and many issues giving value to the assets are subjective and concern people sensitivity. In this assessment, the asset value is obtained by elaborating the outcomes of questionnaires presented to people that know the historic area considered and that are part of the community living in this place. Two types of questionnaires are considered: (1) The first one concerns social-cultural issues, and it collects opinions from people that are members of the community related to the cultural assets. (2) The second one concerns artistic-historic information, and it collects opinions from experts. Two different formats have been elaborated to collect the two types of information.

The criteria guiding the formulation of questions of these surveys are described below. Raw information consists of answers to questionnaires and the outcome can be described by one or more relevant indexes. The first questionnaire should be distributed to a wide range of random samples of people and it could benefit from a diffusion-based smartphone app. The second questionnaire should be distributed to a panel of experts, selected by stakeholders involved in the use, preservation, and promotion of cultural heritage.

6.3.1. *Social-Cultural Issues*

This questionnaire aims to evaluate the importance that inhabitants give to the cultural assets of the area, considering different points of view, for example, the symbolic perspective, the recreational opportunities, the affection to local traditions and their role in reminding the area history and the community origin.

The questionnaire consists of 10 questions, and it takes into exam a list of cultural assets. The respondent is asked for expressing an opinion for each of the assets of the list. In the end, the respondent can add some further objects (building, church, museum, park, painting, artefact, or similar) believed to be important for the community.

The questionnaire is anonymous, but it includes a section about personal information regarding the respondent. This part is not mandatory, but this type of information can be very useful to evaluate the outcomes of the survey and to inform public bodies about the wishes of inhabitants and orient future actions.

As a first proposal, the considered fields include gender, monthly income, nationality, occupation, educational level. To simplify the data handling, answers are organized by multi-choice options. However, the number of classes should be calibrated rationally, considering the number of people participating in the survey and specific issues of the context.

Any processing of personal data must take place in compliance with the principles set out in Article 5 of Regulation (EU) 2016/679.

6.3.2. *Artistic-historic Issues*

This survey aims to provide information about a set of points regarding the artistic/historic value of a list of cultural assets. Differently from the previous case, this type of evaluation should be based on documents, surveys and specific studies on each asset considered in the list. Accordingly, this evaluation must be carried out by a set of experts with knowledge in the specific artistic branches of which the good is expression. The nomination of the expert panel is a key point, and the experts should be carefully selected by the stakeholders having a role in the use, preservation, and promotion of the assets.

For each point, the evaluation is obtained by proposing a set of possible answers (multiple-choice approach). In this case, the number of possible choices varies question by question, and an integer number is associated with each answer (the higher the number, the higher the artistic value is) In this case the choice “I don’t know” is not possible because it is assumed that the set of experts can answer to all the questions. Differently from the previous case (social-value questionnaire), in this survey the experts are required to justify their choice, filling a field “comments and motivations”.

This survey is not anonymous and the persons answering the questions are declared in advance. So, the part collecting information about respondents is not present.

Questions are quite general, and they should work for diverse types of assets (e.g. a church, a museum, or a botanic garden), even if experts will consider different technical parameters in the assessment. However, some adjustments and specializations could be required for particular assets.

A Glossary of technical terms may help to understand the questionnaire and avoid misunderstandings in questions and comments. A (very first) draft of a glossary, mainly based on UNESCO documents, is reported in the appendix.

The questionnaire consists of 9 [A-I] evaluation points. For each point, some illustrative notes are reported (in italic), as well as the multiple-choice answers and the score corresponding to each answer.

6.3.3. *Value assessment and data processing*

The collected data are used to provide synthetic information about the cultural-social value of each asset evaluating an index, which is obtained by a weighted summation of normalized answers. The score of each answer is divided by 4, to vary in the range [0,1], and the final index is obtained by considering the weights reported Table 11. This is a proposal, and weights should be decided by stakeholders or entities involved in the administration of cultural heritage. Different weights could be assigned to different cultural assets, coherently with their specific characteristics.

Table 11: Criteria and weights for cultural-social value.

Asset: XXX	CRITERIA	WEIGHT%
	A. Role of the context	5
	B. Realization Period	15
	C. Transformation level	10
	D. State of Conservation	15
	E. Current Use	10
	F. Documentation/Divulgation	5
	G. Uniqueness	10
	H. Artistic value of unmovable components	15
	I. Artistic value of movable components	15

6.4. Example

The cultural-social value assessment has been experimented on the cultural heritage of Camerino district.

Significant architectural assets which suffered significant damage due to the earthquake have been selected: these are architectural assets belonging to various historical periods, which presented tangible and intangible values for the community and in some cases also contain movable assets of high value. The questionnaires can provide information on the social and historical-artistic values expressed by these significant assets, which can then be extended to the other buildings in the Camerino district to have a general map of the values expressed by local cultural heritage. This example can be extended to other cities, identifying specific local and cultural contexts.

The questionnaire proposed concerns some singular assets (heritage level – stakeholders survey) but also for generic constructions (building aggregation – Community survey) which, although representing examples of minor buildings, have a particular meaning for the entire community.

The Cultural Heritage Asset of Camerino District with Historic-Artistic and Social Values is shown in Table 12.

Table 12: Cultural Heritage Asset of Camerino District

Asset X	Cultural Heritage Asset of Camerino District	
1.	**Cathedral of St. Annunziata** Rebuilt by Andrea Vici and Clemente Folchi in the early nineteenth century on the site of the Romanesque-Gothic cathedral destroyed by the earthquake of 1799. The church has a Latin plan and a façade with an arcade as an extension of the Episcope Palace. Inside and in the sacristy are placed valuable polychrome wooden sculpture of the thirteenth century (Crucifix) and the fifteenth century (Madonna della Misericordia), as well as interesting paintings by artists of the seventeenth century. The painter Carlo Crivelli made a now dismembered polyptych that is now located in various museums.	
2.	**Monastery of St. Philip** The monastery of Saint Philip was designed by Pietro Loni of Lugano and Domenico Cipriani of Cesena for the Oratorians Congregation. The building was completed around 1773 and damaged by the earthquake of 1799 and subsequent seismic events. The church is characterized by an elliptical plan with side chapels that represents a mediation between the baroque tendencies and the classicist instances. The façade is particularly interesting, in brick and stone, with lesene adorned with Ionic capitals. The façade is divided into two orders: the lower has a portal decorated in stone; the upper has a curved eardrum supported by the lesenes.	
3.	**St. Venantius Martyr** The imposing basilica was built in the 12th century on the seat of a previous church located in the place of martyrdom of the saint. From the 13th century the church gained importance and was elevated to Collegiata. Reworked several times over the centuries, it was radically rebuilt after the 1799 earthquake. In the 19th century, Luigi Poletti rebuilt neoclassical naves and modified the primitive façade. The neoclassical front consists of a pronaos supported by six columns on which rests the eardrum with serrated frames. The medieval façade is set back about ten meters and in the centre is adorned with a portal of the mid-fourteenth century made by the Camerino stones worked.	

4.	**Sanctuary of St Maria in Via** The church was designed on the site occupied by a small oratory, purchased by Cardinal Angelo Giori between 1639 and 1642. In 1643, the Cardinal acquired a revered 19th-century image of the Virgin, attributed to the Master of Camerino and started the project of a new church, consecrated in 1654. The plant is elliptical with four lateral semicircular chapels. The chapel of the crucifix and a baptistery occupy the front space, while towards the apses there is the oratory and the sacristy, which open into the newsstand with the icons of the Virgin. The original ceiling collapsed during the earthquake in 1799 and was replaced by a trussed roof. The church was again damaged by the 1997 earthquake and opened in September 2006, only to be damaged again by the 2016 earthquake.	
5.	**Monastery of St. Dominic** The Dominican settlement in Camerino should date back to the day after the Swabian sack of the city in 1259. The first certain news dates back to 1286 when Pope Honorius IV asks the Bishop of Camerino about the use by Dominicans of the Church of St. Sebastian. It is now owned by the University and is used as a museum. The complex was damaged by the 2016 earthquake and the safety work has been carried out.	
6.	**Ducal Palace** The Ducal Palace or Palace of "Da Varano" is a typical Italian Palaces of the 13th-15th centuries. It was built in several phases of which three are the main ones. Three different moments that can be interpreted as an expression of the ambition towards the conquest of political and civil power (the Houses of Gentile, thirteenth century), the affirmation (the Palace of Venazio, 14th-15th century), the complete consecration of power achieved both from a military and political-civil point of view (the Houses Nine or The Palace of Julius, 15th century). The oldest nucleus was built by Gentile Varano in the second half of the 13th century. A passage, called the bridge of the Virgin, united the palace at the Dome. In 1380 Venanzio Varano continued the work incorporating some houses of the Vicomanni of Belforte Family. The most recent building, called "palazzo nuovo" or Palace of Julius was started in the 15th century by Giulio Cesare Varano and has inside a courtyard,. The *Loggiato* allows the access to various rooms including the so-called *Sala degli Sposi* with frescoes from the 15th century XV and to the panoramic terraces from which you can see the surrounding landscape and overlook the botanical garden.	

7.	**Borgesca Fortress** The construction was commissioned by Cesare Borgia who entrusted the drawing to Ludovico Clodio in 1503. Borgia wanted the control of the city from the south-west side: the cylindrical towers and the keep are examples of military architecture of the early Renaissance. The fortress was later restored by Giovanni Maria Varano who had managed to regain the city of Camerino. Other interventions were carried out by Guidobaldo della Rovere, then by Ottavio Farnese and later by the Papal States. Initially, the Fortress was divided by means of an overhang and could only be reached through a drawbridge. The depression was definitively filled in the seventeenth century and over time many of the defensive structures were lost.	
8.	**Foschi – Battibocca Palace** The palace was built around the end of the 18th century by the Foschi family, connecting the adjacent buildings. The decorations, by the local nineteenth-century painters, enrich the internal. In 1885, the palace was sold to the Battibocca family. From 1977 the University buys the palace, and it becomes first the seat of the Rectory and then of administrative offices.	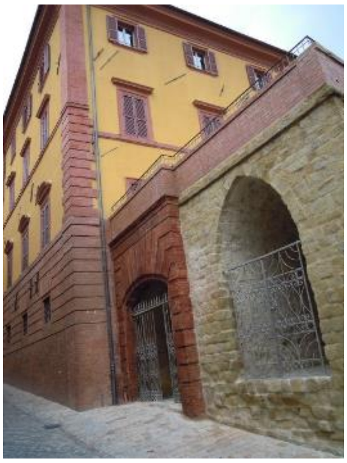
9.	**Pious Institute of the “Esposti”** The origins of the Institute date back to the 15th century with the meeting of various Hospices for pilgrims, exposed and sick existing in the city and gathered in a single entity by Julius Caesar of Varano. In 1782 the pre-existing structures were consolidated with the closure of the ancient loggia through bearing septs and with the realization of masonry reinforcements at the left side. The building has an unusual trapezoidal plan, adapted to the site near to the urban defensive walls.	
10.	**Town Hall and Marchetti teather** Seat of the Bishops of Camerino, the palace was given to the Municipality in 1573 by Bernardo Bongiovanni, after the start of the work of the new episcope. Inside there are interesting decorations. In 1728 the first theatre of Camerino was built under the name “La Fenice”. The next theatre fu costruito was built 1845 by Vincenzo Ghinelli, an important architect who also designed the theatres of Senigallia, Urbino, Cesena, Fabriano and Pesaro. The Sala has a horseshoe plan with three orders of and a balcony. The neoclassical decoration is the work of the decorators Girolamo Domenichini and Giuseppe Rinaldi. Opened in 1990, after the restoration work, it contains ruins of a Roman cryptoporticus in the underground. At present, it has significant damage as a result of the 2016 earthquake.	

6.4.1. *The questionnaire of Social Value*

The purpose of this questionnaire applied to Camerino district is to point out guidelines to design this survey to provide an operational tool for acquiring this type of information. These new data will integrate those already existing on the historical and artistic value of the property to allow a more complete evaluation of cultural heritage value.

The survey aims to provide information about a set of general topics, denoted as macro-criteria, and more specific information for each topic (sub-criteria) (Table 13). For each criterion, opinions are obtained by asking a question to people and proposing a set of possible answers (multiple-choice approach).

The questionnaire of Social Value consists of ten questions concerning a list of cultural assets, previously identified for the research. The respondent can assign a value from 0 to 4 “ (e.g. “very high” = 4, “high” = 3, “medium” = 2, “low” = 1, “no significant” = 0) for each considered asset. The answer "I don't know" = no answer is possible in the case of absence of opinion or lack of knowledge regarding the asset.

The questions that have been submitted to the Community concerning social values are shown in Table 14.

Table 13: Macro-criteria description for the survey

MACRO CRITERION	DESCRIPTION
Perceived historical value	A good understanding of the heritage value of a site, building or object is a value and the major reason underlying its preservation
Symbolic, affective or devotional value	Values and processes of evaluation of symbolic, affective and devotional of cultural heritage that are fundamental parameters for understanding the societies and social groups that build it and find meaning in it.
Social Value	Social value encompasses the significance of the historical environment for contemporary communities, including people's sense of identity, belonging and place, as well as forms of memory and spiritual association. These are specific forms of value created through experience and practice.
Recreational value and other	The economic value of cultural heritage can be defined as the amount of welfare, comfort and entertainment that heritage generates for society.

Table 14: Questions submitted to the Camerino community

Question on perceived historical value						
1	To what extent do you think that the following assets have a significant historical or artistic value, based on your personal knowledge and sensitivity? (*For example, do you think they have a high artistic value thanks to the mastery they were made, or the ability of their authors?)*					
Asset 1	4 [ ]	3 [ ]	2 [ ]	1 [ ]	0 [ ]	no answer [ ]

Asset 2	4 [ ]	3 [ ]	2 [ ]	1 [ ]	0 [ ]	no answer [ ]
…	4 [ ]	3 [ ]	2 [ ]	1 [ ]	0 [ ]	no answer [ ]
Questions on symbolic, affective or devotional value						
2	How important do you think these goods are to you from a symbolic, emotional or devotional point of view? (*For example, are they related to your childhood memories or to important events in your life?)*					
Asset 1	4 [ ]	3 [ ]	2 [ ]	1 [ ]	0 [ ]	no answer [ ]
Asset 2	4 [ ]	3 [ ]	2 [ ]	1 [ ]	0 [ ]	no answer [ ]
…	4 [ ]	3 [ ]	2 [ ]	1 [ ]	0 [ ]	no answer [ ]
3	How important do you think these goods are to the community inhabiting the place, from a symbolic, emotional, or devotional point of view? (*Are they, for example, strongly or weakly related to traditions, popular festivals or religious events?)*					
Asset 1	4 [ ]	3 [ ]	2 [ ]	1 [ ]	0 [ ]	no answer [ ]
Asset 2	4 [ ]	3 [ ]	2 [ ]	1 [ ]	0 [ ]	no answer [ ]
…	4 [ ]	3 [ ]	2 [ ]	1 [ ]	0 [ ]	no answer [ ]
4	How much do you think these cultural goods represent the identity of the place? *(Can for example be a symbol of the city, as the Colosseum for Rome?)*					
Asset 1	4 [ ]	3 [ ]	2 [ ]	1 [ ]	0 [ ]	no answer [ ]
Asset 2	4 [ ]	3 [ ]	2 [ ]	1 [ ]	0 [ ]	no answer [ ]
…	4 [ ]	3 [ ]	2 [ ]	1 [ ]	0 [ ]	no answer [ ]
5	How important is it to transmit this symbolic, emotional or devotional value (question 2/3) to the next generations? *(Considering that young people might no longer know the local traditions related to these goods?)*					
Asset 1	4 [ ]	3 [ ]	2 [ ]	1 [ ]	0 [ ]	no answer [ ]
Asset 2	4 [ ]	3 [ ]	2 [ ]	1 [ ]	0 [ ]	no answer [ ]
…	4 [ ]	3 [ ]	2 [ ]	1 [ ]	0 [ ]	no answer [ ]
Questions on social value						
6	To what extent do you think the following cultural assets could be an adequate location to host cultural events? *(Question refers to events like expositions, debates with experts, conferences, seminars)*					
Asset 1	4 [ ]	3 [ ]	2 [ ]	1 [ ]	0 [ ]	no answer [ ]

Asset 2	4 [ ]	3 [ ]	2 [ ]	1 [ ]	0 [ ]	no answer [ ]
…	4 [ ]	3 [ ]	2 [ ]	1 [ ]	0 [ ]	no answer [ ]
7	How important is it to organize cultural events in these locations in order to make them a cultural reference points for the city and surrounding region? (*For example, would it be important that thematic lectures, workshops, or conferences to be held there?)*					
Asset 1	4 [ ]	3 [ ]	2 [ ]	1 [ ]	0 [ ]	no answer [ ]
Asset 2	4 [ ]	3 [ ]	2 [ ]	1 [ ]	0 [ ]	no answer [ ]
…	4 [ ]	3 [ ]	2 [ ]	1 [ ]	0 [ ]	no answer [ ]
8	To what extent would you like the following goods to be promoted by actions enhancing the knowledge of them at national and international level? (*For example, virtual visits or augmented reality could enhance the interest in these CH goods).*					
Asset 1	4 [ ]	3 [ ]	2 [ ]	1 [ ]	0 [ ]	no answer [ ]
Asset 2	4 [ ]	3 [ ]	2 [ ]	1 [ ]	0 [ ]	no answer [ ]
…	4 [ ]	3 [ ]	2 [ ]	1 [ ]	0 [ ]	no answer [ ]
Questions on recreational value						
9	How important is it to organize recreational events in these places to make them reference points for the city and surrounding region? (*For example, pop music concerts, dancing, happenings, contests)*					
Asset 1	4 [ ]	3 [ ]	2 [ ]	1 [ ]	0 [ ]	no answer [ ]
Asset 2	4 [ ]	3 [ ]	2 [ ]	1 [ ]	0 [ ]	no answer [ ]
…	4 [ ]	3 [ ]	2 [ ]	1 [ ]	0 [ ]	no answer [ ]
10	How much can these goods represent a resource for sustainable tourism? (*For example, offering local products, tour packages combining cultural and natural contents, promoting actions using touristic profits to ensure a continuous asset preservation*					
Asset 1	4 [ ]	3 [ ]	2 [ ]	1 [ ]	0 [ ]	no answer [ ]
Asset 2	4 [ ]	3 [ ]	2 [ ]	1 [ ]	0 [ ]	no answer [ ]
…	4 [ ]	3 [ ]	2 [ ]	1 [ ]	0 [ ]	no answer [ ]

The answers collected were processed taking into account information related to respondents (gender, age, monthly income bracket, nationality, occupation, educational level) (Table 15).

Other analyses of data can be of interest, as the evaluation of the index dispersion or analytical analyses reporting scores for each question or each criterium, e.g. by radar graph (Figure 53).

The collected data will provide an index, which is obtained by a weighted summation of normalized answers.

The score of each answer is divided by 4, to vary in the range [0,1], and the final index is obtained by considering the weights reported in Table 16.

The results of the questionnaire are shown in Figure 45, Figure 46 and

Table 17. Figure 47 shown a map of the outcome extended to the whole historic centre of Camerino.

Table 15: Respondent personal information

Information		Tick
Gender	female	
	male	
	diverse	
Age (years)	6-14	
	15-18	
	19-25	
	25-35	
	36-55	
	55-85	
	>85	
Income bracket (euros monthly)	<1000	
	1000-1500	
	1500-3000	
	3000-5000	
	>5000	
Nationality	Italian	
	UE	
	Extra-UE	
Occupation	student	
	teacher	
	professional	
	employee	
	unemployed	
	artisans	
	traders	
	housekeeper	
	entrepreneur	
	pensioner	
	other	
Educational level	Elementary school	
	lower secondary school	
	upper secondary school	
	degree	
	PhD/master	

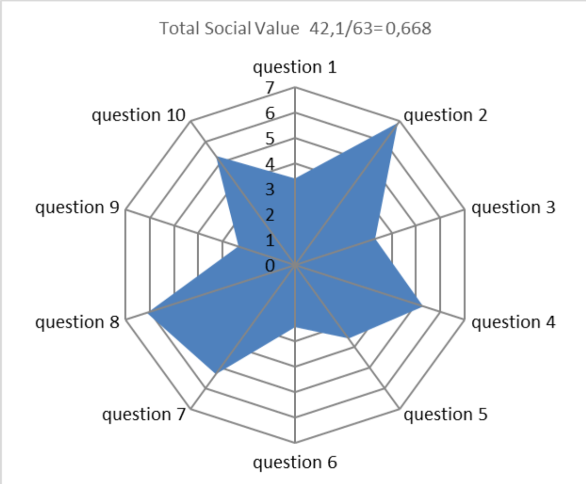

Figure 44: Radar graph reporting scores for each question

Table 16: Weights related to each question of the survey

n.	QUESTION	MACRO-CRITERION	SUB-CRITERION	WEIGHT %
1	To what extent do you think that the following assets have a significant historical or artistic value, based on your personal knowledge and sensitivity?	PERCEIVED HISTORICAL VALUE	Value of knowledge	**15**
2	How important do you think these goods are to you from a symbolic, emotional or devotional point of view?	CULTURAL, SYMBOLIC, EMOTIONAL OR DEVOTIONAL VALUE	Value for the community	**10**
3	How important do you think these goods are to the community inhabiting the place, from a symbolic, emotional, or devotional point of view?		Personal perception value	**10**
4	How much do you think these cultural goods represent the identity of the place?		Identity value	**10**
5	How important is it to transmit this symbolic, emotional or devotional value (question 2/3) to the next generations?		Identity value	**5**
6	To what extent do you think the following cultural assets could be an adequate location to host cultural events?	SOCIAL VALUE	Social value	**5**
7	How important is it to organize cultural events in these locations in order to make them a cultural reference points for the city and surrounding region?		Interest value	**10**
8	To what extent would you like the following goods to be promoted by actions enhancing the knowledge of them at national and international level?		Expectation value	**10**
9	How important is it to organize recreational events in these places to make them reference points for the city and surrounding region?	RECREATIONAL VALUE AND MORE	Recreational value	**10**
10	How much can these goods represent a resource for sustainable tourism?		Resource value	**15**

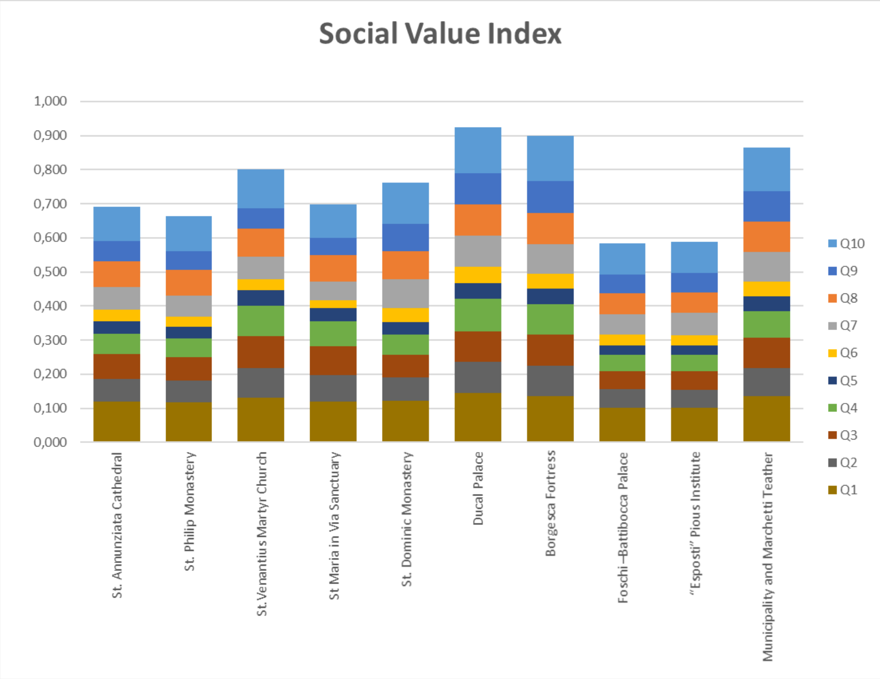

Figure 45: Social Value index with the scores of the different questions

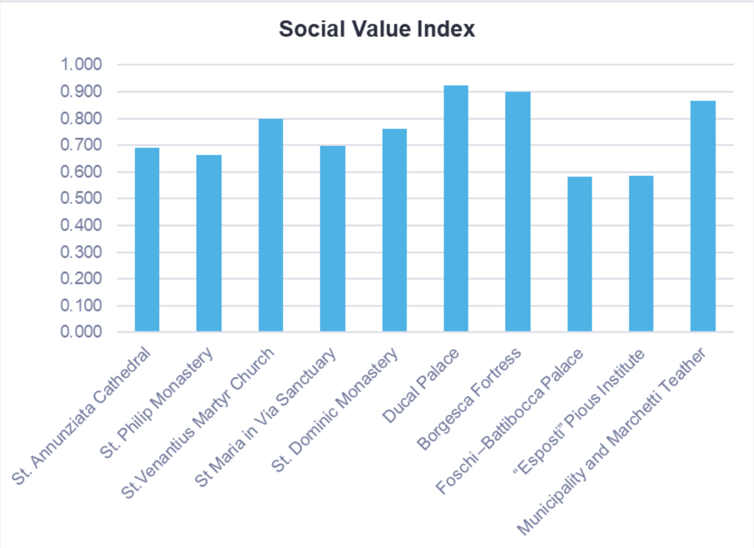

Figure 46: Social Value Index of the 10 most significant architectures of Camerino District

Table 17: Social Value Index - analysis of the values obtained from the questionnaire after their normalization

	Weigth	15	10	10	10	5	5	10	10	10	15	
	Question	Q1	Q2	Q3	Q4	Q5	Q6	Q7	Q8	Q9	Q10	INDEX
Architectural Heritage	St. Annunziata Cathedral	0,120	0,065	0,073	0,061	0,037	0,034	0,065	0,076	0,059	0,100	0,690
	St. Philip Monastery	0,116	0,066	0,067	0,056	0,034	0,031	0,062	0,075	0,056	0,102	0,664
	St.Venantius Martyr Church	0,131	0,088	0,094	0,088	0,046	0,030	0,067	0,084	0,059	0,113	0,800
	St Maria in Via Sanctuary	0,119	0,078	0,085	0,072	0,039	0,024	0,055	0,077	0,051	0,098	0,698
	St. Dominic Monastery	0,123	0,067	0,066	0,059	0,037	0,042	0,083	0,084	0,079	0,122	0,762
	Ducal Palace	0,144	0,091	0,091	0,094	0,047	0,046	0,091	0,093	0,089	0,137	0,925
	Borgesca Fortress	0,136	0,089	0,091	0,091	0,046	0,044	0,087	0,091	0,093	0,134	0,900
	Foschi – Battibocca Palace	0,102	0,055	0,052	0,048	0,028	0,031	0,060	0,063	0,055	0,091	0,584
	“Esposti” Pious Institute	0,100	0,054	0,054	0,048	0,028	0,031	0,064	0,062	0,056	0,091	0,587
	Municipality and Marchetti Teather	0,134	0,084	0,088	0,080	0,043	0,044	0,087	0,087	0,089	0,129	0,865

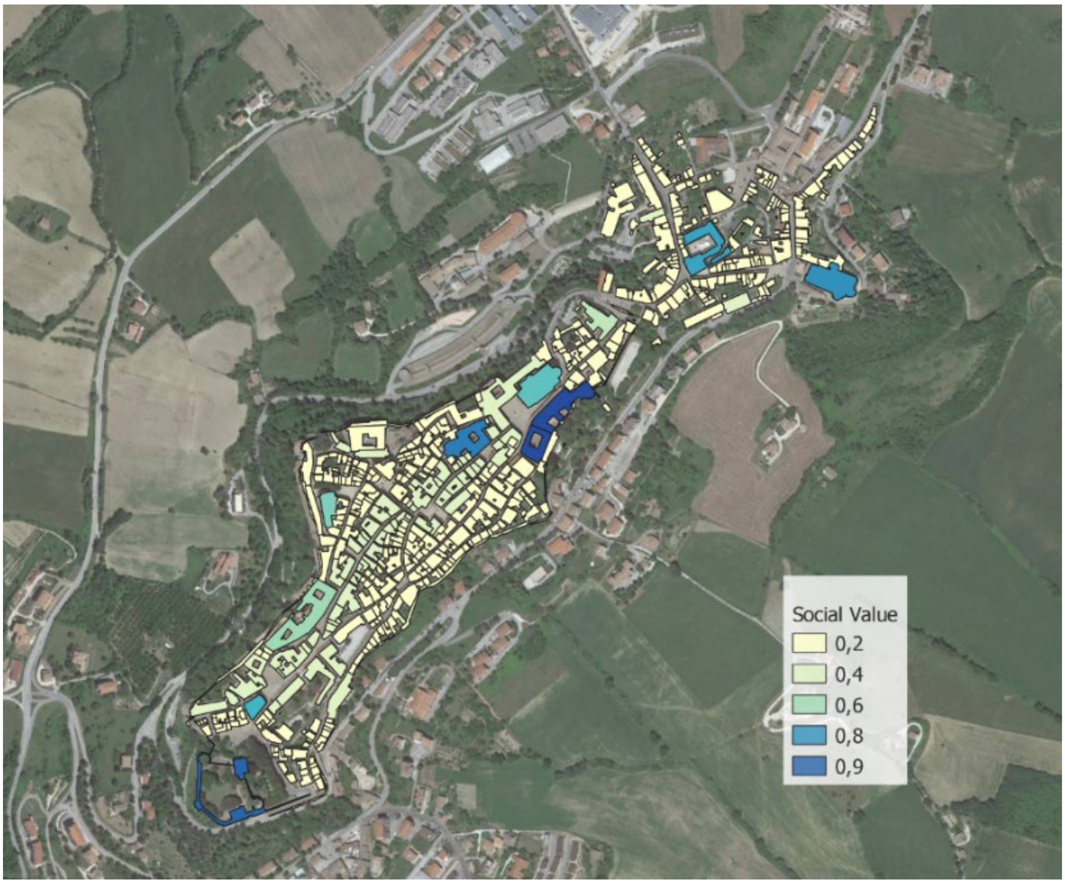

Figure 47: Plan of the historic centre of Camerino with the areas where the social value index is indicated for each building. Some areas are more significant than others, especially those where the main cultural, commercial and social activities took place

6.4.2. *The Artistic Value questionnaire*

As part of the activities of WP5, a structured online questionnaire is applied to some assets of Camerino district but can be applied in other contexts. It is proposed a wide-ranging survey of the cultural heritage to identify a possible classification of the artistic value. The reference documents for the recognition of the Artistic Value Index are represented by the legislation concerning Cultural Heritage. Currently, Italian cultural heritage is subject to the Code of cultural heritage and landscape - Legislative Decree 22 January 2004, n. 42. The recognition of the “artistic value” of a cultural asset can only derive from an evaluation made by the community of experts of the individual branches of art, particularly competent both in the specific artistic branch and in the socio-cultural area.

For these reasons, the questionnaire form is filled by experts, so it is not anonymous and the people answering the questions are declared in advance. Some stakeholders selected with distribution by gender (Male, Female Diverse), can answer various questions that enter into the merits of some technical aspects related to the nature of the goods covered by this questionnaire. Subsequently, the questionnaire can be integrated and corrected based on their observations. The sample to which the questionnaire will be administered, although not probabilistic, meets some criteria that it was intended to adopt for the research.

The *Artistic Value Index* (AVI) is proposed for different types of cultural heritage including churches, palaces, fortresses, museums, but also natural heritage. The heterogeneity of the assets requires a considerable simple and flexible approach useful for general applications in the various case studies.

The recognition of the “artistic value” of a cultural asset can only derive from an evaluation made by the community of experts, particularly competent both in the specific artistic branch and in the socio-cultural currents of which the good is expression.

The Methodology are similar and general framework is used for different assets, and it is based on a selected set of Macro-Criteria chosen for the assessment. The collected data are used to provide synthetic information about the historic-artistic value of each asset, evaluating an index obtained by a weighted summation of answers.

- The questionnaire includes 9 [A-I] multiple-choice closed questions.
- The responses of single fields are scaled to vary in the range.
- To complete the answer, a comment/explanation box is inserted about each answer.

The test is composed of questions shown in Table 18 asked to a significant sample of experts who have already collaborated within the ARCH project.

Table 18: Social Value Index - Questions submitted to the expert audience

General framework
A. Role of Context
The valuation is made based on the context in which the asset is located and this context contributes to the evaluation of the artistic index.
• High (2)

• Medium (1)
• Low (0)
B. Realization Period
of the historical period in which the asset was built (its first origin). The following periods were considered, attributing to each a specific score, which increases according to the greater antiquity of the asset:
• Ancient before 476 (3)
• Middle Ages 476 – 1492 (2)
• Modern 1492 - 1789 (1)
• Contemporary post 1789 (0)
C. Transformation level
The level of transformation of the asset is evaluated in its current state, compared to the initial one, considering whether the transformation has increased the artistic value:
• Significant (2)
• Partially significant (1)
• No significant (0)
D. State of Conservation
The state of conservation of the asset is assessed in relation to possible forms of material and structural degradation, also considering national specific reference documents. (Es. For Camerino district see *Code Nor.Mal 1/88* or *Linee guida per la valutazione e la riduzione del rischio sismico del patrimonio culturale con riferimento alle Norme tecniche per le costruzioni*, Decreto del Ministero delle Infrastrutture e dei trasporti 14 gennaio 2008).
• Good (2)
• Medium (1)
• Poor (0)
E. Current Campatible Function
The current function and its compatibility concerning the conservation of the asset is evaluated
• Compatible Used (2)
• Partially Compatible used (1)
• Unused (0)

F. Documentation/Divulgation
It is evaluated how much the property has been studied and is known not only to the experts but also to the Community.
• Comprehensive (2)
• Essential (1)
• Poor (0)
G. Uniqueness
The uniqueness of the asset is evaluated under a Historic, Artistic, Symbolic perspective
• High (2)
• Medium (1)
• Low (0)
(H+I) Assessment from components
The complexity of the asset is assessed concerning its articulation into parts that are no movable component (facade, apse, transept, atrium, staircase, hall, frescoes, etc.) and to the various movable elements that contribute to its historical-artistic value (paintings, furniture, statues, pottery, etc.)
H. Assessment from components: No Movable Components Goods (facade, apse, transept, atrium, staircase, hall, frescoes, etc.)
• High (2)
• Medium (1)
• Low (0)
I. Assessment from components: Movable components (paintings, furniture, statues, pottery, etc.)
• High (2)
• Medium (1)
• Low (0)

To complete the answer, a comment/explanation box has to be filled.

The scheme can be applied to different assets of Cultural Heritage. The general information of Cultural Heritage of Camerino helps to understand the questionnaire, both for experts and non-experts.

The collected data are used to provide synthetic information about the historic-artistic value of each asset, evaluating an index obtained by a weighted summation of answers. A proposal for the weights is reported in Table 11, and the responses of single fields are scaled to vary in the range [0,1].

The results of the questionnaire are shown in Figure 48, Figure 49, Table 19. Figure 50 is shown a map of the outcome extended to the whole historic centre of Camerino; some areas are more significant than others and coincide with those that are subject to “Vincoli di Tutela” by the Superintendence for architectural heritage and landscape of the Marche Region

An examination of outcomes shows that some architectural assets have a particularly high social and artistic value, as they represent the symbol of the City. Furthermore, wanting to extend the social value also to the smaller building of the historic centre of Camerino, a series of interviews were carried out which allowed the identification of some sectors that are considered most significant in terms of social-artistic value and for which it is necessary to identify a strategy that allows the development of resilient actions.

The indexes from the questionnaires can be useful to define a priority order for interventions combining them with the indications of the Extraordinary Reconstruction Program, an instrument to govern the reconstruction of the entire municipal area aiming at a safe reconstruction, respectful of the historical-architectural, cultural-identity and landscape-environmental characteristics, and reasonably fast.

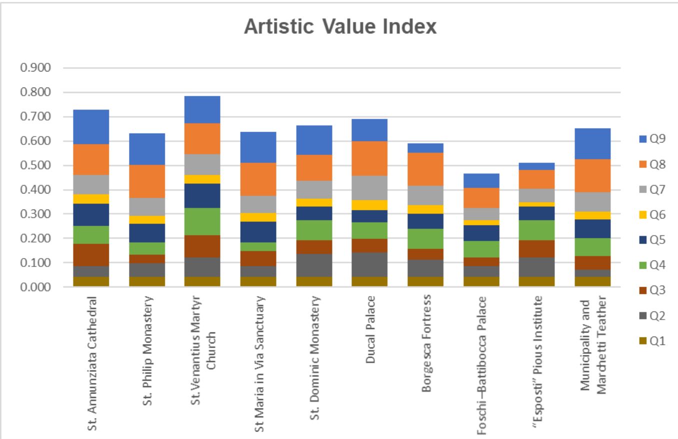

Figure 48: Artistic Value index with the scores of the different questions

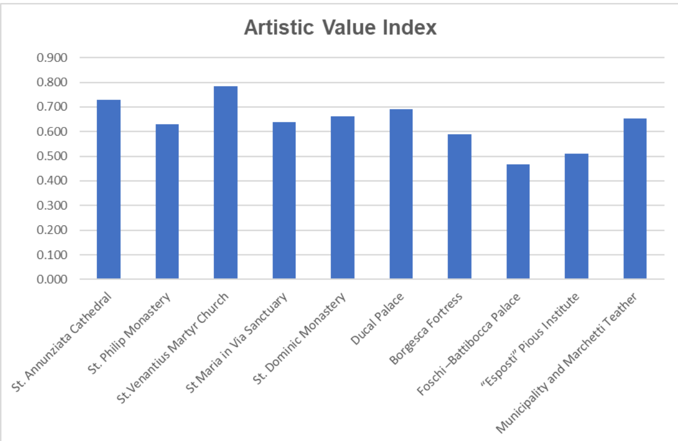

Figure 49: Artistic Value Index of the 10 most significant Architecture of Camerino District

Table 19: Artistic Value Index - Analysis of the values obtained from the questionnaire after their normalization

	Weigth	5	15	10	15	10	5	10	15	15	
	Question	Q1	Q2	Q3	Q4	Q5	Q6	Q7	Q8	Q9	INDEX
Architectural Heritage	St. Annunziata Cathedral	0,043	0,045	0,090	0,075	0,090	0,038	0,080	0,128	0,143	0,730
	St. Philip Monastery	0,043	0,055	0,035	0,053	0,075	0,033	0,075	0,135	0,128	0,630
	St.Venantius Martyr Church	0,043	0,080	0,090	0,113	0,100	0,035	0,085	0,128	0,113	0,785
	St Maria in Via Sanctuary	0,043	0,045	0,060	0,038	0,085	0,035	0,070	0,135	0,128	0,638
	St. Dominic Monastery	0,043	0,095	0,055	0,083	0,055	0,033	0,075	0,105	0,120	0,663
	Ducal Palace	0,043	0,100	0,055	0,068	0,050	0,043	0,100	0,143	0,090	0,690
	Borgesca Fortress	0,043	0,070	0,045	0,083	0,060	0,038	0,080	0,135	0,038	0,590
	Foschi –Battibocca Palace	0,043	0,045	0,035	0,068	0,065	0,020	0,050	0,083	0,060	0,468
	"Esposti" Pious Institute	0,043	0,080	0,070	0,083	0,055	0,020	0,055	0,075	0,030	0,510
	Municipality and Marchetti Teather	0,043	0,030	0,055	0,075	0,075	0,033	0,080	0,135	0,128	0,653

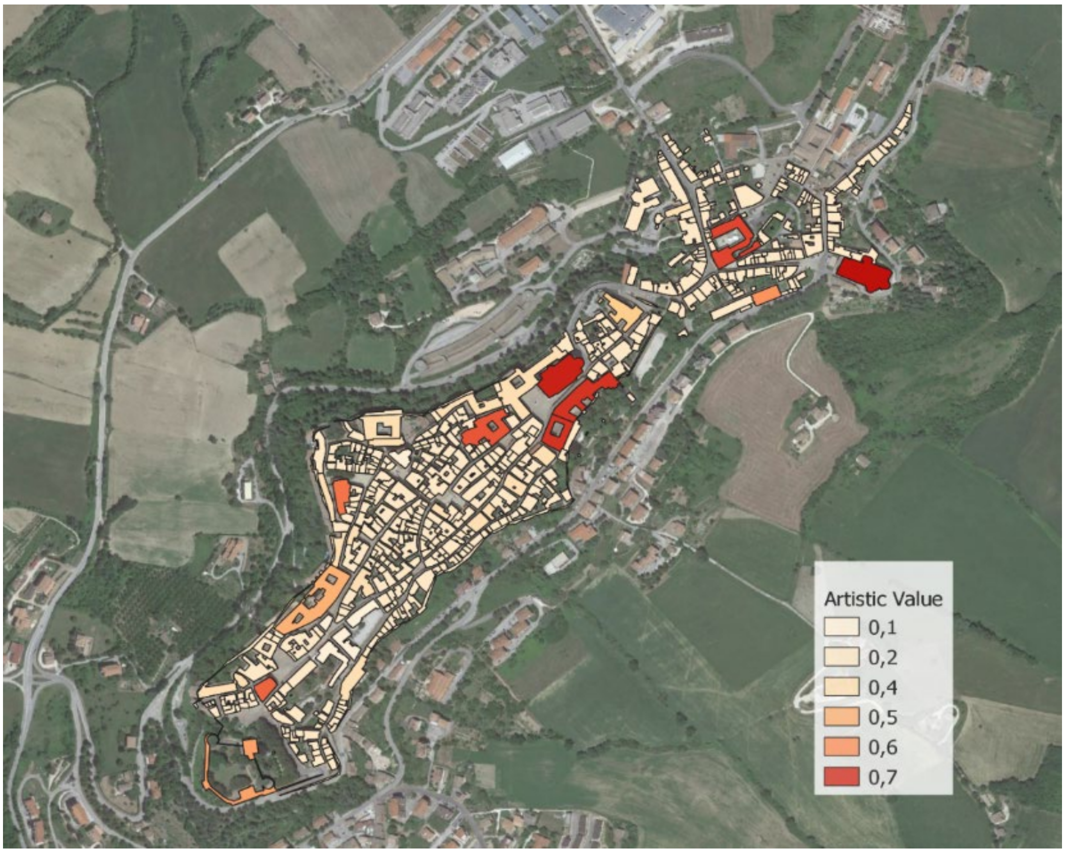

Figure 50: Plan of the historic centre of Camerino with the areas where the Artistic value index is indicated for each building

7. Post-Disaster Road network functionality in Historic Areas

(S. Giovinazzi)

7.1. Introduction to the problem

In the aftermath of a large-scale disaster, the delivery of relief is one of the most important tasks for disaster managers and must be fulfilled in the shortest possible time. Due to its evident role in emergencies, the road network condition plays an important role. The blockage of a road network compromises proper and efficient rescue operation and the evacuation of survivors and art works to safe areas. Similarly, the long-term consequences of road blockage might induce the disruption of customer access, commuting, and the fruition of Historic Area, generally speaking which greatly affects local businesses and employment [111].

The causes of damage to road networks might be diverse [112]. However, It was pointed out that in high-dense urban areas, such as Historic Areas (HAs) mainly depends on the seismic performance of buildings that may interfere network links ([113], [114], [115])

The ARCH project and this deliverable D5.2 therefore focus mainly on the issue road blockages in high-dense historic areas due to the debris from earthquake-induced damages, partial collapses or total collapses of the buildings facing the HAs road network.

A further aspect that might be worth investigating in future projects related to HAs is the management of such debris as due to their historic values it is important to manage them in a proper way, keeping however the focus on their timely removal from the road network to support the timely reestablishment of HAs functions [116].

The Disaster Waste Management Guidelines [117] recommend, as part of the emergency phase, cleaning the main streets within the first 72 h to provide access for search and rescue efforts and relief provisions; the same Guidelines recommend that disaster waste moved should stay in the emergency area until the early recovery phase when appropriate disposal sites will identified.

7.2. Scientific background and model for assessing post-earthquake road network functionality in Historic Areas

Moya et al (2020) [111] provide an exhaustive overview of approaches defined and implemented in the international community to assess road blockages in high-dense urban areas due to the debris from earthquake-induced damages. A summary of the literature review provided by Moya et al (2020) [111] is reported hereafter.

The Italian National Seismic Prevention Program assigns the potential interference of accessibility routes in relation to the height of isolated buildings, the height of structural aggregates, and the width of the street/road [118].

Goretti and Sarli (2006) [114] introduced a methodology to compute the seismic road vulnerability for urban areas, in which the road failure probability, P_f

I, and the number of building blockages when intensity I affects the road, $N_{b|j}$. Further development of the methodology requires the characterization of building vulnerability class, T, and probability that a building with vulnerability T will block the road, $P[b|T,I]$. Moreover, the computation of $P[b|T,I]$. Requires the definition of damage grades, d, the causes of road failure, k, and the probabilities $P[d|T,I]$, $P[b|T,I]$, and $P[k|d,T]$. Considering that the parameters T, k, and d are discrete variables, $P[d|T,I]$, and $P[k|d,T]$ are expressed in matrices and are evaluated based on the statistical analysis on Italian post-earthquake surveys. However, such detailed information is often unavailable in other regions.

Zanini et al. (2017) [115] pointed out that the quantification of the road area potentially obstructed by the debris is rather complex to be performed from an analytical model. Thus, a fuzzy logic system was employed to evaluate the obstructed road width. The fuzzy model was calibrated from a set of masonry building collapses that occurred in previous earthquakes. In the referred work, the percentage of obstructed road width due to a collapsed building i, α_{hbi}, was proposed as a function of the road width, W_{rs}, and the building height, H. The parameters *ahbi* and the debris extent, D, provide a similar information in different formats. For instance, for a collapsed building located beside a road and without any building in the other side of the road, $D = \alpha_{hbi} W_{rs}$ if $\alpha_{hbi} < 1$; otherwise $D > \alpha_{hbi} W_{rs}$. Osaragi and Oki (2017) [119] implemented an integrated simulation model of an earthquake-induced damage scenario. In their model, the safest assumption was made for the value of D, that is, the debris extent was considered to be equal to the building height, $D = H$.

Argyroudis et al. (2015) [113] pointed out that the debris width produced by a collapsed building that is extended further than the initial building's boundary, hereafter referred to as debris extent (D), is required for the road blockage assessment. Because of the complexity and the lack of information, the estimation was based on engineering judgments and assumptions. Thus, four simplified geometrical models of collapsed buildings were defined, each representing a collapse mode. Using such geometrical modes, D is computed as a function of the initial width of the building, W, the inclination angle of the collapsed building, c, the ratio between the volume of the building after collapse and the original volume, k_v, and the height of the building, H.

7.3. Necessary data and suggestion for implementation

The method embedded in the CIPCast-ES (i.e. ARCH DSS module specific for seismic scenario simulation), to assess the road vulnerability to ground failure [120] is based on the model proposed Argyroudis et al. (2015) [113]. As above-mentioned, according to Argyroudis et al. (2015) [113] a functionality level of a road after an earthquake can be estimated by evaluating the possible obstructions due to the presence debris of damaged/collapsed buildings on the road itself with the subsequent reduction of its available width. Argyroudis et al. (2015) [113] correlates the building geometry and shape with the possible resulting debris volume and shape as a function of the level of ground motion sustained by the building (this is a function of the earthquake severity, i.e. earthquake magnitude; the distance of the HAs from the earthquake source, i.e. hypocentre and the soil and morphological conditions of the site) and of the building seismic vulnerability (Ref to Section in this Report).

To apply such a methodology, CIPCast-ES makes use of the following data layers:

– V_i: seismic vulnerability index of the building;

– H_i: average height of the building;

– W_i: width of the building;

– W_r: width of the nearby road pavement;

– W_{br}: distance between the building facade and the nearby road;

– k_v: average building volume reduction after collapse;

According to Argyroudis et al. (2015) [113] a Gaussian distribution is used to estimate the variation of the debris width W_d (Figure 51) based on two parameters: the mean value $E[W_d]$ and the standard deviation σ_{W_d} which can be both calculated given the angle of collapse and the building volume reduction k_v (Figure XX).

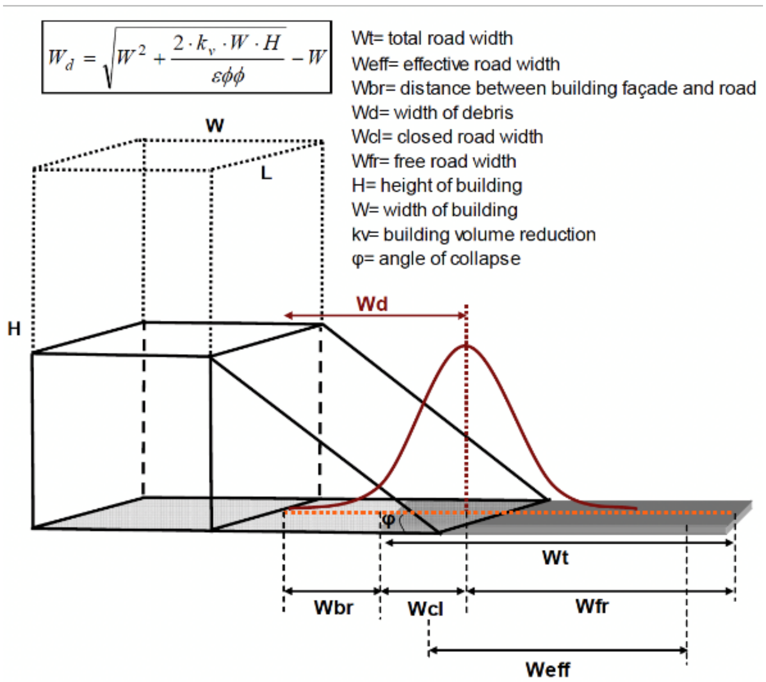

Figure 51: Gaussian distribution used to estimate the variation of the debris

Based on the earthquake simulation described in D5.3, the CIPCast-ES platform produces a physical damage assessment for the buildings that is characterized by the following data:

- Damage Level: for each building, a damage level according to the European Macroseismic Scale EMS-98 [Ref to Section in this Report] (ranging from D1 to D5, plus the absence of damage D0);

– W_d: the width of the debris heap resulting from the collapse of the building (with D5 damage level);

– W_{fr}: the width of the road that remains clear after the debris fall.

In order to evaluate the road blockage due to collapsed buildings (Figure 51), a functionality level FL, based on three thresholds FL0 , FL1 and FL2 , was defined for each building i, assuming a necessary minimum width of 3.5 m for (ordinary, not tracked) emergency vehicles to go through:

– F_{L0} , when $W_{d,i} \leq W_{br}$: the road is open;

– F_{L1} , when $W_{br} \leq W_{d,i} \leq W_{br} + W_r - 3.5$: the road is only open for emergency;

- F_{L2} when $W_{d,i} \geq W_{br} + W_r - 3.5$: the road is closed.

It should be noted that the simulations carried out by this approach were performed under the assumption of a worst-case scenario, i.e. when a generic building collapses, it spreads its debris only in the direction of the road (corresponding to the facade overlooking the road itself).

8. Socio-economic vulnerability

(A. Dall'Asta, S. Giovinazzi)

8.1. Socio-economic vulnerability assessment

8.1.1. *Models for socio-economics vulnerability*

At regional scale, there is a growing recognition that the vulnerability of communities is globally influenced by economic and social conditions and these elements strongly influence both the capability to face the emergency phase following extreme natural events and the capability to recover previous state in a short or long period. Therefore, a vulnerability assessment at large scale must include this type of information and evaluate, in some manner, their influence on the change due to hazardous event.

The economic and social conditions of a community and their dynamic variation triggered by extreme events is quite a complex problem, not yet fully investigated, and satisfactory predictive models are not available.

Some pioneeristic works have been recently developed [121] to relate hazard measures to variation of a reduced number of economic parameters. Conclusions cannot be considered definitive and adequately ample to provide a complete overview of the impact of hazards on communities. It is reasonable to think that these types of studies will find an increasing interest in the next future and will be included in analytical assessment of risk and resilience.

Nowadays, the qualitative approach based on vulnerability indicators is more diffused and a consolidated literature on this topic is available. As discussed in the introductory part of the Handbook, this approach provides information at qualitative level only, however, it is anyway satisfactory for planning purposes because a comparison between different sources of vulnerabilities is possible, as well as a comparison among districts with different socio-economic characteristics.

A recent paper [122] can be assumed as a reference point, because it illustrates, in a critical and exhaustive way, the most of the literature on the topic, ([123], [124], [125] [126], [127], [128]) and proposes a general framework that can be applied to regions with different characteristics and different properties regarding the potential sources of negative impacts. The reader may refer to [122] and to [129] for a comprehensive state of art.

This approach gives a picture of the problem paying attention to the complexity of the system and to the multifaceted nature of the impact.

As mentioned above, it is based on the evaluation of a set of vulnerability indicators considering different aspects that may influence, in a negative or positive manner, the impact of the natural event to the socio-economic layout of the community studied. They take into consideration in an explicit way the following three concepts.

The exposure, intended as the nature and the degree to which a system experiences environmental or socio-political stress, according to [130].

The susceptibility, intended as the pre-existing socioeconomic conditions of communities that increase their vulnerability to external factors, with a special regard to natural disaster and climate change related factors. This point involves impacts on economic activities, infrastructure, demographic structures ([131], [132], [133]).

The third point concerns the resilience, intended as the capacity of the system to absorb, respond, and recover from an external perturbation ([134], [135]).

The three concepts are temporarily related to the event, according to Figure 52 [122].

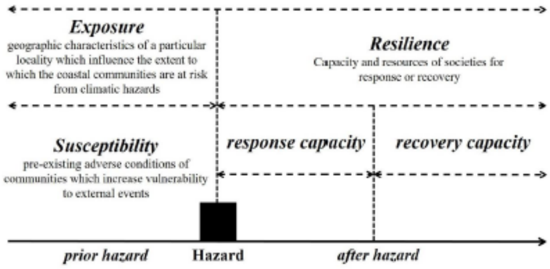

Figure 52: Vulnerability components in relation to the timing of hazard event [Jhan et al. 2021]

A list of potential indicators is reported in the following Figure 53, extracted and slightly modified from [122]. The list collects the most diffused indexes and groups them in "families". This is a list of potential indexes that may play a role in the system vulnerability but a short list should considered, case by case, based on their accessibility (is the data available for all the systems to be assessed?), acceptability (can the indicator apply to the system?), and representativeness (does the indicator significantly influence the vulnerability of the system considered with respect to the hazard of interest?).

Therefore, the previous list must be intended as an initial suggestion for the selection of indicators for the particular chain hazard-vulnerable system-consequence to be evaluated, however a shorter list can be used, applying mentioned selection criteria. Some further indicators can be added in special situations not yet analysed in the literature, or to provide a more refined vulnerability assessment.

Table 20: Potential list of vulnerability indicators

Theme	Indicator
Population structure	Population growth
	Population density
	Dependency ratio
	Young
	Elder
	Lone Parents
	Family Composition
	Race / Ethnicity
	Aging
Access to resources	Literacy
	Educational Level
	Population in the workforce
Physical limitation	Gender
	Disability
	Mortality rate
	Infant mortality
	Maternal mortality
	Birth rate
	Life expectancy
	Special needs populations
Economic Status	Income
	Poor household
	Insurance
	Unemployment
Housing/ Transportation	Housing unit
	Housing tenure
	Available vehicle
	Mobile home
	Crowding
	Residential property
Industrial Development	Employment in primary industry
	Value of primary industry
	Area of primary industry
Physical Infrastructure	Medical service
	Other Public facilities
	Access to water supply
	Access to other supplies
Financial state	Self-financing resources
	Receipts from taxes
Cultural heritage	CH social value
	CH historic-artistical value
	CH related economical activities
	Inhabitants living in CH related buildings or areas

8.1.2. *Analysis methods and index combinations.*

Rough information about different indicators cannot be directly compared, as they concern different objects, so it is necessary to make them uniform by a normalization rule, mapping initial value to value in the range [0,1], or [0,100]. if a percentile value is preferred. Different techniques can be used (e.g. [136], [137], [138]).

A quite diffused normalization rule consists in scaling numerical data, based on extreme values. Denoted by V_i the i-*th* vulnerable indicator, two extreme values $V_{i,min}$ and $V_{i,max}$ can be defined, by considering the maximum and minimum values observed in the whole set of systems to be studied (e.g. if the analysis is carried out at township level, extreme values can be chosen according to the minimum and maximum values observed at national level). The normalized index v_i in [0,1] can be obtained as follows

$$v_i = \frac{\left(V_i - V_{i,min}\right)}{\left(V_{i,max} - V_{i,min}\right)} \tag{15}$$

Once all indicators have been defined, a first analysis of results can be performed by comparing their relative values, in order to give evidence to the most relevant ones, see, for example, Figure 53, where two radar diagrams relevant to two different contexts are presented, recovered from [122].

Indicators	
Indicator 1	I01
Indicator 2	I02
Indicator 3	I03
Indicator 4	I04
Indicator 5	I05
Indicator 6	I06
Indicator 7	I07
Indicator 8	I08

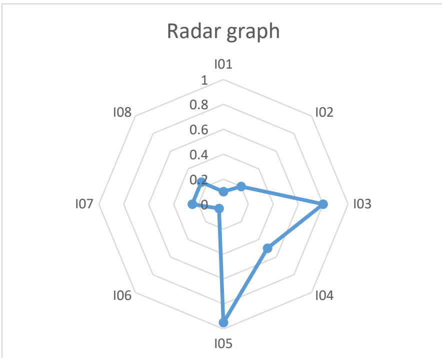

Figure 53: Radar graph for a set of Indicators

The radar diagram provides an efficient description of analytical results and it gives evidence to the most/least important indexes and it is useful for the analysis of a single system. Comparison among different systems requires an averaging of indexes to obtain a single indicator for each system, so that it becomes possible to establish a vulnerability ranking among similar systems.

Also in this case, there are many methods to perform a synthesis of a set of indicators. Two simple combination methods, adequate to the level of knowledge of the problem, are (a) the multiplication of the vulnerability indexes, or (b) the weighted summation of the indexes. Formally, the overall indicators V can be obtained as

$$V_i = v_1 \times \ldots \times v_i \times \ldots \times v_N \tag{16}$$

in the former case (multiplication), or as

$$V_i = w_1 v_1 \times \ldots \times w_i v_i \times \ldots \times w_N v_N \tag{17}$$

in the latter case (weighted summation), where w_i are the weights, and N is the total number of indicators.

Given that indexes are limited in the range [0,1], the multiplication returns a synthetic index in the range [0,1]. In the case of summation, the weights must be selected such that their summation be equal 1, so that the synthetic index is in the range [0.1] too. Multiplication must be considered with special attention because the presence of an index equal or close to 0 drag the synthetic index to 0, even if some single vulnerability indexes are close to 1, thus information about some critical points is lost.

On the other hand, for what concerns the weighted summation, the weight choice makes it possible to give different importance to different vulnerability indicators, but their selection is often based on an expert judgment and can be questionable. In [Marin et al, 2021] a proposal for both the set of indicators and the set of relevant weights is presented, based on a statistical analysis of the previous existing literature.

In a recent paper [139] a combination of the two approaches is used. Firstly, two synthetic indexes relevant to vulnerability and resilience are separately obtained by a weighted summation, then they are combined by multiplication. Some applications of this methodology have been recently developed (e.g. [140]) and some results concerning multi-hazard risk in Italy are reported in Figure 54 (from [139]). For completeness, also the risk analysis is reported in the following Figure 54. The risk index is obtained by multiplying a hazard index, not discussed here, by vulnerability and resilience indexes. In this case, vulnerability/resilience analysis is not influenced by the particular type of hazard.

Previous methodology provides a solid and general framework to evaluate vulnerability of regions or districts subjected to natural hazards. However, districts interested by Cultural Heritage have special characteristics that influence the vulnerability for two reasons, cultural assets are usually more prone to damage with respect to other assets, and the socio-economic system is strongly related to cultural assets located in the region. These aspects should be included in some way in the assessment because they are related to the exposure and susceptibility.

These concerns are not considered in the technical literature yet, and they can be included by adding some specific indicators in the analysis. A proposal of potential indicators could include the following 4 indexes, inserted at the end of the previous Table 20.

An index accounting for the natural, artistic, or historic value, which can be based on assessment described in the Chapter 6, starting from evaluations furnished by experts and including the number of assets placed in the district.

An index accounting for the social value. In this case methods presented in Chapter 6 can be used, starting from perception value based on community replies to questionnaire.

An index concerning the influence of cultural assets on the district economy. It can be based on the share of economic activities related to cultural assets, such as activities in the field of tourism, accommodation capacity, exploitation, and organization of cultural events.

An index based on the share of inhabitants leaving on historical buildings or protected natural areas with a recognized artistic, historical of natural values.

These indexes enlarge the number of parameters and can be handled as described before.

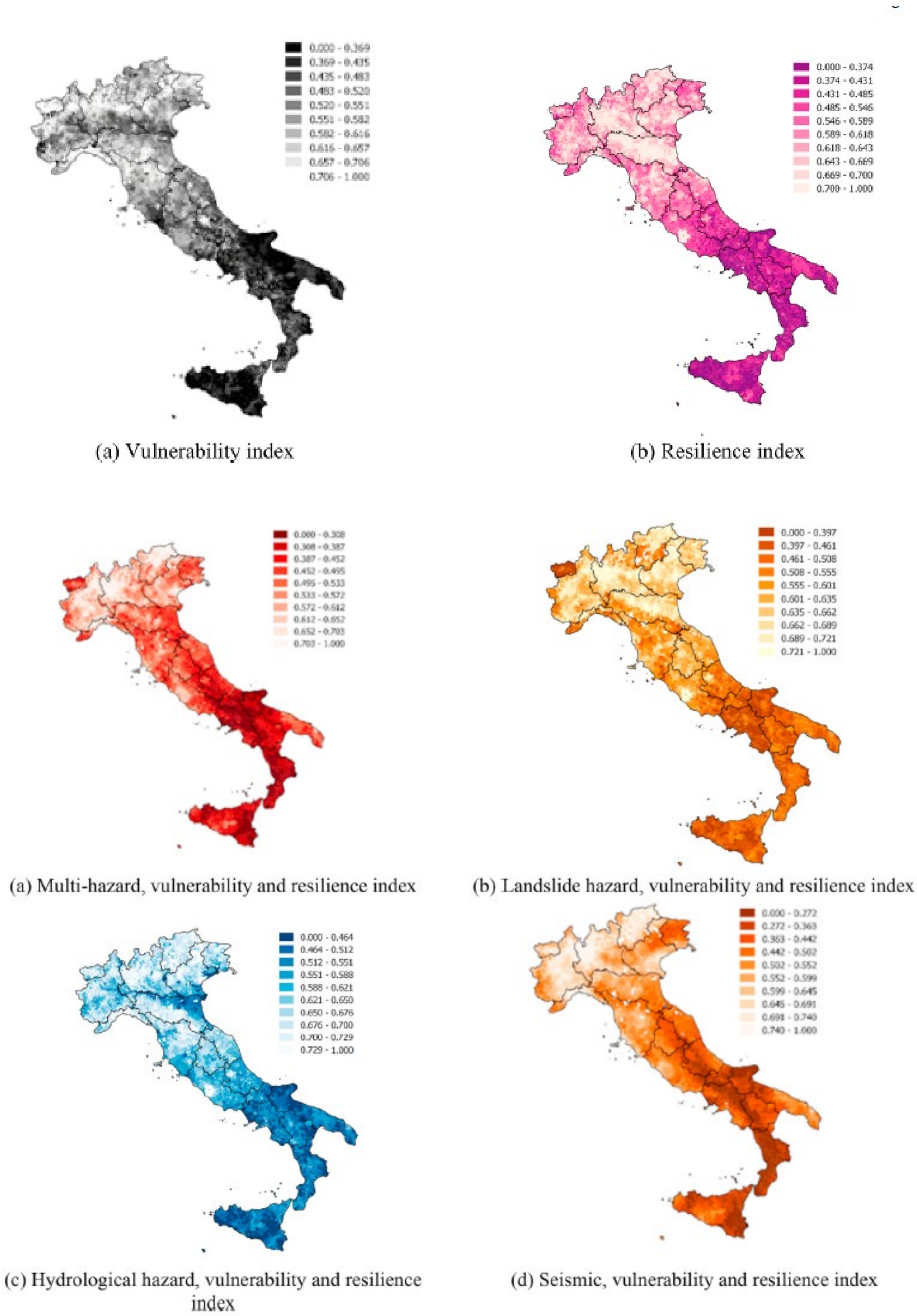

Figure 54: Cultural heritage related vulnerability

8.1.3. *Looking forward*

Many general frameworks for risk and resilience assessment have been presented at international and national level. They are oriented to evaluate the consequences due to extreme natural events, as well as the long-term stresses due to climate change. They generally include evaluation of impacts on communities, considering socio-economic and cultural aspects. A list of recent documents, not exhaustive, is reported in Figure 55.

In this case, a set of indicators concerning the socio-economic impacts are proposed, as reported, for example, in the list of Figure 56, providing a synthesis of indicators suggested in two of the most important documents at international level, the Sendai Framework for Disaster Risk Reduction, and the Global Goals for Sustainable Development.

The Sendai Framework for Disaster Risk Reduction 2015-2030 [141] outlines seven clear targets and four priorities for action to prevent new and reduce existing disaster risks: (i) Understanding disaster risk; (ii) Strengthening disaster risk governance to manage disaster risk; (iii) Investing in disaster reduction for resilience and (iv) Enhancing disaster preparedness for effective response, and to "Build Back Better" in recovery, rehabilitation and reconstruction

Figure 55: Cultural heritage related vulnerability

The Sustainable Development Goals (SDGs) [142], agreed upon in 2015 by world leaders, aim to create a better, fairer, world by 2030, ending poverty, urgently addressing climate change and ending inequality. The listed goals are no Poverty, Zero Hunger, Quality Education, Gender Equality, Clean Water and Sanitation, Affordable and Clean Energy, Decent Work and Economic Growth, Industry, Innovation and Infrastructure, Reduced Inequalities, Sustainable Cities and Communities, Responsible Consumption and Production, Climate Action, Life Below Water, Life on Land, Peace, Justice and Strong Institutions, Partnerships for the Goals,

Both include criteria to measure potential losses and adverse consequences from social and/or economic point of view and some attempts to provide a synthesis of metrics have been developed, as result in the mentioned short list of consequence parameters, (Figure 56) concerning poverty, human settlement resilience, and climate change impacts.

	SDG Indicators	Sendai Framework indicators
	Goal 1. End poverty in all its forms everywhere	
1.5.1	Number of deaths, missing persons and directly affected persons attributed to disasters per 100,000 population	A1 and B1
1.5.2	Direct economic loss attributed to disasters in relation to global gross domestic product (GDP)	C1
1.5.3	Number of countries that adopt and implement national disaster risk reduction strategies in line with the Sendai Framework for Disaster Risk Reduction 2015-2030	E1
1.5.4	Proportion of local governments that adopt and implement local disaster risk reduction strategies in line with national disaster risk reduction strategies	E2
	Goal 11. Make cities and human settlements inclusive, safe, resilient and sustainable	
11.5.1	Number of deaths, missing persons and directly affected persons attributed to disasters per 100,000 population	A1 and B1
11.5.2	Direct economic loss in relation to global GDP, damage to critical infrastructure and number of disruptions to basic services, attributed to disasters	C1, D1, D5
11.b.1	Number of countries that adopt and implement national disaster risk reduction strategies in line with the Sendai Framework for Disaster Risk Reduction 2015-2030	E1
11.b.2	Proportion of local governments that adopt and implement local disaster risk reduction strategies in line with national disaster risk reduction strategies	E2
	Goal 13. Take urgent action to combat climate change and its impacts	
13.1.1	Number of deaths, missing persons and directly affected persons attributed to disasters per 100,000 population	A1 and B1
13.1.2	Number of countries that adopt and implement national disaster risk reduction strategies in line with the Sendai Framework for Disaster Risk Reduction 2015-2030	E1
13.1.3	Proportion of local governments that adopt and implement local disaster risk reduction strategies in line with national disaster risk reduction strategies	E2

Figure 56: Connection of indicators from Sendai Framework and SDG indicators

It is clear that these indicators, and the relevant metrics, concern the potential consequences only, but other information are necessary to develop a vulnerability analysis, as discussed in advance. In particular, metrics to evaluate hazards are necessary and each hazard-consequence pair requires a relationship relating these two quantities. This part of the problem is under investigation and very few results are currently available.

However, a list of consequence indicators is equally useful for the approach previously discussed because it makes it possible to check, from a qualitative point of view, the coherence of the chosen vulnerability indicators with the consequence indicators (a vulnerability parameters is coherent if it is reasonable to conclude that it may affect one or more consequence indicators when the hazard occurs).

8.2. Necessary data and suggestion for implementation

Implementation of a socio-economic vulnerability assessment based on indicators can be organized following the steps below.

1. Identification of the unit element (system) to be evaluated (e.g. county, municipality, …)
2. Identification of a selected list of indicators, starting from the list reported in Table 21 (including cultural heritage related indicators). For each indicator, a numerical evaluation must be proposed, and the data source must be declared. Selection should be based on the criteria of representativeness, acceptability, and accessibility.
3. Definition of the normalization rule to obtain uniform parameters in the range [0,1] from not-homogeneous numerical values associated to different indicators. A first analysis can be carried out at this stage by radar diagram, to give evidence to the most/least important contribute to the system vulnerability.
4. Definition of the combination rule, necessary to provide a single synthetic indicator weighting all the previous indicators. This makes it possible a comparison among global vulnerability of different units.

Special attention should be paid to the normalization rule, that should be calibrated according to the set of units to be studied. Normalization factors should be chosen to span all the range of potential values, avoiding normalization producing very similar values for all the elements.

The final result is also sensitive to weights used in the combination rule. They are generally affected by a level of arbitrariness because they combine sources of vulnerability producing impacts with a different nature. These weights can be proposed from a panel of experts, or they can be defined by an agreement among stakeholders. However, the choice of weights may strongly influence the global assessment and the way chosen for its definition is an essential part of the vulnerability assessment and it must be clearly described.

Table 21: Table for screening of indicators and detail assignment

Theme	Indicator	Code	representativeness	acceptability	accessibility	Numerical evaluation	Data source
Population structure	Population growth	A01					
	Population density	A02					
	Dependency ratio	A03					
	Young	A04					
	Elder	A05					
	Lone Parents	A06					
	Family Composition	A07					
	Race / Ethnicity	A08					
	Aging	A09					
Access to resources	Literacy	B01					
	Educational Level	B02					
	Population in the workforce	B03					
Physical limitation	Gender	C01					
	Disability	C02					
	Mortality rate	C03					
	Infant mortality	C04					
	Maternal mortality	C05					
	Birth rate	C06					
	Life expectancy	C07					
	Special needs populations	C08					
Economic Status	Income	D01					
	Poor household	D02					
	Insurance	D03					
	Unemployment	D04					
Housing/ Transportation	Housing unit	E01					
	Housing tenure	E02					
	Available vehicle	E03					
	Mobile home	E04					
	Crowding	E05					
	Residential property	E06					
Industrial Development	Employment in primary industry	F01					
	Value of primary industry	F02					
	Area of primary industry	F03					
Physical Infrastructure	Medical service	G01					
	Other Public facility	G02					
	Access to water supply	G03					
	Access to other supplies	G04					
Financial state	Self-financing resources	H01					
	Receipts from taxes	H02					
Cultural heritage	CH social value	I01					
	CH historic-artistical value	I02					
	CH related economical activities	I03					
	Inhabitants living in CH related buildings or areas	I04					

8.3. Examples of application

8.3.1. *Coastal system subjected to extreme events (shocks)*

The example of application has been extracted from [122] and synthetic version is reported here, for the purpose of illustrating the main steps of the assessment. Further details can be found in the mentioned paper.

This vulnerability assessment concerns a set of four coastal communities in Taiwan, prone to impacts due to flooding and land subsidence.

The first step consists in the definition of the boundary of the systems studied. In this case analyses haves been developed at township level and results are evaluated for 4 townships.

As a second step, the list of potential indicators has been critically analysed, considering representativeness, acceptability, and accessibility of indicators. Some indicators have been considered as non-representative for the considered systems and a larger number of indicators have been discard because data for their evaluation were not available. On the other hand, some indicators have been described by more than one index. Following Table 22 illustrates the result of this screening.

The third step consists of the evaluation of normalized indexes, starting from available data and using previous discussed normalization procedure. In this case, normalized indicators span the range [0,100] and express a percentage value. Results are reported in the following

Table 23. Result analysis, giving evidence to the different contribution to the township vulnerability, have been performed by using radar diagrams and outcomes are depicted in Figure 57.

The last step consists in the evaluation of a synthetic indicators, combining previous analytic indicators.

In this case the 28 indicators have been averaged to obtain the overall indicators and the vulnerability of the four townships is reported in Figure 58.

Table 22: Indicator selection

Theme	Potential Indicator (reference)	Representativeness	Acceptability	Accessibility	Practical Indictor
Population structure	Population growth (C; D; H; N; P; S)	+	+	+	Population growth
	Population density (A; B; C; E; P)	+	+	+	Population density
	Dependency ratio (B; C; D; E; G; P)	+	+	+	Dependency ratio
	Young (A; C; D; F; G; I; J; K; O;)	+	+	+	Young population
	Elder (A; C; D; F; G; I; J; K; L; O; P; R; S)	+	+	+	Elderly population
	Lone Parents (A; C; D; F; I; K; L)	+	+	+	Lone parents
	Family Composition (A; C; D; F; K; O)	+	+	+	Household size
	Race / Ethnicity (C; D; K; O)	+	+	+	Aborigines population
	Aging (R; S)	+	+	+	Aging index
Access to resources	Literacy (B; E; H; M)	+	+	+	illiteracy
	Educational Level (A; C; K; O; S)	+	+	ND	-
	Population in the workforce (B)	+	+	+	Labor force
Physical limitation	Gender (A; C; D; F; I; O; R)	+	+	+	Gender ratio
	Disability (A; E; F; H; I; M; R)	+	+	+	Disabled population
	Mortality rate (N)	+	+	+	Death rate
	Infant mortality (N)	+	+	ND	-
	Maternal mortality (E; H)	+	+	ND	-
	Birth rate (B; C; E; O; P; Q)	NAP	+	+	-
	Life expectancy (B; E; H; J; Q)	+	+	ND	-
	Special needs populations (C; D; F)	+	+	ND	-
Economic Status	Income (A; B; C; D; I; J; K; M; N; P; R)	+	+	ND	-
	Poor household (D; F; J; K; P; R; S)	+	+	+	Low-income population
	Insurance (R)	+	+	ND	-
	Unemployment (A; C; D; J; K; L; M)	+	+	ND	-
Housing/ Transportation	Housing unit (G; K; M)	NAP	+	ND	-
	Housing tenure (A; C; D; F; L; M)	+	+	ND	-
	Available vehicle (I; K; L; Q)	+	+	ND	-
	Mobile home (A; K; M)	NAP	NA	ND	-
	Crowding (A; K; L; M)	+	+	ND	-
	Residential property (C; M; R)	+	+	ND	-
Industrial Development	Employment in primary industry (A; C; D; E; G; P; Q)	+	+	+	Primary industry employees
	Value of primary industry (C; E; H; N; P)	+	+	ND	-
	Area of primary industry (G; N; P; Q)	+	+	+	Primary industry areas
Physical Infrastructure	Public facility (C)	+	+	+	Relative height of seawall
					Population served per bed in hospitals and clinics
	Medical service (C; D; E; H)	+	+	+	Population served per hospital and clinic
					Population served per medical personnel
	Access to water supply (B; C; E; H; M; N; Q)	+	+	+	Availability of domestic water supply
Financial State	Financial resource				Receipts from subsides and assistance
					Self-financing resources
					Receipts from taxes

NAP: no appropriate
NA: not available
ND: no data

Table 23: Numerical values of the normalized indicators

Socioeconomic Vulnerability Indicator Framework			*p* Scores *			
Dimension	**Criterion (abbreviated name)**	**Indicator (code)**	**Mailiao**	**Kauho**	**Linbian**	**Jiadong**
Susceptibility	Economic structure (ES)	Primary industry areas (I1)	29.5	92.3	20.59	47.38
		Primary industry employees (I2)	29.33	92.79	23.14	42.77
	Infrastructure (I)	Relative height of seawall (I3)	20.08	21.65	64.97	89.22
		Availability of domestic water supply (I4)	26.73	25.8	42.19	92.89
	Population sensitivity (PS)	Population growth (I5)	93.29	29.89	29.29	33.53
		Population density (I6)	31.54	19.71	92.31	46.27
		Household size (I7)	17.13	92.04	37.91	43.99
		Aging index (I8)	7.22	61.74	63.61	79.17
	Age structure (AS)	Young population (I9)	93.2	35.3	31.91	25.99
		Elderly population (I10)	7.05	65.21	62.55	77.66
	Special needs population (SNP)	Aborigines population (I11)	89.95	20.9	62.3	21.71
		Disabled population (I12)	12.9	90.13	40.85	52.92
Resilience	Social dependence (SD)	Low-income population (I13)	20.13	34.15	42.03	92.6
		Dependency ratio (I14)	89.52	40.69	12.27	55.67
		Lone parents (I15)	7.38	65.93	58.1	79.75
		Gender ratio (I16)	81.02	7.89	68.44	52.15
	Human resource capacity (HRC)	Labor force (I17)	89.14	41.73	11.78	56.39
		Illiteracy (I18)	44.69	92.53	20.94	30.86
	Medical services provision (MSP)	Population served per bed in hospitals and clinics (I19)	15.82	90.28	58.64	30.36
		Population served per hospitals and clinics (I20)	29.81	92.37	20.71	46.65
		Population served per medical personnel (I21)	9.83	87.04	47.15	59.25
		Death rate (I22)	7.22	76.04	56.64	72.06
	Financial resources (FR)	Receipts from subsidies and assistance (I23)	28.57	93.29	33.38	30.78
		Self-financing resources (I24)	55.13	91.13	29.18	17.63
		Receipts from taxes (I25)	55.35	91.31	20.06	25.39
Mean scores		All indicators	39.7	62.1	43.6	52.1
		Susceptibility indicators	38.2	54	47.6	54.5
		Resilience indicators	41	69.5	39.8	49.9

* The vulnerability level is between 0 and 100; a high value means a high socioeconomic vulnerability to climate change

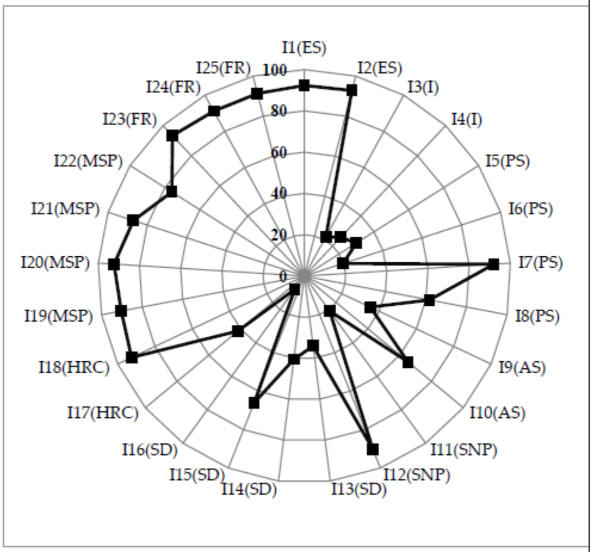

Kauho

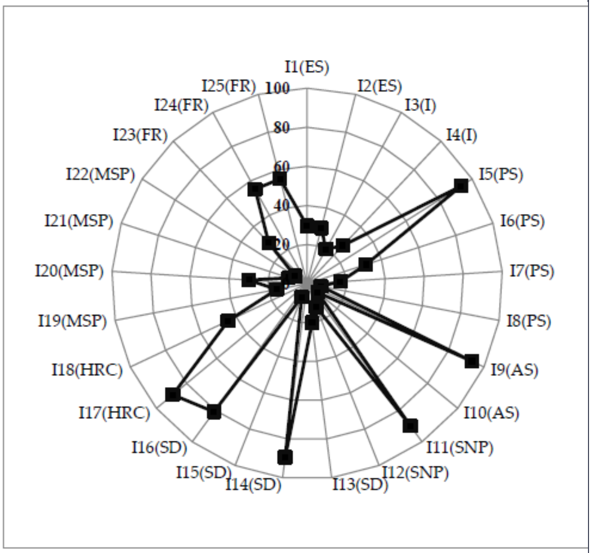

Mailiao

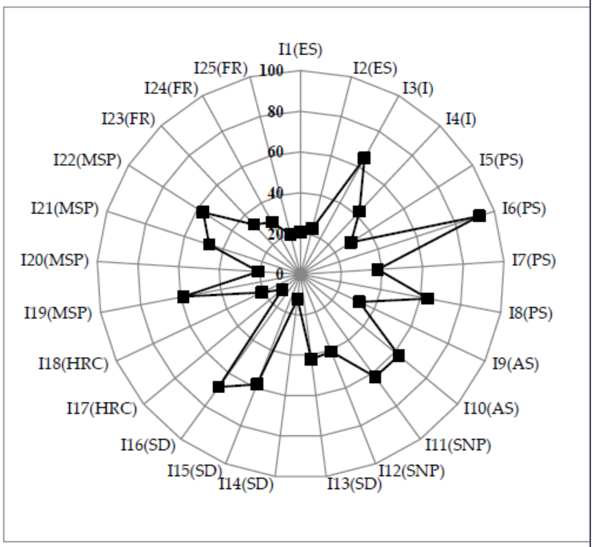

Linbian

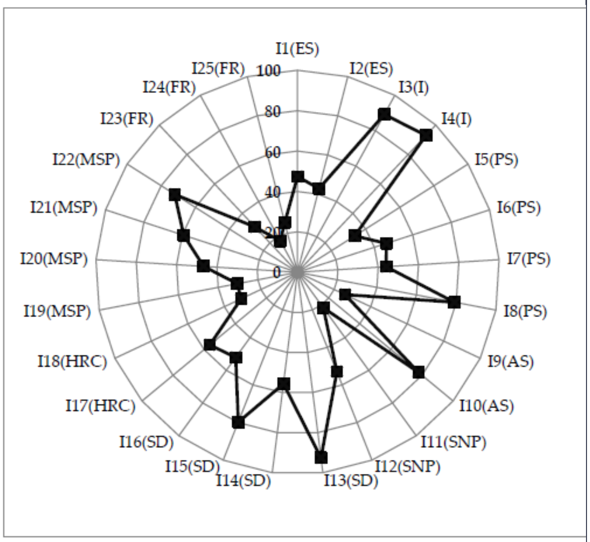

Jiadong

Figure 57: Radar graphs of the four townships studied

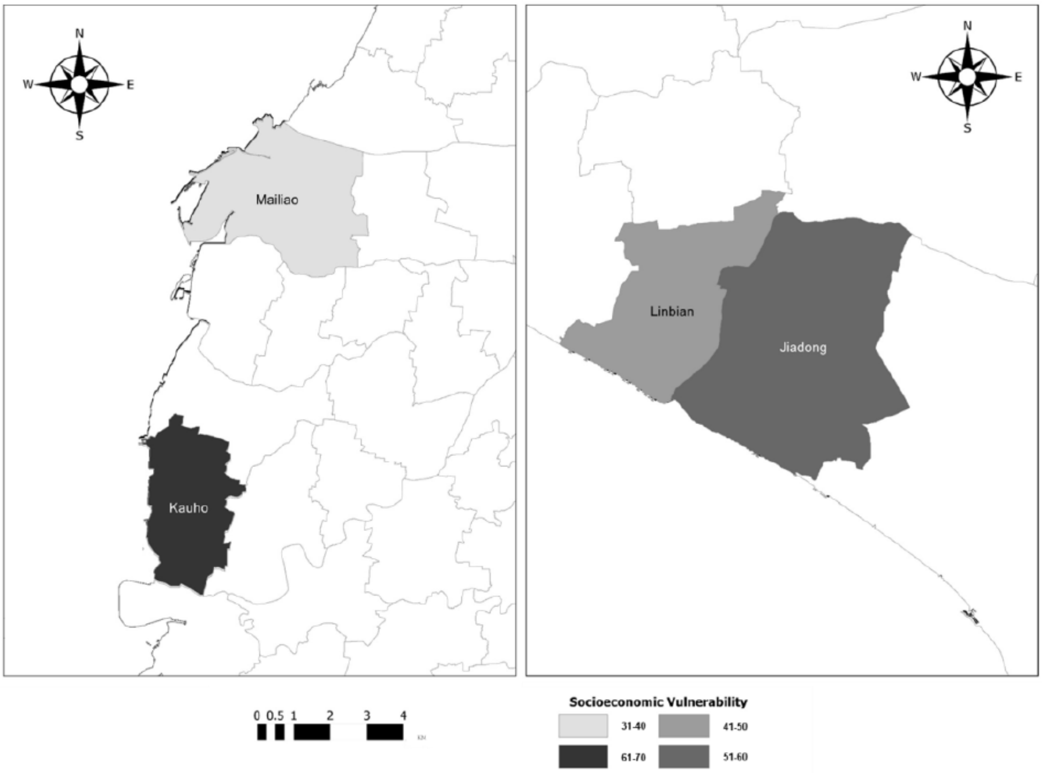

Figure 58: Overall indicators and comparison of vulnerability at township level

8.3.2. *Coastal system subjected to climate changes (stresses)*

This applicative example considers the potential impacts on coastal communities, due to long-term climate changes. Results concern the on-going activities carried out on the coastal system of Valencia, involving many sub-systems sensitive to variations of the environmental conditions. At the current stage of the research, indicator selection is only illustrated (points 1 and 2 of Section 8.2) while data collection and combination rules are on-going (points 3 and 4 of Section 8.2)

More precisely, vulnerability parameters have been selected to provide information about the people wellness and health, the economic systems related to the farming activities and the tourism sector. Climate changes can be monitored by a number of characteristic parameters reported and discussed in Deliverable 5.1, as frequencies of heatwaves, amplitude of temperature variations, pluvial intensity and location of flooding prone areas.

Following the approach based on indexes, a group of people consisting of experts and stakeholders have selected a list of indicators related to the specific vulnerabilities of this area and have identified the relevant metrics. These indicators fit with the three necessary requirements of representativeness, acceptability, and accessibility.

The list of indicators is reported in Figure 59 and they are grouped following criteria proposed in Section 8.2.

Theme	Indicator	Code	data
Population structure	Foreign population EU	OthPopEU	Double
	Foreign population Non-EU	OthPopNoEU	Double
	Total pop aged<15	POP_15	Double
	Total pop aged 15-65	POP_15_65	Double
	Male population aged 15-65	POP_15_65_	Double
	Female population aged 15-65	POP_15_651	Double
	Female pop aged<15	POP_15_F	Double
	Male pop aged<15	POP_15_M	Double
	Total pop aged>65	POP_65	Double
	Female population aged>65	POP_65_F	Double
	Male population aged>65	POP_65_M	Double
	Population Density (pop/kmq)	POP_DEN_KM	Double
	Total population	POP_TOT	Double
	Female population	POP_TOT_F	Double
	Male population	POP_TOT_M	Double
Access to resources	Edu - Graduates	EDU_GRADUA	Double
	Edu - High level of education	EDU_HIGH_L	Double
	Edu - Illiterates	EDU_ILLITE	Double
	Edu - Low level of education	EDU_LOW_LE	Double
Economic status (general)	Male unemployed	M_UNEMPLOY	Double
	Female unemployed	F_UNEMPLOY	Double
	Unemployed in industry	IND_UNEMPL	Double
	Unemployed in services	SERV_UNEMP	Double
	Unemployed Total	TOT_UNEMPL	Double
	Not previously occupied	NOPREVIOUS	Double
	Bank offices for 10k inhabitants	BANKS_10K_	Double
	Unemployed in construction activities	CONSTR_UNE	Double
Economic status (agricultural)	Unemployed in Agriculture	AGR_UNEMPL	Double
Industrial development (general)	Professional Econ Actvs - Professionals finance, law, insurance	FIN_ASS__1	Double
	Commercial Econ Actvs - Financial institutions and insurance	FIN_ASS_AC	Double
	Commercial Econ Actvs -Trade, restaurants, hospitality and repairs	HOSP_REST_	Double
	Industrial Econ Actvs - Mineral extraction and transformation	INDACExtMi	Double
	Industrial Econ Actvs - Energy and water	INDACTENE	Double
	Industrial Econ Actvs - Metal transformation	INDACTraMe	Double
	Industrial Econ Actvs - Other manufacturing industries	INDACTotMa	Double
	Professional Econ Actvs - Industry and construction Technical Staff	INDUST_ACT	Double
	Professional Econ Actvs - Other professionals	OTHER_AC_1	Double
	Commercial Econ Actvs - Other services	OTHER_ACTV	Double
Industrial development (agricultural)	Professional Econ Actvs - Agriculture Technical Staff	AGRIC_ACTP	Double
Industrial development (tourism)	No. Tourism Actvs	NoACTTour	Double
	Tourism - Apartments	APARTMENTS	
	Tourism - No. of Hostels	HOSTELS	Double
	Tourism - No. of Hotels	HOTELS	Double
	Tourism - No. of place in Hostels	NOPLACE__1	Double
	Tourism - No. of place in Apartments	NOPLACE_Ap	Double
	Tourism - No. of place in Hotels	NOPLACE_HO	Double
Informative	No. District	NUMDISTR	Long
	Council	JUNTA	Long
	District name	NAM_DISTR	Text
	District name	NAMEDISTR	Text
	No. District	NO_DISTR	Long
	Council name	NOMBRE	Text
	shape	Shape	Geometry
	ID object	FID	Object ID

Figure 59: list of indicators

References

Chapter 2

[1] Cerè, G., Rezgui, Y., Zhao, W., 2017. Critical review of existing built environment resilience frameworks: Directions for future research. Int. Journal of Disaster Risk Reduction 25 (2017) 173–189.

[2] EM-DAT The international disaster database (www.emdat.be).

[3] Porter, K., 2021. A Beginner's Guide to Fragility, Vulnerability, and Risk. University of Colorado Boulder, 139 pp., https://www.sparisk.com/pubs/Porter-beginners-guide.pdf.

[4] Dall'Asta A. (2020) Some short remarks on risk assessment. Researchgate (https://www.researchgate.net/publication/340096794_Some_short_remarks_on_Risk_Assessment).

[5] Roca, P., Cervera, M., Gariup, G., Pela', L., 2010. Structural Analysis of Masonry Historical Constructions. Classical and Advanced Approaches. Arch Computat Methods Eng 17, 299–325. https://doi.org/10.1007/s11831-010-9046-1

[6] Lagomarsino, S., Giovinazzi, S., 2006. Macroseismic and mechanical models for the vulnerability and damage assessment of current buildings. Bull Earthquake Eng 4, 415–443. https://doi.org/10.1007/s10518-006-9024-z.

[7] Polese, M., Di Ludovico, M., Gaetani d'Aragona, M., Prota, A., Manfredi, G., 2020. Regional vulnerability and risk assessment accounting for local building typologies. International Journal of Disaster Risk Reduction 43, 101400. https://doi.org/10.1016/j.ijdrr.2019.101400.

[8] Morici, M., Canuti, C., Dall'Asta, A., Leoni, G., 2020. Empirical predictive model for seismic damage of historical churches. Bull Earthquake Eng 18, 6015–6037. https://doi.org/10.1007/s10518-020-00903-2.

[9] Peduto, D., Korff, M., Nicodemo, G., Marchese, A., Ferlisi, S., 2019. Empirical fragility curves for settlement-affected buildings: Analysis of different intensity parameters for seven hundred masonry buildings in The Netherlands. Soils and Foundations 59, 380–397. https://doi.org/10.1016/j.sandf.2018.12.009.

[10] Piciullo, L., Ritter, S., Lysdahl, A.O.K., Langford, J., Nadim, F., 2021. Assessment of building damage due to excavation-induced displacements: The GIBV method. Tunnelling and Underground Space Technology 108, 103673. https://doi.org/10.1016/j.tust.2020.103673.

[11] Polese, M., Gaetani d'Aragona, M., Prota, A., 2019. Simplified approach for building inventory and seismic damage assessment at the territorial scale: An application for a town in southern Italy. Soil Dynamics and Earthquake Engineering 121, 405–420. https://doi.org/10.1016/j.soildyn.2019.03.028.

[12] Vettore, M., Donà, M., Carpanese, P., Follador, V., da Porto, F., Valluzzi, M.R., 2020. A Multilevel Procedure at Urban Scale to Assess the Vulnerability and the Exposure of Residential Masonry Buildings: The Case Study of Pordenone, Northeast Italy. Heritage 3, 1433–1468. https://doi.org/10.3390/heritage3040080.

Chapter 3

[13] Knotkova, D., 1993. ''Atmospheric Corrosivity Classification. Results from the International Testing Program ISOCORRAG,'' Corrosion Control for Low-Cost Reliability, 12th International Corrosion Congress, Vol. 2, Progress Industries Plant Operations, NACE International, Houston, Texas, pp. 561–568.

[14] Zallmanzig, J.,1985. Investigation on the rates of emission and effects in selected places of Europe for the quantitative examination of the influence of air pollution on the

destruction of ashlar. Report of the NATO/CCSM Pilot Study on Conservation and restoration of Monuments, Number 158 Umwelbundesamt, Berlin.
[15] Svensson, J.E., Johansson, L.G., 1993. A laboratory study of the effect of ozone, nitrogen dioxide and sulphur dioxide on the atmospheric corrosion of zinc, J. Electrochem. Soc., Vol 140, No 8, pp. 2210–2216.
[16] Brown, B.F., Burnett, H.C., Chase, W.T., Goodway, M., Kruger J., Pourbaix, M., 1977. Corrosion and Metal Artifacts – A Dialogue between Conservators and Archaeologists and Corrosion Scientists. Washington, DC: National Bureau of Standards.
[17] Weil, P.D., Naude, V.N., 1985. Patina, a historical perspective artistic intent and subsequent effects of time, nature and man. pp. 21–27. 1985. Philadelphia, Pennsylvania Academy of the Fine Arts.
[18] Hamilton, R.S., Mansfield, T.A., 1991. Airborne particulate elemental carbon: its sources, transport and contribution to dark smoke and soiling, Atmos. Env. 25, 715–723.
[19] Harrison, R.M., Jones, A.M., Lawrence R.G., 2004. Major component composition of PM10 and PM2.5 from roadside and urban background sites, Atmos. Env. 38, 4531–4538.
[20] Brimblecombe, P., 2003. The effects of air pollution on the built environment. Imperial College Press, London.
[21] Bailey, D.L.R., Clayton, P., 1982. The measurement of suspended particle and total carbon concentrations in the atmosphere using standard smoke shade methods, Atmos. Env. 16, 2683–2690.
[22] BSI 1969. BS1747 Methods for the measurement of air pollution. BSI London.
[23] ISO 1995. Air quality – particle size fraction definitions for health-related sampling, ISO 7708, International Organisation for Standardization, Geneva.
[24] ISAC 2004. Noah's Ark, Global Climate Change Impact on Built Heritage and Cultural Landscapes. http://noahsark.isac.cnr.it/
[25] Hinds, W.C., 1999. Aerosol Technology: properties, behaviour and measurements of airborne particles, 2nd edition. Wiley ISBN 978-0-471-19410-1.
[26] Friedlander, S.K., 2000. Smoke, dust and haze: fundamentals of aerosol dynamics (second edition), Oxford University Press ISBN-13:978-0-19-512999-1Hamilton, R., Kucera, V., Tidblad, J., Watt, J. (Eds.), 2009. The Effects of Air Pollution on Cultural Heritage. Springer US, Boston, MA. https://doi.org/10.1007/978-0-387-84893-8
[27] Gatz, D.F., 1991. Urban Precipitation Chemistry: A Review and Synthesis. Atmospheric Environment Vol. 25B, no. no. 1: 1–15.
[28] Mikhailov, A.A., Tidblad, J., Kucera, V., 2004. ‘‘The Classification System of ISO 9223 Standard and the Dose-Response Functions Assessing the corrosivity of Outdoor Atmospheres’’ Protection of Metals. 2004. Vol. 40. N 6. pp. 541–550 (In Russian variant pp. 601–610).
[29] Hamilton, R., Kucera, V., Tidblad, J., Watt, J. (Eds.), 2009. The Effects of Air Pollution on Cultural Heritage. Springer US, Boston, MA. https://doi.org/10.1007/978-0-387-84893-8
[30] Cramer, S.D., McDonald, L.G., 1990. Atmospheric factors affecting the corrosion of zinc, galvanized steel, and copper. In: ASTM STP 1000 Corrosion Testing and Evaluation. Committee G1 Symposium, eds. S. Dean and R. Baboian, Philadelphia, PA: ASTM.
[31] Lins, A., Power, T., 1991. The Corrosion of Bronze Monuments in Polluted Urban Sites: A Report on the Stability of Copper Mineral Species at Different pH Levels. Scott, D. A., Podany, J., and Considine, B. B. Ancient and Historic Metal Conservation and Scientific Research. pp. 119–151. 1991. Marina del Ray, Getty Conservation Institute.
[32] Lipfert, F.W., 1991. Historic Urban SO2 Levels. APT Bulletin XXIII, no. 4: 72. Notes adapted from F. W. Lipfert, 1987, Estimates of historic urban air quality trends and

precipitation acidity in selected U.S. cities (1880–90), Brookhaven National Laboratory Report 39845.
[33] Sherwood, S.I., Gatz, D. F., Hosker, Jr. R.P., Davidson, C.I., Dolske, D.A., Hicks, B.B., Langmuir, D., Linzey, R., Lipfert, F.W., McGee, E.S., Mossotti, V.G., Schmiermund, R.L., Spiker, E.C., 1990. Processes of Deposition to Structures. Acidic Deposition: State of Science and Technology, ed. P. Irving, Vol. III, Report 20. Washington, D.C.: National Acidic Precipitation Assessment Program. (SOS/T 20).
[34] Gentilucci, M., Materazzi, M., Pambianchi, G., Burt, P., Guerriero, G., 2019. Assessment of variations in the temperature-rainfall trend in the province of Macerata (Central Italy), comparing the last three climatological standard normals (1961–1990; 1971–2000;1981–2010) for biosustainability studies. Environ. Process., 6, 391–412.
[35] Mattias, P.; Capaccioni, B.; Vaselli, O., 1996. L'arenaria di palazzo Ducale in Camerino (MC): Caratteristiche mineralogico-petrografiche e considerazioni sullo stato di conservazione. Studi Geologici Camerti, XIV (1996-97), 67-82. (In Italian).

Chapter 4

[36] Giuffrè, A., (1993). Sicurezza e conservazione dei centri storici in area sismica, il caso Ortigia. Laterza, Bari, Italy.
[37] Binda, L., Baronio, G., Gambarotta, L., Lagomarsino, S., Modena, C., (1999a). Masonry constructions in seismic areas of central Italy: a multi-level approach to conservation. VIII North American Masonry Conference - 8NAMC, Austin, USA, pp. 44-55.
[38] Binda, L., Gambarotta, L., Lagomarsino, S., Modena, C., (1999b). A multilevel approach to the damage assessment and seismic improvement of masonry buildings in Italy. Seismic damage to masonry buildings, Balkema, Rotterdam, Netherlands.
[39] Borri, A., Avorio, A., Cangi, G., (1999a). Considerazioni sui cinematismi di collasso osservati per edifici in muratura. IX Convegno Nazionale "L'ingegneria Sismica in Italia", ANIDIS, Torino, Italy.
[40] Borri, A., De Maria, A., (2009). Eurocode 8 and italian code. A comparison about safety levels and classification of interventions on masonry existing buildings. Eurocode 8 Perspectives from the Italian Standpoint Workshop, 3 April, Naples, Italy, pp. 237-246.
[41] Doglioni, F., Moretti, A., Petrini, V., (1994). Le chiese ed il terremoto. LINT, Trieste, Italy.
[42] Lagomarsino, S., Brencich, A., Bussolino, F., Moretti, A., Pagnini, L.C., Podestà, S., (1997). Una nuova metodologia per il rilievo del danno alle chiese: prime considerazioni sui meccanismi attivati dal sisma. Ingegneria Sismica, No. 3, pp. 70-82.
[43] D'Ayala, D., Speranza, E., (1999a). Identificazione dei meccanismi di collasso per la stima della vulnerabilità sismica di edifici nei centri storici. IX Convegno Nazionale "L'ingegneria Sismica in Italia", ANIDIS, Torino, Italy.
[44] D'Ayala, D., (1999b). Correlation of seismic vulnerability and damages between classes of buildings: Churches and houses, in Seismic Damage to Masonry Buildings. Balkema, Rotterdam, pp. 41-58.
[45] Official Bulletin of Marche Region n.15 (2000). Codice di pratica (linee guida) per la progettazione degli interventi di riparazione, miglioramento sismico e restauro dei beni architettonici danneggiati dal terremoto umbro-marchigiano del 1997, a cura di Canofeni, G., Marino F., Minardi, G., Moretti, A., Regazzo, P., Serafini G., 29 settembre 2000.
[46] Carocci C.F., Guidelines for Safety and Preservation of Historical Centres in Seismic Areas. (carocci2001) In: Historical Constructions. Guimaraes, Portugal, ISBN 972-8692-01-3, pp. 145-166
[47] Pavić, G., Hadzima-Nyarko, M., Bulajić, B., Jurković, Ž., 2020. Development of Seismic Vulnerability and Exposure Models—A Case Study of Croatia. Sustainability 12, 973. https://doi.org/10.3390/su12030973.

[48] Dall'Asta, A., Leoni, G., Meschini, A., Petrucci, E., Zona, A., 2019. Integrated approach for seismic vulnerability analysis of historic massive defensive structures. Journal of Cultural Heritage 35, 86–98. https://doi.org/10.1016/j.culher.2018.07.004.

[49] Carbonari, S., Dall'Asta, A., Dezi, L., Gara, F., Leoni, G., Morici, M., Petrucci, E., Prota, A., Zona, A., 2019. First analysis of data concerning damage occurred to churches of the Marche region following the 2016 central Italy earthquakes. BGTA. https://doi.org/10.4430/bgta0271.

[50] Canuti, C., Carbonari, S., Dall'Asta, A., Dezi, L., Gara, F., Leoni, G., Morici, M., Petrucci, E., Prota, A., Zona, A., 2021. Post-Earthquake Damage and Vulnerability Assessment of Churches in the Marche Region Struck by the 2016 Central Italy Seismic Sequence. International Journal of Architectural Heritage 15, 1000–1021. https://doi.org/10.1080/15583058.2019.1653403

[51] ISTAT (Italian National Institute of Statistics). Website and Data Warehouse. 2011. Available online: https://www.istat.it/it/censimenti-permanenti/censimenti-precedenti/popolazione-e-abitazioni/popolazione-2011 (accessed on 1 November 2020).

[52] Braga, F., Dolce, M., Liberatore, O., (1982). A statistical study on damaged buildings and an ensuring review of the MSK-76 scale. In Proceedings of the Seventh European Conference on Earthquake Engineering, Athens, Greece, 20–25 September 1982; Building Seismic Safety Council: Athens, Greece, 1982; pp. 431–450.

[53] Rota, M., Penna, A., Strobbia, C.L., 2008. Processing Italian damage data to derive typological fragility curves. Soil Dynamics and Earthquake Engineering 28, 933–947. https://doi.org/10.1016/j.soildyn.2007.10.010

[54] Rosti, A., Rota, M., Penna, A., 2021. Empirical fragility curves for Italian URM buildings. Bull Earthquake Eng 19, 3057–3076. https://doi.org/10.1007/s10518-020-00845-9

[55] D'Ayala, D., Meslem, A., Vamvatsikos, D., Porter, K., Rossetto, T., Silva, V, (2015). Guidelines for Analytical Vulnerability Assessment of Low/Mid-Rise Buildings; Vulnerability Global Component Project; Global Earthquake Model Foundation: Pavia, Italy.

[56] Del Gaudio, C., Ricci, P., Verderame, G.M., 2018. A class-oriented mechanical approach for seismic damage assessment of RC buildings subjected to the 2009 L'Aquila earthquake. Bull Earthquake Eng 16, 4581–4605. https://doi.org/10.1007/s10518-018-0365-1

[57] Kappos, A.J., Panagopoulos, G., Panagiotopoulos, C., Penelis, G., 2006. A hybrid method for the vulnerability assessment of R/C and URM buildings. Bull Earthquake Eng 4, 391–413. https://doi.org/10.1007/s10518-006-9023-0

[58] Pitilakis, K., Crowley, H., Kaynia, A. (Eds.), 2014a. SYNER-G: Typology Definition and Fragility Functions for Physical Elements at Seismic Risk: Buildings, Lifelines, Transportation Networks and Critical Facilities, Geotechnical, Geological and Earthquake Engineering. Springer Netherlands. https://doi.org/10.1007/978-94-007-7872-6

[59] Pitilakis, K., Franchin, P., Khazai, B., Wenzel, H. (Eds.), 2014b. SYNER-G: Systemic Seismic Vulnerability and Risk Assessment of Complex Urban, Utility, Lifeline Systems and Critical Facilities: Methodology and Applications, Geotechnical, Geological and Earthquake Engineering. Springer Netherlands. https://doi.org/10.1007/978-94-017-8835-9

[60] Bradley, B.A., Dhakal, R.P., Cubrinovski, M., MacRae, G.A., Lee, D.S., 2008. Seismic loss estimation for fficient decision-making. BNZSEE 42, 96–110. https://doi.org/10.5459/bnzsee.42.2.96-110

[61] Porter, K.A., 2003. An overview of PEER's performance-based earthquake engineering methodology. Proceed. of Ninth International Conference on Applications of Statistics and Probability in Engineering, San Francisco, California, 2003.
[62] Günay, S., Mosalam, M. K., 2013. PEER Performance-Based Earthquake Engineering Methodology, Revisited. Journal of Earthquake Engineering, 17(6), 829-858.
[63] Grünthal, G., 1998. Cahiers du Centre Européen de Géodynamique et de Séismologie: Volume 15 – European Macroseismic Scale 1998. European Center for Geodynamics and Seismology, Luxembourg, 1998.
[64] Lagomarsino, S., Giovinazzi, S., 2006. Macroseismic and mechanical models for the vulnerability and damage assessment of current buildings. Bull Earthquake Eng 4, 415–443. https://doi.org/10.1007/s10518-006-9024-z
[65] Morici, M., Canuti, C., Dall'Asta, A., Leoni, G., 2020. Empirical predictive model for seismic damage of historical churches. Bull Earthquake Eng 18, 6015–6037. https://doi.org/10.1007/s10518-020-00903-2.
[66] RISK-UE (2004), An Advanced Approach to Earthquake Risk Scenarios with Applications to different European Towns, FP5 European Project (2001-2004), www.risk-ue.net.
[67] Lallemant, D., Kiremidjian, A., Burton, H., 2015. Statistical procedures for developing earthquake damage fragility curves: STATISTICAL PROCEDURES FOR DAMAGE FRAGILITY CURVES. Earthquake Engng Struct. Dyn. 44, 1373–1389. https://doi.org/10.1002/eqe.2522
[68] Rosti, A., Rota, M., Magenes, G., Penna, A., September, 2019a. Derivazione di curve di fragilità empiriche per edifici residenziali in muratura, in: ANIDIS 2019 - XVIII Convegno.
[69] Del Gaudio, C., Rosti, A., Rota, M., Ricci, P., Penna, A., Verderame, G., 2019. Derivazione di curve di fragilità empiriche per edifici residenziali italiani in c.a., in: ANIDIS 2019 - XVIII Convegno.
[70] Rosti, A., Del Gaudio, C., Di Ludovico, M., Magenes, G., Penna, A., Polese, M., Prota, A., Ricci, P., Rota, M., Verderame, G., 2019b. Uso di curve di fragilità empiriche per la valutazione del rischio sismico a scala nazionale, in: ANIDIS 2019 - XVIII Convegno.
[71] Dolce, M., Speranza, E., Giordano, F., Borzi, B., Bocchi, F., Conte, C., Di Meo, A., Faravelli, M., Pascale, V., 2019. Observed damage database of past Italian earthquakes: the Da.D.O. WebGIS. BGTA. https://doi.org/10.4430/bgta0254
[72] Faccioli, E., Cauzzi, C., 2006. "Macroseismic intensities for seismic scenarios estimated from instrumentally based correlations," Proceedings of the First European Conference on Earthquake Engineering and Seismology, Ginevra, Switzerland, 3-8 September, CD-ROM.
[73] Murphy JR and O'Brien LJ (1977) "The correlation of peak ground acceleration amplitude with seismic intensity and other physical parameters," Bulletin of the Seismological Society of America, 67: 877-915.
[74] Zuccaro, G., Dolce, M. , De Gregorio, D. , Speranza, E. , Moroni, C., 2015. La scheda CARTIS per la caratterizzazione tipologico-strutturale dei comparti urbani costituiti da edifici ordinari. Valutazione dell'esposizione in analisi di rischio sismico. In Proceedings of the 34th Conference Gruppo Nazionale di Geofisica della Terra Solida, Trieste, Italy, 17–19 November. (In Italian).
[75] Polese, M., Di Ludovico, M., Prota, A., Tocchi, G., Gaetani d'Aragona, M., 2019. Utilizzo della scheda Cartis per aggiornamento dell'inventario ed e etto sulle stime di vulnerabilità a scala territoriale. In Proceedings of the 18th Conference ANIDIS: L'ingegneria Sismica in Italia, Ascoli Piceno, Italy, 15–19 September. (In Italian).
[76] Saretta, Y., Sbrogiò, L., Molinari, F., Vettore, M., Valluzzi, M.R., 2020. Proposta di un nuovo strumento multilivello per la valutazione del danno e della vulnerabilità a scala

urbana: la procedura MUSE-DV masonry per la valutazione empirica del comportamento di edifici consolidati. Progettazione Sismica 12, 5–30. https://doi.org/10.7414/PS.12.1.1.

[77] Baggio, C., Bernardini, A., Colozza, R., Corazza, L., Della Bella, M., DI Pasquale G., Dolce M., Goretti, A., Martinelli A., Orsini, G., Papa, F., Zuccaro, G., 2007. Field Manual for post-earthquake damage and safety assessment and short term countermeasures (AeDES). JRC Scientific and Technical Report, European Commission, Joint Research Centre Institute for the Protection and Security of the Citizen.

[78] Borri, A., Corradi, M., Castori, G., De Maria, A., 2015. A method for the analysis and classification of historic masonry. Bull Earthquake Eng 13, 2647–2665. https://doi.org/10.1007/s10518-015-9731-4.

Chapter 5

[79] Skempton, A.W., Macdonald, D.H., 1956. THE ALLOWABLE SETTLEMENTS OF BUILDINGS. Proceedings of the Institution of Civil Engineers 5, 727–768. https://doi.org/10.1680/ipeds.1956.12202

[80] Bjerrum, L., 1963. Allowable settlement of structures. Proceedings of the 3rd European Conference on Soil Mechanics and Foundation Engineering, Wiesbaden, 2, Brighton, England, pp. 135–137.

[81] Bhattacharya, S., Singh, M.M., 1984. Proposed criteria for subsidence damage to buildings. Rock mechanics in productivity and protection. American Rock Mechanics Association the 25th U.S. Symposium on Rock Mechanics (USRMS), 25-27 June, Evanston, Illinois, pp. 747–755.

[82] Boscardin, M.D., Cording, E.G., 1989. Building response to excavation induced settlement. J. Geotech. Eng. 115, 1–21.

[83] Burland, J.B., Wroth, C.P., 1974. Settlement of buildings and associated damage. SOA Review. Proc of the Conf on Settlement of Structures, Cambridge. Pentech Press, London, pp. 611–654.

[84] Burland, J.B., Broms, B.B., de Mello, V.F.B., 1977. Behaviour of foundations and structures. In: SOA Report, Proc of the 9th Int Conf on Soil Mechanics and Foundation Engineering, Tokyo, vol. 2, pp. 495–546.

[85] Burland, J.B., 1995. Assessment of risk of damage to buildings due to tunnelling and excavation. Invited Special Lecture, Proceedings of the 1st International Conference on Earthquake Geotechnical Engineering, IS-Tokyo 95, pp. 1189–1201.

[86] Chiriotti E., Marchionni. V. Grasso, P., 2000. Porto Light Metro System, Lines C, S and J. Interpretation of the Results of the Building Condition Survey and Preliminary Assessment of Risk. Methodology for Assessing the Tunnelling Induced Risks on Buildings along the Tunnel Alignment. Normetro – Transmetro, Internal technical report (in Italian and Portuguese).

[87] Chiriotti, E., Grasso, P., 2001. Porto Light Metro System, Lines C, S and J. Compendium to the Methodology Report on Building Risk Assessment Related to Tunnel Construction. Normetro – Transmetro, Internal technical report (in English and Portuguese).

[88] Dzegniuk, B., Hejmanowski, R., Sroka, A., 1997. Evaluation of the damage hazard tobuilding objects on the mining areas considering the deformation course in time. In: Proceedings of Xth International Congress of the International Society for Mine Surveying. https://doi.org/10.13140/2.1.3356.3520.

[89] Kruse, G.A., & Haan, E.J. (2006). Characterisation and engineering properties of Dutch peats.

[90] Eurocode 7, 2004: Geotechnical design - Part 1: General rules. Final Draft, EN 1997-1:2004 (E), (F) and (G), November 2004. European Committee for Standardization, Brussels, p. 168.

[91] Giardina, G., Hendriks, M.A.N., Rots, J.G., 2009. Assessment of the settlement vulnerability of masonry buildings. In: 1st WTA International PhD Symposium – Buildings Materials and Building Technology for preservation of the Built Heritage, Leuven, Belgium.

[92] GNDT, 1993. Rischio Sismico Di Edifici Pubblici, Parte I: Aspetti Metodologici, Proceedings of CNR-Gruppo Nazionale per la Difesa dai Terremoti, Roma, Italy (1993) (in Italian).

[93] Polsby, D., Popper, R., 1991. The Third Criterion: Compactness as a procedural safeguard against partisan gerrymandering. Yale Law J. 9 (2), 301–353. https://doi.org/10.2139/ssrn.2936284.

[94] Polshin, D.E., Tokar, R.A., 1957. Maximum Allowable Non-uniform Settlement of Structures. Proc. 4th Int. Conference Soil Mechanics and Foundation Engineering. Butterworths Scientific Publications, London, pp. 402–405.
[95] Saeidi, A., Deck, O., Verdel, T., 2012. Development of building vulnerability functions in subsidence regions from analytical methods. Geotechnique 62 (2), 107–120. https://doi.org/10.1680/geot.9.P.028.
[96] Skempton, A.W., MacDonald, D.H., 1956. Allowable settlement of buildings. In: Proc. of the ICE (Institute of Civil Engineers), Pt. III, vol. 5, pp. 727–768.
[97] Son, M., Cording, E.J., 2007. Evaluation of building stiffness for building response analysis to excavation-induced ground movements. J. Geotech. Geoenviron. Eng. 133 (8), 995–1002.
[98] Yu, Z., Karmis, M., Jarosz, A., Haycocks, C., 1988. Development of damage criteria for buildings affected by mining subsidence. In: 6th Annual Workshop Generic Mineral Technology Center Mine System Design And Ground Control, pp. 83–92.
[99] Palla, A., Colli, M., Candela, A., Aronica, G.T., Lanza, L.G., 2018. Pluvial flooding in urban areas: the role of surface drainage efficiency. J Flood Risk Management 11 (2018) S663–S676.
[100] Ball, J.E., Alexander, M., 2006. Modeling street surface runoff. In: Pro- ceedings of the 7th International Conference on Hydroinfor- matics, Nice, France, 2006, 288–295.
[101] Maksimović, C., Prodanović, D., Boonya-Aroonnet, S., Leitão, J.P., Djordjević, S., Allitt, R., 2009. Overland flow and pathway analysis for modelling of urban pluvial flooding. J Hydraul Res 2009, 47, (4), 512–523.
[102] Despotovic, J., Plavsic, J., Stefanovic, N., Pavlovic, D., 2005 Inefficiency of storm water inlets as a source of urban floods. Water Sci Technol 2005, 15, (2), 139–145.
[103] Djordjević, S., Prodanović, D., Maksimović, C., Ivetić, M., Savic, D., 2005. SIPSON – simulation of interaction between pipe flow and surface overland flow in networks. Water Sci Technol 2005, 52, (5), 275–283.
[104] ten Veldhuis, J.A.E., Clemens, F.H.L.R., 2011. The efficiency of asset management strategies to reduce urban flood risk. Water Sci Technol 2011, 64, (6), 1317–1324.
[105] Huizinga, J., Moel, H. de, Szewczyk, W. (2017). Global flood depth-damage functions. Methodology and the database with guidelines. EUR 28552 EN. doi: 10.2760/16510
[106] Nastev, M., Todorov, N., 2013 Hazus: A standardized methodology for flood risk assessment in Canada, Canadian Water Resources Journal, 38:3, 223-231, DOI: 10.1080/07011784.2013.801599.
[107] NIWA Technical Report: WLG2010-45 August 2010 NIWA Project: RSKA113
[108] Ferretti, A., Prati, C., Rocca F., "Permanent scatterers in SAR interferometry," Jan. 2001 in IEEE Transactions on Geoscience and Remote Sensing, vol. 39, no. 1, pp. 8-20, doi: 10.1109/36.898661.

Chapter 6

[109] Giannini, M.S., 1967. Cultural Heritage. In Rivista trimestrale di Diritto Pubblico. 26: 3–38.
[110] Mazzanti, M., 2006. Methods and analysis tools for the economic evaluation of cultural heritage. Milan: FrancoAngeli.
[111] Moreschini, L., 2003. Methods of economic evaluation of cultural heritage. In International Centre for Research on the Economics of Culture, Institutions and Creativity (EBLA) Working paper. 1.
[112] Brosio, G., Piperno, S., 2013. Government and Local Finance. An introduction to the theory and institutions of fiscal federalism. Turin: Giappichelli.

[113] Rugolo, A., 2013. Il giudizio di valore tra conservazione e democrazia. In A. Bianco, Articolo 9. Rome: Aracne: 11–20.
[114] Baldioli, A., 2012. Conservation and priority: quantitative and qualitative criteria for a weighted evaluation process. In ANANKE. 65: 39–46.

Chapter 7

[115] Moya, L., Mas, E., Yamazaki, F., Liu, W., Koshimura, S., 2020. Statistical analysis of earthquake debris extent from wood-frame buildings and its use in road networks in Japan. Earthquake Spectra 36, 209–231. https://doi.org/10.1177/8755293019892423.
[116] Anbazhagan, P., Srinivas, S., Chandran, D., 2012. Classification of road damage due to earthquakes. Nat Hazards 60, 425–460. https://doi.org/10.1007/s11069-011-0025-0.
[117] Argyroudis, S., Selva, J., Gehl, P., Pitilakis, K., 2015. Systemic Seismic Risk Assessment of Road Networks Considering Interactions with the Built Environment: Systemic seismic risk assessment of road networks. Computer-Aided Civil and Infrastructure Engineering 30, 524–540. https://doi.org/10.1111/mice.12136.
[118] Goretti, A., Sarli, V., 2006. Road Network and Damaged Buildings in Urban Areas: Short and Long-term Interaction. Bull Earthquake Eng 4, 159–175. https://doi.org/10.1007/s10518-006-9004-3.
[119] Zanini, M.A., Faleschini, F., Zampieri, P., Pellegrino, C., Gecchele, G., Gastaldi, M., Rossi, R., 2017. Post-quake urban road network functionality assessment for seismic emergency management in historical centres. Structure and Infrastructure Engineering 13, 1117–1129. https://doi.org/10.1080/15732479.2016.1244211.
[120] Brown, C., Milke, M., Seville, E., Giovinazzi, S., 2010. Disaster Waste Management on the Road to Recovery: L'Aquila Earthquake case study. Ohrid, Macedonia: 14th European Conference on Earthquake Engineering (14ECEE), 30 Aug-3 Sep 2010.
[121] UNEP/OCHA, 2011. Disaster Waste Management Guidelines (Technical Report). Geneva: Joint UNEP/OCHA Environment Unit.
[122] Dolce, M., 2012. The Italian national seismic prevention program. In: Proceedings of the 15th world conference on earthquake engineering (Invited Lecture), Lisbon, 24–28 September 2012.
[123] Osaragi, T., Oki, T., 2017. Wide-area evacuation simulation incorporating rescue and firefighting by local residents. Journal of Disaster Research 12: 296–310.
[124] D'Agostino, G., Di Pietro, A., Giovinazzi, S., Porta, L.L., Pollino, M., Rosato, V., Tofani, A., 2019. Earthquake Simulation on Urban Areas: Improving Contingency Plans by Damage Assessment, in: Luiijf, E., Žutautaitė, I., Hämmerli, B.M. (Eds.), Critical Information Infrastructures Security, Lecture Notes in Computer Science. Springer International Publishing, Cham, pp. 72–83. https://doi.org/10.1007/978-3-030-05849-4_6

Chapter 8

[125] Porcelli F., Trezzi R (2014). The Impact Of Earthquakes On Economic Activity: Evidence From Italy, SIEP, Working paper 419
[126] Jhan H.T., Ballinger R., Jaleel A. Ting K.H (2020). Development and application of a Socioeconomic Vulnerability Indicator Framework (SVIF) for Local Climate Change Adaptation in Taiwan. Sustainability, 12, 1585; doi:10.3390/su12041585. www.mdpi.com/journal/sustainability
[127] Brooks, N. Vulnerability, Risk and Adaptation: A Conceptual Framework; Tyndall Centre for Climate Change Research: Norwich, UK, 2003; pp. 5–7.
[128] Birkmann, J. Measuring Vulnerability to Natural Hazards: Towards Disaster Resilient Societies; TERI Press: New Delhi, India, 2006; pp. 185–213.

[129] Patt, A.G.; Schröter, D.; de la Vega-Leiner, A.C.; Klein, R.J.T. Vulnerability research and assessment to support adaptation and mitigation: Common themes from the diversity of approaches. In Assessing Vulnerability to Global Environmental Change—Making Research Useful for Adaptation Decision Making and Policy; Patt, A.G.,
[130] Schröter, D., Klein, R.J.T., de la Vega-Leiner, A.C., Eds.; Earthscan: London, UK, 2009; pp. 1–26. Tapsell, S.M.; Penning-Rowsell, E.C.; Tunstall, S.M.; Wilson, T.L. Vulnerability to flooding: Health and social dimensions. Philos. Trans. R. Soc. A: Math. Phys. Eng. Sci. 2002, 360, 1511–1525. [CrossRef]
[131] Clark, G.; Moser, S.C.; Ratick, S.J.; Dow, K.; Meyer, W.B.; Emani, S.; Jin, W.; Kasperson, J.X.; Kasperson, R.E. Schwarz, H.E. Assessing the Vulnerability of Coastal Communities to Extreme Storms: The Case of Revere,
[132] McLaughlin, S.; McKenna, J.; Cooper, J. Socio-economic data in coastal vulnerability indices: Constraints and opportunities. J. Coast. Res. 2002, 36, 487–497. [CrossRef]
[133] Thrush, D.; Burningham, K.; Fielding, J. Vulnerability with Regard to Flood Warming and Flood Event: A Review of the Literature; Environment Agency: Bristol, UK, 2005; pp. 10–15.
[134] Adger,W.N. Vulnerability. Glob. Environ. Change 2006, 16, 268–281. [CrossRef] Sustainability 2020, 12, 1585 23 of 27
[135] Cutter, S.L. The Vulnerability of Science and the Science of Vulnerability. Ann. Assoc. Am. Geogr. 2003, 93, 1–12.
[136] O'Brien, K.L.; Leichenko, R.M. Double exposure: Assessing the impacts of climate change within the context of economic globalization. Glob. Environ. Chang. 2000, 10, 221–232.
[137] Klein, R.J.T.; Nicholls, R.J. Assessment of coastal vulnerability to climate change. Ambio 1999, 28, 182–187.
[138] Timmerman, P. Vulnerability, Resilience and the Collapse of Society: A Review of Models and Possible Climatic Applications; University of Toronto: Toronto, ON, Canada, 1981; pp. 17–19.
[139] Klein, R.J.T.; Nicholls, R.J.; Thomalla, F. Resilience to natural hazards: How useful is this concept? Glob. Environ. Chang. B Environ. Hazards. 2003, 5, 35–45.
[140] Li, Y.J. Social vulnerability indicator as a sustainable planning tool. Environ. Impact. Assess. Rev. 2014, 44, 31–42.
[141] Siagian, T.H.; Purhadi, P.; Suhartono, S.; Ritonga, H. Social vulnerability to natural hazards in Indonesia: Driving factors and policy implications. Nat. Hazards 2013, 70, 1603–1617.
[142] Zhou, Y.; Li, N.; Wu, W.; Wu, J.; Shi, P. Local Spatial and Temporal Factors Influencing Population and Societal Vulnerability to Natural Disasters. Risk Anal. 2014, 34, 614–639.
[143] Marin G., Modica M., Paleari S., Zoboli R., (2021). Assessing disaster risk by integrating natural and socio-economic dimensions: A decision-support tool, Socio-Economic Planning Sciences 77 101032
[144] Modica M., Reggiani A., Nijkamp P., (2018). Vulnerability, resilience and exposure: methodological aspects and an empirical application to shocks. SEEDS Working Paper 13/2018
[145] United Nations (2015). Sendai framework for disaster risk reduction 2015–2030. Downloadable at https://www.prevention-web.net/files/43291_sendaiframeworkfordrren.pdf.
[146] United Nations (2021). The Sustainable Global Goals Report 2021. Downloadable at https://unstats.un.org/sdgs/report/2021/The-Sustainable-Development-Goals-Report-021.pdf